Immunological and Conformational characterization of synthetic peptide probes for autoimmune diseases

Matthaia Ieronymaki

PhD THESIS OF

THE UNIVERSITY OF CERGY-PONTOISE

Immunological and conformational characterization of synthetic peptide probes for autoimmune diseases

presented by :

Matthaia Ieronymaki

PhD discussed on December 16th 2016,

Composition of the evaluation committee:

Pr. Paolo Rovero	examinateur
Pr. Thierry Brigaud	examinateur
Pr. Delphine Joseph	rapporteur
Dr. Jean-Maurice Mallet	rapporteur
Pr. Anna-Maria Papini	directrice de thèse
Dr. Maud Larregola	co-directrice de thèse

PhD THESIS OF

THE UNIVERSITY OF CERGY-PONTOISE

Immunological and conformational characterization of synthetic peptide probes for autoimmune diseases

presented by:

Matthaia Ieronymaki

This thesis was held at LCB Laboratory of the University of Cergy-Pontoise in France while from February 2015 to February 2016, experiments were performed at NEUROFARBA department of the French-Italian laboratory 'Peptide and Protein Chemistry & Biology ", Universita degli Studi in Florence, thanks to Erasmus Program Traineeship, under the direction of Pr. Paolo Rovero.

Acknowledgements

Undertaking this PhD has been a truly life-changing experience for me and it would not have been possible to do without the support and guidance that I received from many people.

I would like to first express my appreciation and thanks to my supervisor Professor Anna Maria PAPINI that she has been a tremendous mentor for me. I would like to thank her for the opportunity that she gave me to be part of the c/o French-Italian Laboratory of Peptide & Protein Chemistry & Biology (PeptLab) where I grew as a research scientist.

Words cannot express how grateful I am to my co-supervisor Dr. Maud LARREGOLA whose advices, not only on my research but also in my life, have been priceless. Her guidance was significant during the research, the writing and the defense of this thesis. I could not have arrived until the end without her help and her support. Even if our collaboration came to the end she will always continue to inspire me.

I would also like to acknowledge Professor Paolo ROVERO of the University of Florence, who is not only an "examinateur" of my thesis committee but he also hosted me to his laboratory, PeptLab, NEUROFARBA, Universitá degli Studi in Florence, thanks to Erasmus^{+} Learning Program. He gave me the opportunity to explore a new scientific field, to broad my horizons and to increase my competences.

Moreover, I would like to thank the rest of my committee members, Professor Delphine JOSEPH of the University of Paris Sud and Dr. Jean-Maurice of CNRS - Ecole Normale Supérieure who accepted to be my thesis "rapporteurs" even at hardship. Their import was crucial for the improvement of the manuscript. Last by not least, I would like to thanks Professor Thierry BRIGAUD of the University of Cergy-Pontoise, "examinateur" of my research work and president of the defense committee, who accepted me and gave me access to Laboratory of Chemical Biology (LCB) and research facilities where I met and worked with skilled researches.

During these years, I worked with people expert on their field and I had the chance to learn many things by their side. I would especially like to thank Dr. Francesca Nuti, Dr. Elisa Peroni, Dr. Olivier Monasson, Dr. Feliciana Real, Dr. Giulia Pacini, Dr. Gada Rossi. All of you have been there to teach me and to support me although your busy schedule. I would like to express my gratitude and best wishes to all the laboratory members of LCB and PeptLab.

I would like to thanks all of my friends.. friends from my childhood (Danae and Athena) who support me all over these years and are a priceless part of my life, my “new” friends who met them thanks to this PhD; in France, with whoμ I share beautiful moments and I shared many experiences and in Italy, with who I spent a wonderful winter which will be unforgivable (via del Moro_2015-2016). I’m glad having all of you in my life and surely more amazing moments are coming..

Last but not least, a special thanks to my family; my parents and my sister for supporting me spiritually and encouraging me throughout this thesis and in my life in general. Even if a kilometric distance was between us I always had them by my side.

TABLE OF CONTENTS

To patients suffering
from autoimmune diseases

Summary

Autoimmune diseases refer to chronic and heterogeneous diseases with acquired immune system reactions against the body own healthy tissues. Autoimmune diseases affect more than 5% of the population worldwide and especially young adults. The complexity of their spectrum is enormous and even if their etiology is still unclear, it was demonstrated that both genetic and environmental factors are involved in triggering the pathological mechanism. Hence, a reliable diagnostic and /or prognostic tool for an early diagnosis of autoimmune diseases before irreversible cellular damage occurs and for monitoring their progression is demanded.

Numerous studies have revealed the presence of different autoantibodies (auto-Abs) in sera of patients suffering from autoimmune diseases. Autoantibodies that are specific for a disease can be used as biomarkers for its diagnosis while autoantibodies that differ depending on the disease state can be used in the follow up of the patients. Actually, in the case of autoimmunity, an easily detectable and reliable biomarker may be represented by the titer of a specific auto-Ab.

In this context, we aimed to identify target(s) of the response for two different autoimmune diseases, multiple sclerosis and monoclonal gammopathy, using the chemical reverse approach, which involves the screening of focused antigen libraries with patient serum.

In particular, the significance of anti-myelin antibodies, and especially, anti-Myelin Oligodendrocyte Glycoprotein (anti-MOG) antibodies is still matter of debate, underscoring the highly controversial issue of a putative pathogenetic role of anti-MOG antibodies in Multiple Sclerosis. In this research project we investigated the role of MOG as putative auto-antigen in Multiple Sclerosis using the experimental autoimmune encephalomyelitis (EAE) model. Moreover, in order to assess the presence of a B-cell epitope spreading mechanism, i.e. the occurrence of a response directed toward epitopes distinct from the disease-inducing agent, we synthesized and tested as antigenic probes five synthetic peptides covering the 1-117 sequence of MOG.

The second issue of the present research focused on the selection of a peptide mimicking the minimal epitope recognized by the commercial available monoclonal antibody anti-human natural killer cell-1 (anti-HNK-1) using Surface Plasmon Resonance (SPR) technique. HNK-1 epitope, is considered as the antigenic determinant of myelin-associated glycoprotein (MAG), a quantitatively minor component of myelin sheaths. It is observed that patients affected by autoimmune neurological disorders, such as IgM monoclonal gammopathy and demyelinating polyneuropathy, often develop anti-MAG antibodies specifically targeting the HNK-1 epitope. Accordingly, identification and characterization of these antibodies are relevant. The selected peptide could be subsequently used in earlier stage patients for the development of a novel and reliable diagnostic tool for anti-HNK-1 antibody identification in sera of patients affected by autoimmune neurological disorders monitoring disease activity.

Résumé

Les maladies auto-immunes sont des maladies chroniques et hétérogènes caractérisées par des réactions du système immunitaire acquis contre les propres tissus sains de l'organisme. Ces maladies affectent presque 5% de la population mondiale et en particulier les jeunes adultes. La complexité de leur spectre est énorme et même si leur étiologie est encore incertaine, il a été démontré que des facteurs génétiques et environnementaux sont impliqués dans le déclenchement du mécanisme pathologique. Cependant, il est nécessaire d'utiliser des outils diagnostiques et / ou pronostiques fiables pour le diagnostic précoce avant que des dommages cellulaires irréversibles ne se produisent et pour surveiller la progression de la maladie.

De nombreuses études ont mis en évidence la présence de différents auto-anticorps dans le sérum de patients atteints de maladies auto-immunes. Les auto-anticorps qui sont spécifiques d'une maladie peuvent être utilisés en tant que biomarqueurs pour son diagnostic alors que les auto-anticorps qui diffèrent en fonction de l'état de la maladie peuvent être utilisés dans le suivi des patients. En fait, dans le cas de l'auto-immunité, un biomarqueur facilement détectable et fiable peut être représenté par le titre d'un auto-anticorps spécifique.

Dans ce contexte, nous nous intéressons à deux maladies différentes, la sclérose en plaques (SEP) et la gammapathie monoclonale, en utilisant l'approche chimique inverse via le criblage de librairies de peptides par des sérums de patients.

En particulier, l'importance des anticorps anti-myéline, et surtout, des anticorps anti-MOG (myéline oligodendrocyte glycoprotéine) est toujours l'objet de débats, soulignant la question très controversée d'un rôle pathogène putatif d'anticorps anti-MOG dans la SEP. Dans cette thèse, nous avons étudié le rôle de MOG comme auto-antigène putatif dans la SEP en utilisant le modèle expérimental d'encéphalomyélite auto-immune (EAE). Ainsi, afin d'évaluer la présence d'un mécanisme d' « epitope spreading » des cellules B, à savoir l'apparition d'une réponse dirigée vers des épitopes distincts de l'agent pathogène induisant la réponse immunitaire, nous avons synthétisé et testé en tant que

sondes antigéniques cinq peptides synthétiques qui couvrent la séquence 1-117 de MOG.

La seconde étude a porté sur la sélection d'un peptide mimant l'épitope minimal reconnu par l'anticorps monoclonal commercial anti- natural killer cell-1 humain (anti-HNK-1) en utilisant la résonance plasmonique de surface (SPR). L'épitope HNK-1 est considéré comme le déterminant antigénique de la glycoprotéine associée à la myéline (MAG), un composant quantitativement mineur des gaines de myéline. On observe que les patients atteints de troubles neurologiques auto-immuns, tels que la gammapathie monoclonale à IgM et la polyneuropathie démyélinisante, développent souvent des anticorps anti-MAG ciblant spécifiquement l'épitope HNK-1. Par conséquent, l'identification et la caractérisation de ces anticorps est pertinente. Le peptide choisi suite à notre étude pourrait ensuite être utilisé chez des patients atteints de troubles neurologiques pour le développement d'un outil de diagnostic fiable ou de surveillance de l'activité de la maladie par l'identification d'anticorps anti-HNK-1 dans le sérum des patients.

CHAPTER 1

Introduction

I. Immune system and immunity

The immune system is a sophisticated defense that specifically recognizes and eliminates foreign agents thereby protecting the host against infection. Immunity is divided into two different types – innate and adaptive.[1] Innate immune responses are not specific to a particular pathogen in the way that the adaptive immune responses are. On one hand, innate responses depend on a group of proteins and phagocytic cells that recognize conserved features of pathogens and become quickly activated to help destroy the invaders. Therefore, during the first critical hours of exposure to a new pathogen, our innate immune system protects us from infection. On the other hand, the adaptive immunity is called into action when a pathogen is able to evade and overcome the innate immunity. Its activation takes much longer, usually over a few days. A major advantage of adaptive immune responses, not seen with innate immunity, is that they generate memory so that a second infection with the same microbe elicits a stronger, faster and usually more effective response (Figure 1.1).[2]

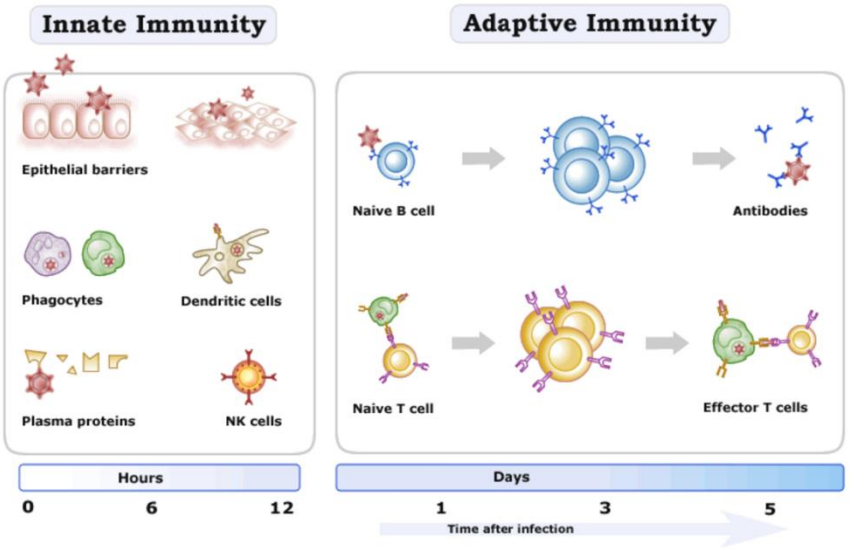

Figure 1.1: The main components of the innate and adaptive immune systems.[3]

I.1. Types of adaptive and cell-mediated immune responses

There are two broad classes of adaptive immune responses, the antibody responses and the cell-mediated immune responses, and they are carried out by different classes of lymphocytes, called B cells and T cells, respectively (Figure 1.2). In antibody response, B cells are activated to secrete antibodies, which are proteins called immunoglobulins. The antibodies circulate in the bloodstream and permeate the other body fluids, where they bind specifically to the foreign antigen that stimulated their production. Binding of antibody inactivates viruses and microbial toxins by blocking their ability to bind to the receptors on host cells. Antibody binding also marks invading pathogens for destruction, mainly by making it easier for phagocytic cells of the innate immune system to ingest them. In cell-mediated immune responses, the second class of adaptive immune response, activated T-cells react directly against a foreign antigen. This pathogen is presented to T-cells on the surface of a host cell (Antigen Presenting Cell, APC) by certain delivery molecules, called Major Histocompatibility Complex (MHC) or Human Leukocyte Antigen (HLA) for humans. APC could be various types of cells, such as microglia, fibroblasts, but mostly dendritic cells of myeloid origin. The antigens are recognized by cytotoxic T-cells (Tc), also known as $CD8^+$ T cells because they express the CD8 glycoprotein on their surface, and by helper T-cells (Th), also known as $CD4^+$ T cells because they express the CD4 glycoprotein on their surface. Specifically, Tc- cells recognize their targets by binding to antigens associated with MHC I molecules, which is found on the surface of all nucleated cells. Through different molecules secreted by regulatory T cells (Treg), Tc- cells can be activated to an anergic state, which prevents autoimmune diseases. On the other side, Th-cells became activated when they are presented with peptides antigens by MHC class II molecules, which are expressed on the surface of APCs. Once activated, they divide rapidly and secrete small proteins called cytokines that regulate or assist in active immune response. The T-cell receptor (TCR) recognizes a peptide antigen on the cell surface carried by the MHC molecule and then a complex between T cell receptor (TCR), the antigen (peptide) and histocompatibility protein (MHC) is created. The T-cell should kill a virus-infected host cell that has viral antigens on its surface, thereby eliminating the infected cell before the virus had the

chance to replicate. In other cases, the T-cell produces signal molecules that activate macrophages to destroy the invading microbes that they have phagocytosed.[2,4]

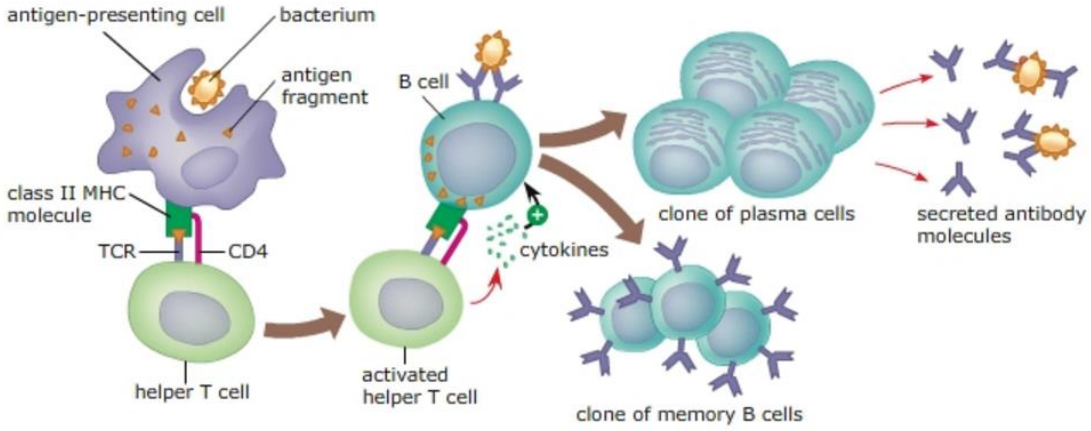

Figure 1.2: The two main classes of adaptive immune responses.[5]

II. Autoimmune Diseases

During maturation of the immune system, immune cells that react against self-tissues are eliminated providing an immune system that is 'tolerant' to self. Autoimmunity was believed to be an aberrant response. Nowadays, researchers have realized that autoimmunity is a natural phenomenon in which recognition of self-antigens by lymphocytes is mainly involved in pathologic organ damage.[6] Human autoimmune diseases affect almost more than 5% of the population worldwide, and are responsible for the morbidity and the mortality of the human population.[7] The complexity of this spectrum of autoimmune diseases is enormous and their etiology is still unclear. There are over 80 autoimmune diseases known and they have been categorized as organ specific or systemic or both. In organ-specific autoimmune diseases, the immune responses are "misdirected" against a self-antigen or organ (e.g., thyroid, β-cells of the pancreas). By contrast, in systemic autoimmune diseases, multiple organs are targets for immune attack, and chronic activation of innate and adaptive immune cells is usually present. However, it should be mentioned that the categorization of an autoimmune disease as organ-specific or systemic is based primarily on clinical observations rather than on the expression pattern of the self-antigen that appears to be targeted in the attack.

II.1. The development of autoimmune diseases

The complexity of autoimmune diseases comes from the fact that autoimmunity is triggered by a variety of agents and molecular and cellular pathways and is not set off by a single cause. It is difficult to understand the mechanisms of autoimmunity because autoimmune diseases are only recognizable after their development and appearance. According to recent findings [7,8,9], the development of autoimmune diseases can be divided in four phases (Figure 1.3):

(i) *Susceptibility phase* that could be either inherited, acquired, or both.

(ii) Initiation phase, abnormalities in tolerance induction, regulatory T-cell (Treg) development, or immune signaling thresholds allow the development of self-sustaining tissue damage.

(iii) *Propagation phase,* immune effector pathways cause damage and provide antigen to provoke the immune response. It should also be noted that in many cases during this phase, immunoregulatory pathways are also activated, which may result in natural inhibition of clinical disease over time.

(iv) *Resolution phase*, involves the induction and activation of regulatory mechanisms that limit the effector response and restore the effector/regulatory balance.

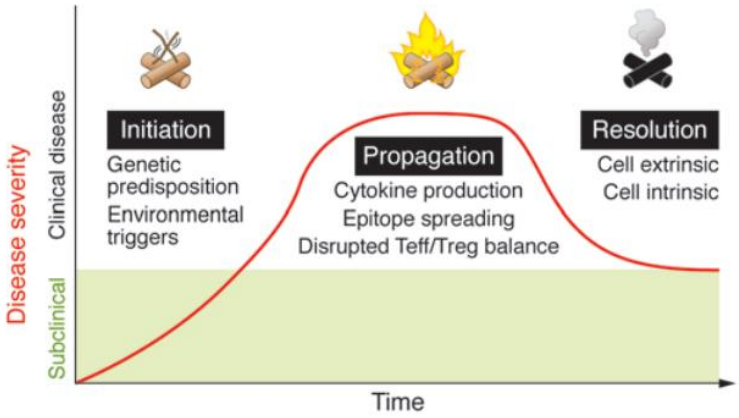

Figure 1.3: The main phases of autoimmune disease.[10]

II.2.Determinants of Autoimmune Diseases

During the last decade many attempts have been done to understand the ongoing deregulation of self-tolerance mechanisms. For many autoimmune diseases, a particular pathogen, chemical, drug, toxin, or hormone is thought to lead to an anti-self immune response. However, the genetic make-up of the host is considered as the single most important factor contributing to autoimmune disease.[11] The development of an autoimmune disease is characterized as “mosaic of autoimmunity” as it depends on a combination of genetic and environmental factors[12] as well as hormonal influences.[13]

II.2.1. Genetic predisposition

Studies performed on several mouse models[14,15] highlight a crucial role for pathways of tolerance induction, immune regulation, and immune signaling in avoiding to trigger autoimmunity. Certain human leukocyte antigen (HLA) allele(s) have been associated with the predisposition to an autoimmune response. An antigen, which could not be

presented by the host major histocompatibility complex (MHC), cannot induce a response thus would not be an autoantigen in that host. The presence or absence of the appropriate MHC is able to determine whether the potential autoantigen is presented and furthermore the induction of a response to the presented antigen. However, no genetic pattern is specific to any disease and some patients with specific genetic pattern manifest different diseases.

II.2.2. Environmental factors

The evidence of the role of environmental factors in the etiology of autoimmune diseases is clearly apparent when considering that more than 50 and sometimes 70 or 80% of monozygotic twins are discordant for major autoimmune diseases.[16] Environmental factors could be divided into two categories: the infectious agents and non-infectious agents such as stress[17], smoking, vitamin D deficiency[18], drugs, glue-sniffing or exposure to silica dust, exposure to UV irradiation (particularly UV-B rays).[19] It is reported that workers in industries such as furniture re-finishing, spray-painting, perfume or cosmetic manufacturing also have a slightly increased risk of developing autoimmune diseases.

Drug treatment has been suspected for the initiation of a response in some autoimmune diseases. For example, thiol-containing drugs and sulfonamide derivatives, as well as certain antibiotics and non-steroidal anti-inflammatory drugs, appear to trigger the onset of pemphigus. Drugs such as hydralazine and procainamide or similar aromatic amine drugs prescribed can induce SLE-like symptoms such as arthritis, pleuropericarditis, and myocarditis.

Infections with certain viruses, bacteria, fungi and vaccines appear to lead to systemic autoimmune diseases in genetically predisposed individuals. A severe bacterial or viral infection may trigger an increase in autoreactive antibodies or conventional T cells that leads to initiate an autoimmune disease or an exacerbation of existing symptoms.[20,21] With respect to viruses, the onset of various autoimmune diseases has been variably associated with infection by HSV-1, Coxsackie virus, Epstein- Barr virus (EBV), human immunodeficiency virus (HIV), human papilloma virus (HPV), or influenza virus. In particular, viral infections have been closely associated with flare-ups of SLE. Similarly,

the development of Guillain Barre Syndrome (GBS) may follow infection with herpes simplex virus (HSV), EBV, or cytomegalovirus (CMV), and the onset of acute idiopathic thrombocytopenic purpura (ITP) may be preceded by varicella infection. Infections with various bacterial species have also been associated with autoimmune diseases. The most striking example is the development of rheumatic fever (RF) following recovery from infection with a virulent member of the Group A streptococci.

II.2.3. Hormonal influences

Last but not least, hormones seem to have an influence to trigger autoimmune diseases. It has been reported that females are more susceptible to autoimmune conditions than males.[22,23] More than 85% of patients with thyroiditis, scleroderma, lupus, and multiple sclerosis are females.[24] X-chromosome abnormalities, sex hormones such as estrogens and androgens are believed to play a significant role in the sex-based susceptibility to many autoimmune diseases.

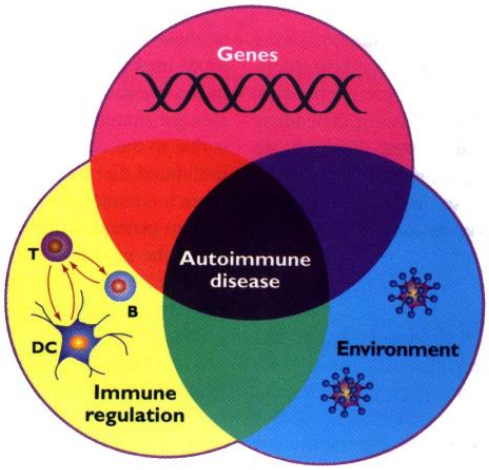

Figure 1.4: Genetic susceptibility, environmental stimuli, and defective regulation are responsible for initiating autoimmunity.[25]

II.3. Possible mechanisms triggering autoimmune diseases

The mechanisms of the autoimmune responses still remain unclear but there are numerous and diverse hypothesizes that are considered to contribute to the progress of autoimmune diseases in susceptible individuals. We could categorize them into *pathogen-related* and *cellular* mechanisms.

II.3.1. Pathogen-related mechanisms

i) The most common pathogen-related hypothesis is *molecular mimicry*. This process is relevant to those autoimmune responses that are clearly associated with preceding infections, thus it has frequently been proposed as a potential initiator of autoimmune diseases. During several infections, proteins which usually are recognized as self could become non-self after a tissue injury, oxidation stress, cell death, free radical production or reparative changes inducing an autoimmune response. These changes to the self-proteins could come from post-translational modifications (PTMs), denaturation, misfolding or mutations. However, it is important to realize that molecular mimicry alone is not able to explain self-sustaining autoimmune diseases, which are driven by self-antigens and autoreactive T cells but is necessary to overcome T-cell tolerance to the self-protein. Due to the simultaneous liberation of self-antigen in the presence of the cross-reactive antibody response, activated cross-reactive B cells may present cryptic epitopes in the self-antigen to autoreactive T cells.[26] Release of self-antigen could lead to adaptive immune response to self. Thereby, it is possible that this process could end up to the exposure of other regions on the same self-antigen that will then stimulate the emergence of further antibodies, some of them pathogenic, through the mechanism of "epitope spreading".

ii) A second putative mechanism of an autoimmune response is called *"adjuvant effect"*. It is known that an infectious agent may activate lymphocytes in an antigen-specific manner although it can also provide a non-specific antigen second signal which is necessary to induce a pathogenic adaptive immune response. This secondary signaling has been referred to as the "adjuvant effect".[27] The hypothesis is that bacterial DNA, bacterial components, and endogenous nucleic acids released upon pathogen-induced cell death are particularly potent adjuvants because they engage the Toll-like receptors

(TLRs) of immature dendritic cells (DCs). Following TLR engagement, DCs are induced to mature and upregulate their expression of co-stimulatory molecules. When such mature DCs encounter autoreactive T cells in the lymph node, activation leading to an autoimmune response may result if the pMHC derived from a pathogen or self antigen is recognized by the T cell. Thus, autoreactive T cells regain their capacity for activation. While the precise mechanism by which DC function is enhanced by stress molecules remains to be clarified, the results of *in vitro* as well as *in vivo* studies show that autoimmune diseases can be induced by endogenous host stress molecules in the absence of pathogen infection.

iii) Another theory to account for at least some episodes of pathogen-linked autoimmune diseases involves *microbial superantigens*. Superantigens are called proteins that produced especially by bacteria, mycoplasma and virus-effected cells and have the ability to bind to the variable of T cell receptors independently their antigen. These molecules can non-specifically activate a large number of different T cell clones by binding directly to particular T-cell receptor (TCR) Vβ sequences.[28] Superantigens are considered to have a role in relapses of autoimmune diseases or the aggravation of ongoing autoimmune diseases, but they do not appear to be able to initiate autoimmune diseases.

Proteins to which the immune system is self-tolerant might, if altered, elicit autoimmune responses. Self-proteins can be altered in many ways such as mutations, posttranslational modifications and disordering.

II.3.2. Cellular mechanisms

Apart from pathogen-related mechanisms, there are cellular mechanisms that lead or enhance an autoimmune response. Both T and B cells play an important role in autoimmunity. Four basic mechanisms describing how Treg cells are involved in immunosuppression are reported[29]: the modulation of antigen presenting cell (APC) maturation and function, the killing of target cells, the disruption of metabolic pathways and the production of anti-inflammatory cytokines (Figure 1.5).[28,30] Studies suggest that the nature of the Treg impairment depends on the autoimmune disease that is under investigation.

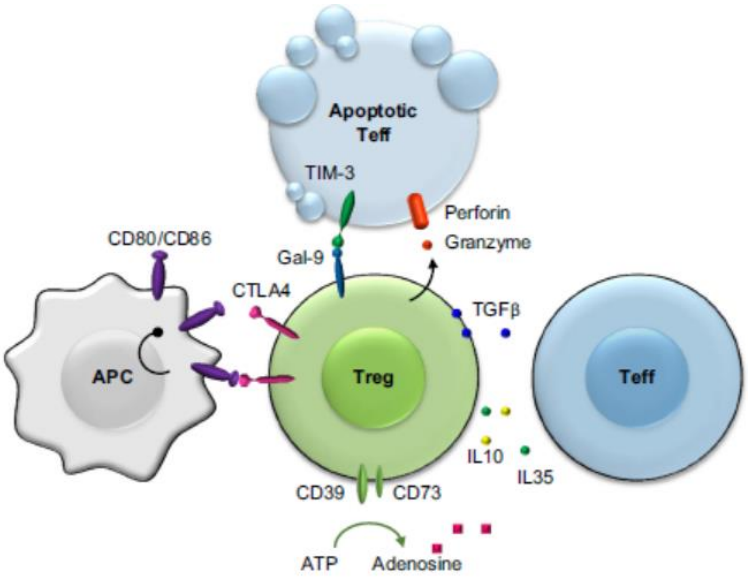

Figure 1.5: Treg cell mechanism of suppression.[28]

Treg impairment has been reported in several autoimmune diseases, both non-organ specific (SLE) and organ specific (Multiple Sclerosis, RA, autoimmune thyroid disease, psoriasis etc). Studies on animal models describe that the absence of Treg cell populations can be the cause of uncontrolled immune responses and widespread autoimmune inflammation of tissues. Because of difficulties in isolation of human Treg, reports are sometime inconsistent or even contradictory.

Due to the production of antibodies, including autoantibodies, B cells are generally thought to be positive regulators of the immune response. The production of antibodies facilitates optimal $CD4^+$ T-cell activation because B cells serve as antigen-presenting cells and exert other modulatory functions in immune responses. However, certain B cells, which produce regulatory cytokines and directly interact with pathogenic T cells via cell-to-cell contact, can also result in negative regulation of the immune response. These types of B cells are defined as regulatory B (Breg) cells.[31] Certain Breg cells that produce IL-10 or TGF-β have been shown to possess inhibitory functions in autoimmune diseases.[32] Recent studies from numerous mouse models have suggested that B-cell depletion results in an increased Breg cell subset in the reconstituted B-cell population. Thus, the effects of the adaptive transfer of Breg cells alone or in combination with B-cell depletion could be an interesting approach for the treatment of autoimmune diseases.

III. The role of post translational modifications (PTMs) in autoimmunity

As already described above, one of the mechanisms able to trigger an immune response is represented by PTMs, changes occurring at the amino or carboxyl terminus of a protein or at individual amino acid side-chains (Table 1.1). It is estimated that around 50-90% of proteins in human body are post-translationally modified.[33] PTMs play a crucial role to the primary and tertiary structure of the proteins, their biological and / or enzymatic functions and proteolytic degradation.[34] These modifications can be enzyme-mediated, as in the case of glycosylation and phosphorylation, or can occur spontaneously, as in the deamidation reaction that converts asparagine to aspartic acid or isoaspartic acid. The probability of a post-translational modification could depend on different parameters:

i) the sequence motif, as in the case of the *N*-glycosylation where the motif Xaa-Asn-Xaa-[Ser/Thr] is required,[35]

ii) the sequence-regulated conformations that can influence the accessibility to the particular enzyme that mediates the modification,

iii) the intra- and extracellular locations of individual modifying enzymes,

iv) the changes in the substrate itself, like proteolytic cleavages and previous modifications.

Table 1.1: Common post-translational modifications

Modification	Residue Modified
Additions	
Glycosylation	Asn/Ser
Phosphorylation	Ser/The/Tyr
Acetylation	Lys/Ser
Methylation	Arg/Lys
Conversions	
Deamidation	Asn
Deimination/Citrullination	Arg

Some post-translationally modified self-Ags (i.e., proteins) that arise temporally over the course of development (e.g. during adolescence) can create neo-self Ags, to which the immune system has never been exposed in the periphery. Even if it is still unclear, that could be a general hypothesis on how the normal tolerance to self-proteins is disturbed and elicit an autoimmune response.

Mamula M. et al.[31] observed that B-cell response tends to be promiscuous because of the ability of antibodies (Abs) elicited by modified self-proteins to bind either the modified or unmodified form of proteins. On the other hand, T-cell response leans toward specificity to the modified self-Ag with little or no crossreactivity with the unmodified self Ag. Although, the mechanisms by which T cells specific for the neo self Ags escape tolerance are not clearly understood. A possible explanation could be that some PTMs of self-peptides inside a protein are not present at the time of T-cell selection within the thymus thus autoreactive T cells migrate to the periphery. Once in the periphery, T cells and/or B cells recognize the modified self Ag as 'foreign' promoting the mechanisms of intramolecular epitope-spreading, by which the immune response diversifies to include epitopes beyond the site(s) inducing the initial reaction.

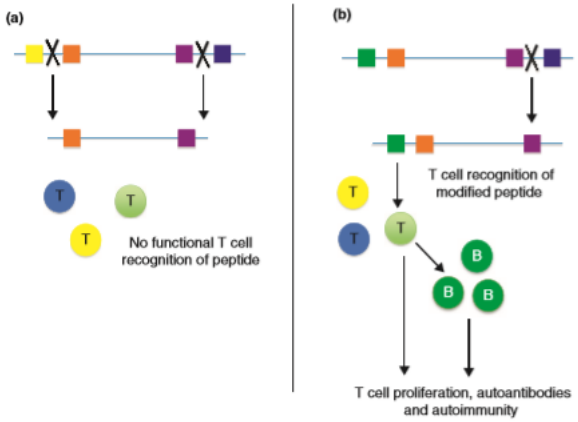

Figure 1.6: Alteration of Ag processing by aberrant PTMs. (A) Proteases (represented by X) cleave native proteins into peptides. T and B cells do not recognize self-peptides. (B) Proteins bearing aberrant PTMs are not properly cleaved by proteases, creating neo-Ag for T cells.[35]

IV. Biomarkers

The term biomarker refers to any measurement that indicates the biological state of an individual, the disease risk, diagnosis and progression, the treatments of choice as well as the response to them and their efficacy.[36] It is already mentioned above that autoimmune diseases affect around 5% of the population, particularly young adults and in most cases their etiology and pathogenesis remain unclear. As there are many asymptomatic patients or patients to whom the first clinical symptoms appeared in a later state, it is necessary to use reliable diagnostic and / or prognostic tools for an early diagnosis before irreversible cellular damage occurs and for monitoring the disease progression. Numerous studies have demonstrated the presence of different autoantibodies in sera of patients suffering from autoimmune disorders. Autoantibodies that are specific for a disease can be used as biomarkers for its diagnosis while autoantibodies that differ depending on the disease state can be used in the follow up of the patients.[37] In 1906, first Wassermann reported a routine diagnostic assay to detect anti-cardiolipin autoantibodies[38] for syphilis and since then autoantibodies have been used as disease markers. For example, anti-cyclic citrullinated peptide antibodies (anti-CCP) can predict the development of rheumatoid arthritis (RA) in subjects with undifferentiated arthritis.[39] Whether the use of biomarkers is very useful in screening strategies on healthy or already diagnosed population requires detailed methodological, clinical and ethical evaluations. It is important to note that as no antibody assay offers 100% specificity and as the assay method used influence the positive results, the greatest challenge is to distinguish between the false positive and the true positive results in order to predict correctly the onset and the development of a disease.[40] In this concept it is essential to use methods with high diagnostic specificity to minimize false positives.

Taking into account that native antigens could be used in simple biological assays for the identification of autoantibodies, as disease biomarkers as well as the fundamental role of the PTMs for specific autoantibody recognition in autoimmune diseases led PeptLab laboratory to develop the innovative **“Chemical Reverse Approach”.** This approach is useful to identify and optimize synthetic peptides as antigenic probes for fishing out autoantibodies circulating in biological fluids as biomarkers.[41]

V. The “Chemical Reverse Approach”

Synthetic peptide probes derived from native protein sequences, reproducing specific epitopes, or mimicking immunogenic modifications could be even more effective and specific than native proteins to detect antibodies. This approach was defined “Reverse” because autoantibodies circulating in patient blood guide the screening of the synthetic antigenic probe. “Chemical” because autoantibody recognition drives selection and optimization of the “chemical” structure from defined peptide libraries,[42] often through the evaluation of different PTMs. The “Chemical Reverse Approach” uses patient sera to screen specific libraries of synthetic modified peptides in order to identify peptide probes capable to characterize highly specific autoantibodies as biomarkers of autoimmune diseases. Peptide epitopes identified by this approach can be used as antigenic probes in immunoenzymatic assays, like Enzyme Linked Immunosorbent Assays (ELISA). The “Chemical Reverse Approach” focuses on two different parameters regarding Ab recognition. On one hand, the identification of the side-chain modification, which is involved in the pathogenic mechanism and on the other hand the selection of the best peptide fitting with the antibody-antigen binding site regarding to conformational features. As a proof-of-concept this approach has been successfully applied for the identification of autoantibodies as biomarkers of an autoimmune mediated form of Multiple Sclerosis, Reumathoid Arthritis (RA),[43] and more recently Rett Syndrome.

VI. CSF114(Glc), the first antigenic probe able to recognize disease-specifc auto-Ab as biomarkers of Multiple Sclerosis

In 1999, the team of Anna-Maria Papini[44] reported that a synthetic glucosylated peptide of human Myelin Oligodendrocyte Glycoprotrein (hMOG), the [Asn31(Glc)]hMOG(30-50), is able to recognize auto-Abs in Multiple Sclerosis patient sera. Subsequently, it was demonstrated that even if its conformation is similar to the N-glucosylated peptide, the unglucosylated analogue hMOG(30-50) displayed negligible inhibitory activity in competitive enzyme-linked immunosorbent assay (ELISA) and failed to detect IgG autoantibodies in solid-phase ELISA (SP-ELISA) giving evidence that *N*-glucosylation is one of the PTMs associated with the antibody-mediated demyelination in Multiple Sclerosis. Hence, the ability of [Asn31(Glc)]hMOG(30-50) analogue to detect auto-Abs is related to the *N*-glucose moiety and it is not conformation-dependent.[45] Taking into account these findings, a series of peptides and glycopeptides unrelated to MOG was synthesized in order to further investigate the role of glycosylation in triggering an autoimmune response in Multiple Sclerosis.[46,47] Using SP-ELISA, high Ab titers are identified in Multiple Sclerosis patient sera with all glycopeptides containing glucose on Asn but mainly with a completely MOG-unrelated sequence, termed CSF114(Glc). CSF114(Glc) is a structure-based designed type I' β-turn sequence, in which the glucose moiety is optimally exposed.[48] At clinical level, the glucopeptide CSF114(Glc) reveals IgM and IgG antibody titers and the latter ones even if with less specificity paralleled the occurrence of magnetic resonance imaging lesions and disease progression in 40% of analyzed patients. Therefore, quantification of the IgG titers has been found to have a high prognostic value. Lastly, at the *N*-terminus of CSF114(Glc) was introduced a ferrocenyl carboxylic acid (Fc) or a ferrocenyl-thio-phosphine of 1-aminobutyric acid [4-FcPhP(S)Abu] in order to develop an electrochemical assay, more sensible than ELISA.[49]

VII. Multiple Sclerosis

One of the most common autoimmune and neurodegenerative disorders of the central nervous system (CNS) is Multiple Sclerosis. It is a chronic, demyelinating and inflammatory disease in which the immune system triggers an attack against its own tissues. The main objective of the immune system attack, is myelin resulting in its loss (demyelination). Myelin is a white substance that surrounds most axons, forming an electrically insulating layer that helps propagate nerve impulses. Loss of myelin can cause a variety of symptoms such as weakness in one or more members (in 40% of patients), visual disturbance as optic neuritis (in 22% of patients), paresthesia (in 21% of patients), diplopia (in 12% of patients), while less frequently (in 5% of patients) vertigo, heartburn and burning electrical discharge in the spine and legs, trigeminal neuralgia in the face, paroxysmal symptoms and dysarthria. As in most autoimmune diseases, Multiple Sclerosis primarily affects young adults, without excluding its appearance in younger or elderly people.

There are several different forms of Multiple Sclerosis.[50] Since these classifications were based upon clinical characteristics, they do not reflect specific biological pathophysiology but they provide an organized framework for diagnosis and long-term management. The *Relapsing-Remitting* Multiple Sclerosis form (RRMS) is the most common form of the disease, where symptoms appear for several days to weeks, after which they usually resolve spontaneously. After tissue damage accumulates over many years, patients often enter the *Secondary Progressive stage* (SPMS), where pre-existing neurologic deficits gradually worsen over time. Relapses can be seen during the early stages of SPMS, but are uncommon as the disease further progresses. About 15% of patients have gradually worsening manifestations from the onset without clinical relapses, which defines the *Primary Progressive* Multiple Sclerosis form (PPMS). Patients with PPMS tend to be older, have fewer abnormalities on brain MRI, and generally do not respond very effectively to standard Multiple Sclerosis therapies.[51] Finally, *Progressive Relapsing Multiple Sclerosis* is defined as gradual neurologic worsening from the onset with subsequent superimposed relapses. Progressive Relapsing Multiple Sclerosis (and

possibly a proportion of PPMS) is suspected to represent a variant of SPMS, where the initial relapses were unrecognized, forgotten, or clinically silent.

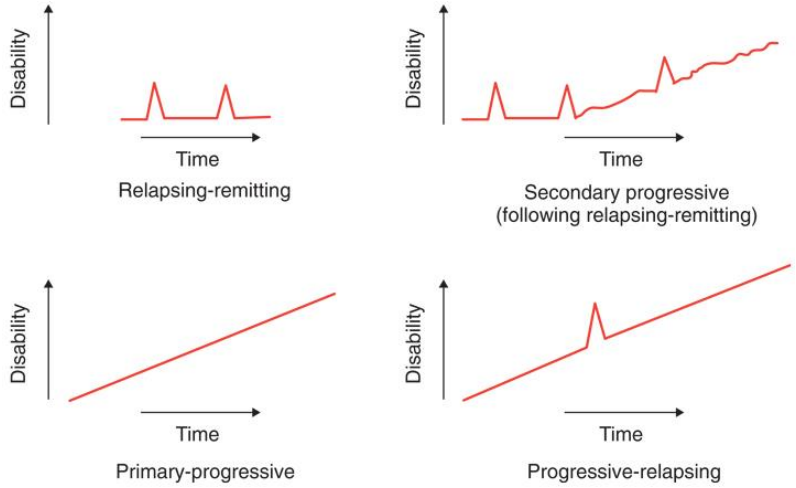

Figure 1.7: Illustration of clinical courses of Multiple Sclerosis.

The pathogenesis of the disease still remains unclear but an autoimmune mechanism against myelin antigens is thought to influence its immunopathological mechanisms.

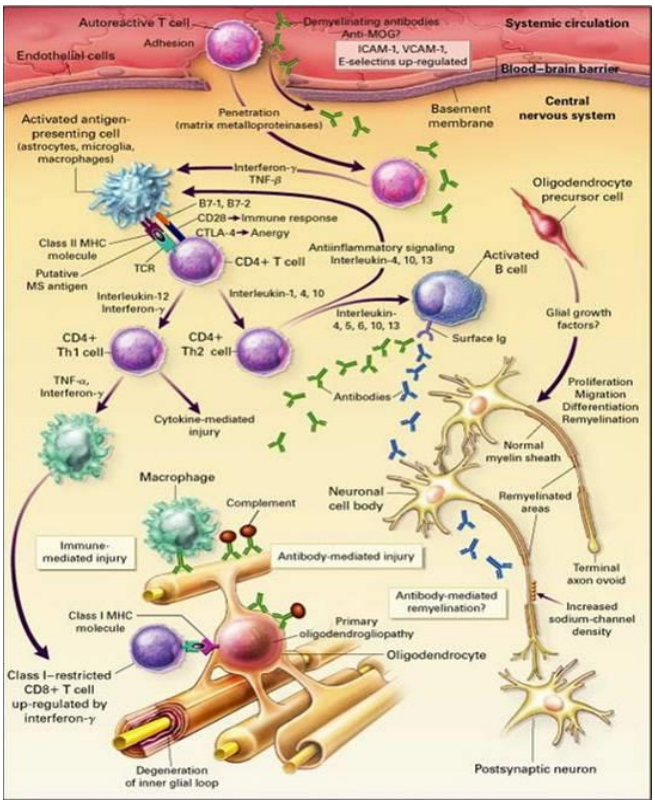

Figure 1.8: Possible mechanism for the pathogenesis of Multiple Sclerosis.

Different myelin proteins have been studied as putative antigens for trigging T or B cell response in Multiple Sclerosis. The most extensively studied candidates are Myelin Basic Protein (MBP), Proteolipid Lipoprotein (PLP), Myelin Oligodendrocyte Glycoprotein (MOG), etc. In this PhD research project, we mostly focus on MOG.

VII.1. MOG and anti-MOG antibodies

Autoantibodies play an important role in different encephalopathies and inflammatory diseases of the central nervous system (CNS)[52,53,54,55], like Multiple Sclerosis, immune-mediated, demyelinating and neurodegenerative diseases.[56] Myelin oligodendrocyte glycoprotein (MOG) has been one of the most studied candidates as target CNS autoantigen for both humoral and cell-mediated immune responses. MOG is one of the few myelin proteins that is localized on the outer lamellae of myelin sheath.[57,58] Its localization makes the protein an accessible target for pathogenic autoantibodies.[59,60] The role of MOG and antibodies to MOG in CNS demyelination has been explored for decades, immunizing an important animal model of Multiple Sclerosis, the experimental autoimmune encephalomyelitis (EAE). MOG was firstly characterized by the mouse IgG1 monoclonal antibody 8-18C raised against cerebellar glycoproteins. Passive transfer of this monoclonal antibody resulted in a hyperacute inflammatory response in animals with acute EAE, in fatal relapses or in formation of demyelinating plaques in those with chronic relapsing EAE. In addition, studies using enzyme linked immunosorbent assays (ELISA) showed that anti-MOG antibodies titers are correlated with *in vivo* demyelination in animal models with relapsing EAE.[61] Nowadays it is known that MOG can be involved in CNS autoimmunity in principally two different ways. Firstly, MOG specific T cells evoke CNS inflammation and secondly, anti-MOG antibodies lead to the induction of demyelination.[62] The encephalitogenic T-cell response leading to acute demyelinating EAE was shown to target the Ig-like extracellular N-terminal domain (MOG_{1-117}) and especially the epitope MOG_{35-55}.[63] On the other hand the importance of the B cell response is still less clear.

It is important to note that only the anti-MOG antibodies, which binding is conformational driven, have shown to be pathogenic in EAE, while MOG peptide-specific autoantibodies were unable to recognize the native protein.[64,65] Crystallographic studies

on rMOG demonstrated that the mAb 8-18C5 binds mainly at the amino acids 101-108 that comprise the FG loop, protruding from the top of the Ig domain of MOG as a hairpin loop.[66] Maybe the inability of the anti-MOG antibodies to recognize linear epitopes is due to the absence of this loop. The two central amino acids (His[103] and Ser[104]) of the FG loop have been demonstrated to have an important role for the pathogenic demyelinating anti-MOG antibody response according to studies in which these residues were substituted with other amino acids. As it is reported by de Graaf *et al.* rats immunized with correctly refolded recombinant human MOG developed severe acute EAE and had a higher amount of anti-MOG antibodies in serum, as well as enhanced T cell responses against encephalitogenic MOG 91-108 peptide.[67] Generally, by ELISA experiments, antibodies to native and glycosylated MOG were associated with demyelination in rat EAE models whereas antibodies to recombinant MOG were not found to be associated with inflammation and / or demyelination.[68]

Although MOG is a protein highly conserved among species, with a 90% sequence homology of the extracellular domain, a single substitution of the amino acid at position 42 from Ser in rodents to Pro in humans is able to change the mechanism of encephalitogenicity from B cell dependent to independent.[69] It is evident that translating the findings in animal models to human diseases has to be done with caution.

Early studies reported that the amino acids H[103] and S[104] bound by 8-18C5 mAb were not the most frequently recognized residues in humans. With the use of different MOG mutants to evaluate the epitope specificity of seropositive anti-MOG antibody pediatric patients with demyelinating diseases, Mayer *et al.*[7] found that the most frequently recognized single epitope was identified as P42 on the membrane proximal CC'-loop, a site that is not present in murine MOG. In humans, contrary to rodents, the region at the tip of the FG loop was the second most frequent epitope. Additionally, this study highlights that the absence of the single glycosylation site at the position 31 did not significantly reduce the binding.

For many decades researchers using different methods like ELISA and Western blots have been trying to evaluate the presence of anti-MOG antibodies in the serum and the CSF of patients with Multiple Sclerosis. There are studies showing the importance of MOG in the immune response of patients with demyelination[70,71] but there are also

other studies indicating the seropositivity with anti-MOG IgM and IgG antibodies in patients with other inflammatory neurological diseases as well as healthy controls.[72,73,74] There is a series of explanations that try to understand these differences in the studies, i.e., the different techniques that have been used for the antigen preparation and the antibody determination. In some studies, recombinant hMOG expressed in *E.coli* was used, so with lack of glycosylation, while other authors translated native full length MOG and used it but once again without a specific post-translational modification. Furthermore, the fact that in most assays, like ELISA and Western blots, linearized or denatured MOG antigens were used might have a crucial role for antibody recognition as it is known from animal models that anti-MOG antibodies can bind conformational epitopes. Last but not least, patient populations were heterogeneous and research groups evaluated different immunoglobulin isotypes.

Apart from ELISA and Western blot studies, cell-based assays have been performed in order to identify anti-MOG antibodies in patient sera.[75,76,77,78,79] The majority of these studies reported that both prevalence and intensity of MOG antibody titers were low in Caucasian adult patients with Multiple Sclerosis. Contrary to studies using ELISA, the use of cell-based assays to investigate anti-MOG antibodies demonstrated that these were almost not detected in healthy controls or other immune systemic diseases.

In 2007, anti-MOG antibodies were associated for the first time with acute disseminated encephalomyelitis (ADEM).[80] Surprisingly, high-titer antibodies have been found to be more frequently positive in pediatric onset demyelination including ADEM and clinical isolated syndromes (CIS) than adult onset MS.[73,81] It is interesting to mention that in children with a first episode of demyelination, anti-MOG antibody positive patients were less likely to continue fulfilling the criteria for clinically defined MS than the seronegative patients.[82]

VII.1.1. The role of MOG in the CNS

It has been already shown in an animal model that the 8-18C5 mAb, which binds a MOG epitope, is pathogenic. Although, the question whether anti-MOG antibodies have a pathogenic role in demyelinating diseases in humans still remains. An antibody is considered pathogenic if it is produced within the CNS or passes through the blood brain

barrier (BBB) from the periphery into the CNS. A direct CNS infection could be associated with an inflammatory response, a breakdown of the BBB and leakage of CNS antigens into the peripheral circulation, where a peripheral immune response could be mounted against accessible central antigens, like MOG.[83] Another possibility is the stimulation of the adaptive immune responses by an infection and the activation of B and T cells. The BBB is disrupted and the circulating lymphocytes pass to the CNS with restimulation upon contact with the MOG antigen and then clonal expansion within the CNS.[79] Ramanatan *et al.*[84] propose an increased incidence of an infection in patients with MOG antibody-associated demyelination. The infection could trigger immunity in MOG antibody-positive disease. Further work is required to identify how the process of CNS inflammation is initiated and propagated in case of MOG antibody-associated demyelination.

VII.1.2. Structure of MOG

Full length MOG is made up of 218 amino acids. A pattern of MOG topology was proposed by Kroepfl *et al*.[85] According to this model, the protein contains an extracellular domain (MOG_{ED}) that comprises an Ig-like portion and the N-linked carbohydrate moiety (N-terminal), a first typical transmembrane domain, a second hydrophobic domain and a small intracellular domain (C-terminal).

The crystal structures of $rMOG_{ED}$[62] and $mMOG_{ED}$[86] were resolved by X-ray crystallography. The reported studies proposed that the overall structure of MOG_{ED} adopts a topology of an Ig-V domain structure, which consists of a compact β-sandwich domain with one antiparallel β-sheet (strands A, B, E, and D) packing against a mixed β-sheet (strands A', G, F, C, C', and C''). The N- and C-termini are at opposite ends of the molecule. Moreover, at the periphery of the protein there are four 3_{10} helices. There is a canonical disulfide bond (Cys24–Cys98) and a salt bridge between Arg68 and Asp92. The glycosylation site of MOG (Asn31) is located in the BC loop, exposed at the top, membrane-distal side of MOG_{ED} (Figure 1.9).

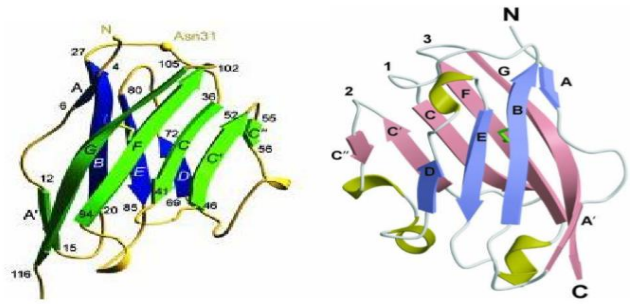

Figure 1.9: X-ray crystal structure of $rMOG_{ED}$ (on the left) and $mMOG_{ED}$ (on the right).

Even if MOG_{ED} was crystallized as a monomer, the observed interactions within the crystalline lattice were suggestive of a biologically relevant MOG_{ED} dimer. Indeed, there are three regions of crystal contacts observed within the lattice of MOG, and only one of these was observed to lie on a crystallographic twofold, forming an antiparallel, head-to-tail dimer within the lattice. The shape complementarity index at the dimer interface is high, representing a value that is comparable to that observed in antibody – antigen interactions. These interactions involve mainly extreme N-terminus, the A-A' loop (residues 8–11), the C–C' loop (residues 40–46), and the F–G strand β-hairpin (residues 95–112).

After further investigations, it was confirmed that native MOG exists as a mixture of monomeric and dimeric species.[87] It was demonstrated that the monoclonal Ab (mAb) 8-18C5 (which is able to mediate demyelination *in vitro* and *in vivo* and to increase clinical EAE in rats),[55] is capable to recognize proteins with relative mass of 26–28 kDa (monomeric MOG) and 54 kDa (dimeric MOG) in CNS myelin from mouse and human brain as well as native hMOG purified from brain. It was also confirmed that the observed dimer was not merely due to crystal packing artifacts using several biochemical techniques (e.g. native gel electrophoresis).

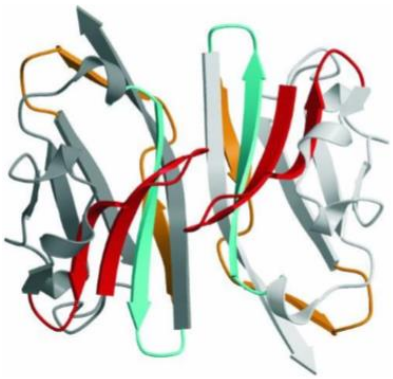

Figure 1.10: Schematic representation of the dimeric structure of MOG.

VIII. Monoclonal gammopathy of undetermined significance (MGUS)

While Multiple Sclerosis is an inflammatory demyelinating disease of the central nervous system, which attacks the brain and the spinal cord, MGUS is a demyelinating neuropathy of the peripheral nervous system (PNS). PNS consists of the nerves and ganglia outside the brain and spinal cord. The main function of the PNS is to transmit instructions from the CNS to any part of our body. Monoclonal gammopathy (MG) is related to the presence of a plasma M-protein as a result of an accumulation of bone marrow plasma cells derived from a single abnormal clone.[88] M-protein, also known as paraprotein, is an abnormal immunoglobulin fragment or immunoglobulin light chain that is produced in excess by an abnormal clonal proliferation of plasma cells. In most cases in which monoclonal gammopathy is due to a benign clonal expansion, the disease is called monoclonal gammopathy of undetermined significance (MGUS) and is a common age-related demyelinating sensor-motor polyneuropathy.[89] Patients suffering from this disease are estimated around 2% over 50 years-old and 3% over 70 years old. The clinical picture of the disorder usually consists of a chronic sensory polyneuropathy with ataxia and tremor of progressive worsening. Motor involvement, if present, usually occurs lately in the course of the disorder.[90] MGUS is usually associated with different classes of immunoglobulin, especially with IgG for approximately 60% of patients, followed by IgM in about 10-27% of cases, and the rest are of IgA class. However MGUS with IgM is the most frequent case, which later develops a neuropathy.

It was previously reported that around 70% of patients with MGUS have anti-myelin associated glycoprotein (MAG)[91,92] antibodies detected by ELISA. Therefore, the presence of anti-MAG antibodies suggests diagnosis of active autoimmune demyelinating sensory-motor neuropathies, inflammatory neuropathies, and some other motor neuron diseases. It is believed that MAG plays a crucial role in cell-cell interaction within the nervous system. Anti-MAG antibodies cross react with several other components of peripheral nerve myelin, as the glycolipids sulfoglucoronyl paragloboside (SGPG), sulfoglucoronyl lactosaminyl paragloboside, and sulfatide,[93] which are also involved in demyelinating neuropathies. It was previously reported that IgM antibodies reacting with MAG can also cross-react with SGPG or some other nerve glycoproteins, *i.e.* P0, a major structural component of the myelin sheath.[94,95] The antigenic determinant is

considered to be the HNK-1 (Human Natural Killer cell-1), a carbohydrate epitope which is found not only in MAG but also in neural cell adhesion molecules (NCAM), myelin protein zero (P0), extracellular matrix proteins (Tenascin-R, Phospgacan), and peripheral nerve glycoconjugates (SGPG).[96,97] The majority of patients with anti-MAG antibodies have also serum antibodies to SGPG. Therefore, the HNK-1 epitope could be the putative antigen involved in chronic demyelination and the interest of diverse research groups was concentrated on peptides that possibly mimic this epitope. The latter one could be used for the development of a novel diagnostic tool for patients affected by autoimmune neurological disorders.

Peripheral neuropathies, such as MGUS, are one of the most etiologically diverse group of neurological disorders in which biomarkers are widely used in both clinical classification and understanding of the disease. In the present research project the synthesis of a series of rationally synthesized peptides mimicking the minimal epitope recognized by the anti-HNK-1 IgM monoclonal antibody is reported in order to develop a useful tool for the diagnosis of patients affected by PNS autoimmune disorders.

VIII.1. Myelin associated glycoprotein (MAG)

MAG is a quantitatively minor component of myelin which was first detected in isolated rat CNS myelin by metabolic labeling experiments.[98] It is a 100kDa transmembrane glycoprotein localized in periaxonal Schwann cell and oligodendroglial membranes of myelin sheathes. The supportive function of glial cells helps to define synaptic contacts and maintain signaling abilities of neurons. Glial cells are more numerous than nerve cells in the brain, outnumbering them by a ratio of 3 to 1. Therefore, MAG has important functions in glia-axon interactions in both PNS and CNS but also for the normal formation and maintenance of myelinated axons of the PNS. When the normal physiological functions are disrupted, neurological disabilities are accumulated. It is noteworthy that in hypomyelinated mutants, MAG is not reduced as much as proteins of compact myelin, due to the fact that myelin-related glial membranes containing MAG are preserved relative to compact myelin.[99] The identification of MAG in the PNS was more difficult than in the CNS as its amount is smaller and it is masked by the P0 glycoprotein which is a major component (Figure 1.11).

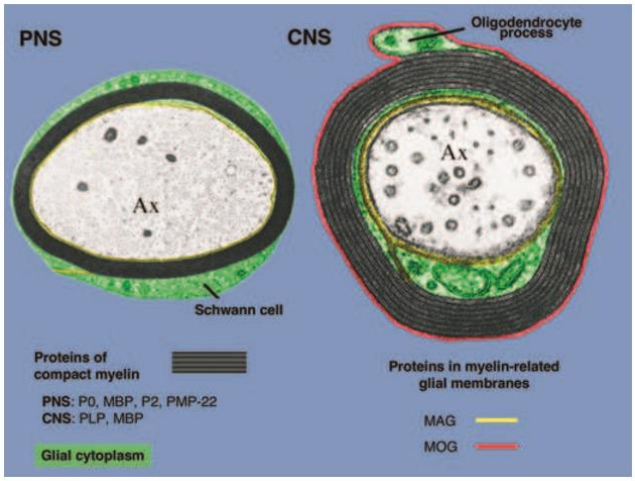

Figure 1.11: Location of MAG in PNS and CNS.[99]

Immunocytochemistry experiments show that MAG is also present in membranes of Schmitt-Lanterman incisures, lateral loops, and inner and outer mesaxons of PNS sheaths where its functions are different.

In 1987, three groups published the structure of MAG, which was revealed by cloning of the rat MAG gene.[100] MAG consists of five extracellular immunoglobulin (Ig)-link domains, a single transmembrane domain, and a cytoplasmic domain with two different C-termini for the L- and S- isoforms. So, it belongs to the immunoglobulin superfamily. The large isoform (71 kDa) and small isoform (67 kDa) arise from alternative splicing of mRNAs. A soluble form of MAG containing the extracellular domain is released from myelin in large quantities and identified in normal human tissues and in tissues from patients with neurological disorders. This soluble MAG may contribute to the lack of neuronal regeneration after injury.

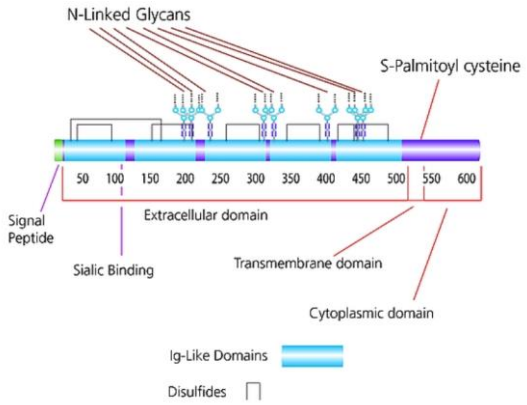

Figure 1.12: Myelin Associated Glycoprotein in rat.

MAG contains around 30% carbohydrates by weight, consisting of eight heterogenous N-linked oligosaccharides present at extracellular sites.[100] Most of the carbohydrate moieties contain the HNK-1 epitope, which is usually recognized by anti-MAG antibodies.

VIII.2. Human Natural Killer cell-1 (HNK-1)

The HNK-1 epitope is a sulfated carbohydrate epitope firstly described in 1981 on HNK cells.[94] It has a 3'-sulfated glucuronic acid attached to *N*-acetyllactosamine, and it is described on *O*-glycans of glycoproteins, on proteoglycans, and on glycolipids (Figure 1.13).[101] Its biosynthesis is regulated mainly by glucuronyltransferases (GlcAT-P and GlcAT-S) and a sulfotransferase.[102] There are results suggesting that the two glucuronyltransferases synthesize structurally and functionally different HNK-1 carbohydrates.[103] More specifically, there are evidences that the HNK-1 epitope is synthesized by GlcAT-S as the non-sulfated form in mouse kidney while the sulfated is expressed predominately in the nervous system.

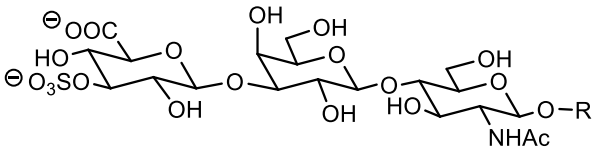

Figure 1.13: The sulfated HNK-1 epitope.

As already mentioned the sulfated HNK-1 carbohydrate is involved in the formation and maintenance of myelin and is thought to be the target for IgM autoantibodies in demyelinating neuropathies of the peripheral nervous system in humans. Moreover, HNK-1 has also other roles that are reported below. It is an essential ligand for many neural cell adhesion molecules, i.e., the integrins (NCAM, P0, etc.) and the extracellular matrix glycoproteinglycans (Tenascin-R, phosphacan, etc.). HNK-1 has effects on correct reinnervation after an injury because it is considered as an intrinsic molecular effector for Schwann cells associated with motor neurons.[104,105] The HNK-1 epitope is also associated with neuron to glial cell adhesion and with the outgrowth of astrocytic processes, and is involved in cell interactions that control cell type-specific neurite outgrowth and regeneration.[106] Recently, the HNK-1 glycan function was also studied in brain tumors and it was shown that its expression is inversely correlated with astrocytic

tumor aggressiveness in human patients. Almost all brain tissues free from cancer cells were positive for the HNK-1 glycan. It is thus proposed its function as a tumor suppressor and may be sufficient to stimulate the migration of cerebellar granule neurons.[107] Two monoclonal antibodies have been identified for their reactivity with the HNK-1 carbohydrate epitope, the HNK-1[108] on neurite outgrowth and the 412 antibodies on neuron-astrocyte and astrocyte adhesion.[109] Even if it is not fully clear, it seems that the HNK-1 antibody can exclusively recognize the epitope when the glucuronic acid is sulfated while the 412 antibody binds with the sulfated and non-sulfated forms.[110]

CHAPTER 2

Epitope mapping of anti-MOG antibodies in EAE: application of microwave-assisted strategy to the synthesis of peptide antigens and ELISA screening

I. Introduction

The involvement of MOG as a putative auto-antigen in the pathogenesis of demyelinating autoimmune diseases and especially in Multiple Sclerosis is reported by diverse research groups and has already been highlighted in this PhD thesis. However, its role remains a matter of debate even if a possible explanation could be the exposition of its IgG-like extracellular domain on the outermost surface of myelin sheath, allowing the access of potential auto-antibodies to the protein.[87]

To further investigate Multiple Sclerosis and to elucidate the anti-MOG antibody response, animal models are an extremely powerful tool. This study was carried out using a widely used Multiple Sclerosis animal model, the EAE, induced by active immunization with MOG(35-55) peptide in C57BL/6 mice, which reflects aspects of chronic progressive Multiple Sclerosis. In this context, we used the properly refolded extracellular domain of the MOG protein as well as five peptide fragments, i.e., MOG(1-34), MOG(35-55), MOG(56-75), MOG(76-95), and MOG(96-117), which arose by splitting the full sequence to analyze the antibody response. A shortened protein fragment, the $MOG_{1-117,}$ instead of the standard extracellular domain MOG_{1-125} was used in an attempt to avoid solubility issues. This more soluble fragment is more appropriate to be employed as an antigen in immunological solid-phase assays. Our attempt was focused firstly on the characterization of both linear and conformational epitopes and secondly on the investigation of possible involvement of an intramolecular epitope spreading phenomenon in EAE pathogenesis. Epitope spreading is involved in many autoimmune disorders,[111,112] including Multiple Sclerosis[113,114] and several EAE models.[115,116] For this study, a solid-phase immunoenzymatic assay testing both naïve and EAE mice sera was set up using as antigenic probes the extracellular MOG_{1-117} protein domain, properly refolded, and the peptide fragments, synthesized by an optimized protocol for solid phase peptide synthesis (SPPS) using microwave irradiation. The obtained results indicate an intense IgG antibody response against both the recombinant protein and the immunizing peptide MOG(35-55), while no response was observed against the other synthetic fragments, enabling us to exclude the presence of an intramolecular epitope spreading mechanism. Furthermore, by CD spectroscopy experiments we studied the

conformational propensity of both MOG_{1-117} and MOG(35-55). Combination of the results obtained by SP-ELISA and CD characteristics allowed us to hypothesize the presence of both linear and conformational epitopes in MOG(35-55) sequence.

II. Results and Discussion

II.1. Design and synthesis of MOG antigens

The recombinant MOG protein was obtained at NEUROFARBA PeptLab (Section of Pharmaceutical Sciences, University of Florence, Italy), by subcloning the cDNA of the 1-117 extracellular portion of rat MOG into the His-tag expression vector pET-22. The need of soluble products to perform solid-phase immunoassays forced us to use the shortened protein fragment $MOG_{1-117.}$ The choice of this fragment was done in order to avoid solubility issues observed with the canonical extracellular domain $MOG_{1-125,}$ which comprises a highly hydrophobic transmembrane portion ($F^{119}YWI^{122}$). With the removal of this short sequence a more soluble recombinant product was obtained, that is more appropriate to be employed as an antigen in solid-phase immunoassays. The final product was refolded according to the protocol previously reported,[117] using a gradient of denaturating buffer versus non-denaturating buffer over 10 h on a Ni-NTA affinity chromatography column.

The design of the synthetic peptides used was guided by the immunogenic peptide MOG(35-55), which was described in the literature as the immunodominant epitope of MOG.[118] Afterwards, the C-terminal fragment MOG(56-117) was divided in three 20-mer portions. Moreover we investigated also the residual N-terminal fragment MOG(1-34) (Table 2.1). Practically, we splitted the sequence into five peptide fragments: MOG(1-34), MOG(35-55), MOG(56-75), MOG(76-95), and MOG(96-117).

Table 2.1. Sequences of the designed synthetic antigenic probes.

No	Antigen	Sequence
2	**MOG(1-34)**	GQFRVIGPGYPIRALVGDEAELPCRISPGKNATG
3	**MOG(35-55)**	MEVGWYRSPFSRVVHLYRNGK
4	**MOG(56-75)**	DQDAEQAPEYRGRTELLKET
5	**MOG(76-95)**	ISEGKVTLRIQNVRFSDEGG
6a	**MOG(96-117)**	YTSFFRDHSYQEEAAMELKVED
6b	**MOG(96-117)KKKK**	YTSFFRDHSYQEEAAMELKVEDKKKK

The synthesis of MOG peptide fragments **2-6b** was performed following an optimized process for solid phase peptide synthesis (SPPS) using microwave irradiation for the coupling and the deprotection steps combined with the Fmoc/tBu strategy (see chapter 4, I).This protocol offers a remarkable reduction not only of total chemical waste (~90%) but also of the time needed for a complete cycle (approximately 4 minutes/cycle). In particular, the coupling reaction was performed in two short coupling steps at 90 °C and not in one longer step at 75 °C, as previously reported.[119] A big issue to be overcome during peptide synthesis and especially during coupling reaction is racemization.[120,121,122] The degree of racemization depends on diverse factors, like the electron-withdrawing effect of the amino-acid side chain, the temperature and the solvent of the reaction, and the base used during activation. In order to overcome the problem of racemization the microwave conditions mentioned before were applied to all amino acids except His, Cys and Arg residues, for which specific parameters are required. Therefore, the coupling of both Cys and His residues was performed at 50 °C. Once these amino acids were incorporated into the peptide chain, higher temperatures and MW conditions were applied for the rest of the synthesis. Moreover, during the coupling of Arg residue the nucleophilic side chain of Arg is susceptible to form a δ-lactam during the coupling reaction.[139] For this reason, a first coupling of the activated Arg was performed at conventional conditions (25 min at room temperature) then microwave energy was applied for 2 min. A second coupling was typically performed to ensure that deletion

sequences, resulting from lactam formation, are minimized. For the activation the well-known carbodiimide DIC[123] based techniques with Oxyma were used.[124] We avoided the use of derivatives like HOBt and HOAt because they are classified as Class 1c explosives, and they are less stable at elevated temperatures. The deprotection step was performed with 20% piperidine in DMF, employing a short initial microwave deprotection step for 15 sec at 75 °C followed by a second step of 50 sec deprotection at 90 °C.

At the end, crude peptides were cleaved form the resin according to the general protocol described in chapter 4. For the peptides containing more than one Arg residue an approximately 5 h cleavage was requested because of the uncompleted removal of the Pbf side-chain protecting group after 2 h. Crude peptides were purified to a final HPLC purity >95% and characterized by analytical RP-HPLC with UV detection at 215 nm, coupled with ESI-MS (see Annexes II, III). Analytical data are reported in Table 2.2.

Antigens were tested on a cohort of 47 EAE mice sera, together with 9 naïve mice sera as control, measuring separately IgG and IgM.

II.2. Solid Phase ELISA (SP-ELISA)

The presence of Ab response against recombinant refolded MOG and MOG peptides in EAE mice sera (in cooperation with Dr. Rina Aharoni of the Department of Immunology of the Weizmann Institute, Rehovot, Israel) was evaluated by SP-ELISA, with an optimized method set up in our PeptLab for both recombinant MOG[136] and synthetic peptides (see Annexe V.1). According to the results obtained (Figure 2.1) high and specific IgG response against mMOG(35-55) and recombinant $rMOG_{1-117}$ was detected in sera of all the EAE induced mice (manifesting clinical scores 2-4) at all the time points tested (2-4 weeks after disease induction), while no response was detected against any other peptide fragment.

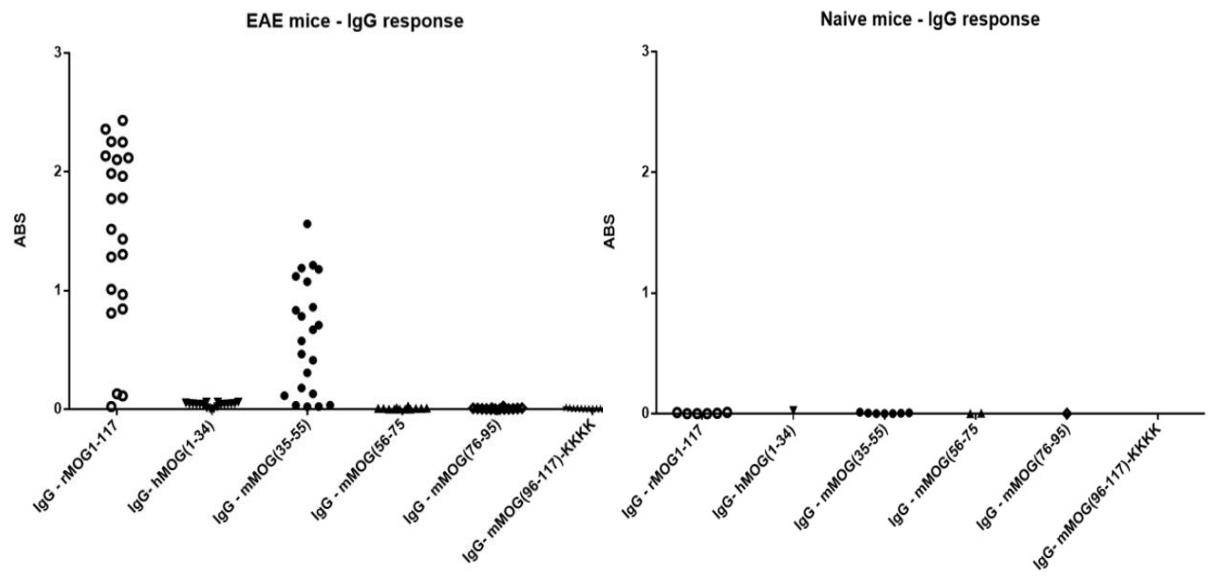

Figure 2.1: Data distribution of IgG in EAE (left) and naïve mice (right).

On the contrary, no significant response was detected against any Ag in the case of IgM comparing EAE with naïve mice (Figure 2.2). Finally, none of the tested antigens was recognized by auto-antibodies, either IgG or IgM, in naïve mice sera (Figures 2.1, 2.2).

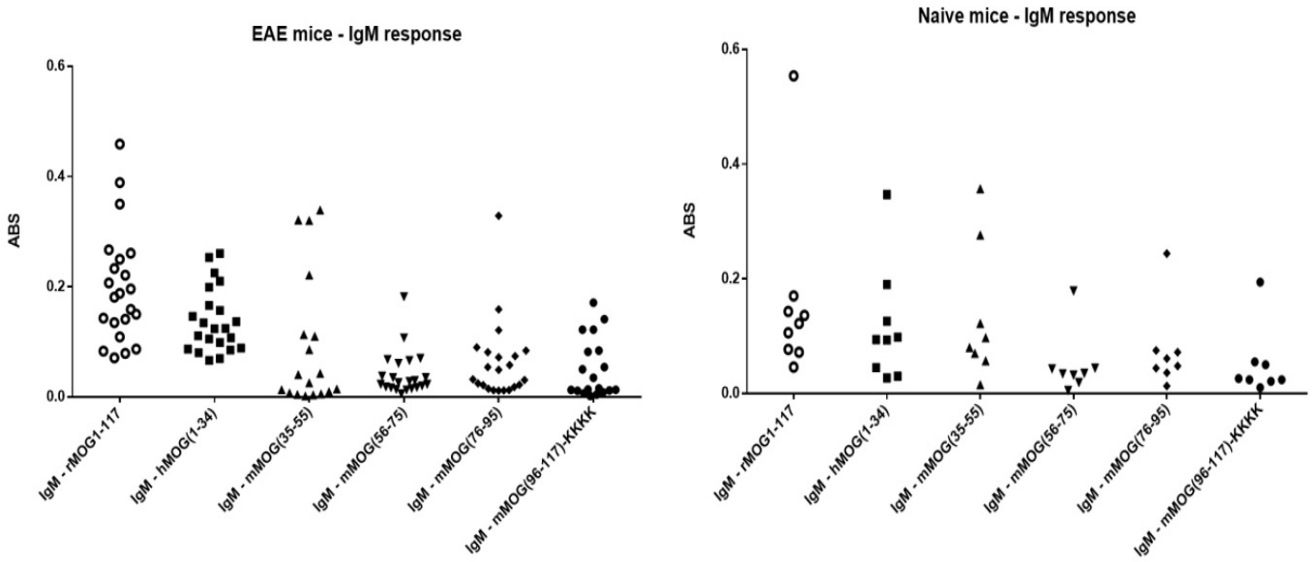

Figure 2.2: Data distribution of IgM in EAE (left) and naïve mice (right).

The data distribution of IgG in EAE showed stronger response against the recombinant protein compared to the immunogenic peptide. With this result we could hypothesize the presence of a MOG conformational epitope recognized by auto-antibodies in EAE mice sera. Indeed, the recombinant refolded protein could reproduce both the primary

amino acid sequence and the conformation of the native antigen, and correctly expose the latter in the context of the solid-phase ELISA coating phase. On the other hand, the immunogenic peptide, MOG(35-55) reproduce only a linear, short portion of the protein and was unable to mimic a conformational epitope on the ELISA plate.

After the synthesis and purification of the peptide probe **6a** we had to deal with solubility issues. For this reason, we decided to add a C-terminal 4-Lys tag (peptide **6b**) to enhance the solubility of the sequence, as we previously reported for other peptide sequences.[125] SP-ELISA experiments performed using the two peptides **6a** and **6b** on the same sera samples and conditions showed no difference in the values of the IgM response (Figure 2.3) demonstrating that the Lys tag did not influence the antibody recognition.

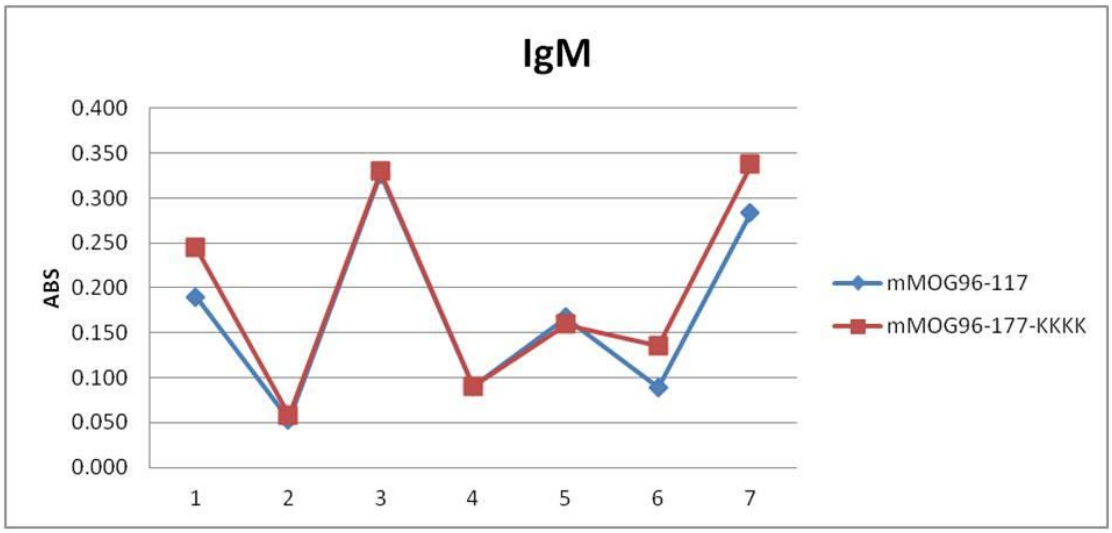

Figure 2.3: IgM Ab value detected against MOG(96-117) (peptide 6a) (blue) and MOG(96-117)-KKKK (peptide 6b) (red) in 7 EAE mice sera.

CD spectroscopy experiments were performed to confirm conformational differences between the protein MOG(1-117) and the peptide MOG(35-55).

II.3. Circular Dichroism (CD)

Circular dichroism (CD) studies in the far-UV region (240 nm to 190 nm) were performed to estimate the secondary structure of recombinant MOG_{1-117} and MOG(35-55) (see Annexe IV). Both the protein MOG(1-117) and the peptide MOG(35-55) were studied at the same concentration in PBS (pH 8.0) at 25 °C and their spectra were recorded. Based on previously published CD results on MOG_{1-125}[126] (see Chapter 1, VII.1.2), as expected refolded recombinant MOG_{1-117} displays a beta-sheet conformation, which is characterized by a minimum at 218 nm and a positive peak near 200 nm. Conversely, we have assessed that MOG(35-55) displays a random coil conformation, characterized by a negative peak around 195nm (Far-UV Circular dichroism spectra).

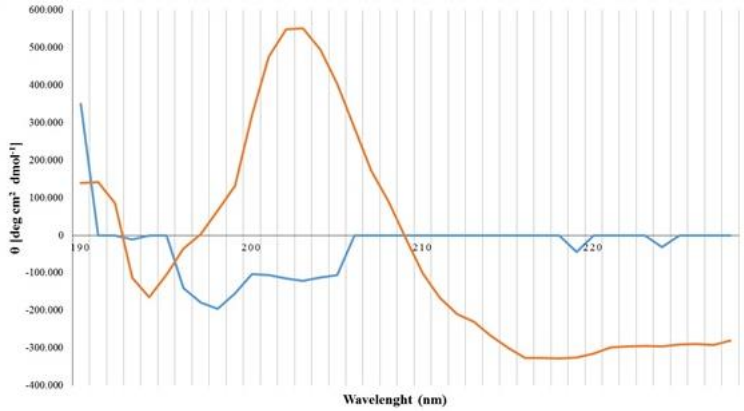

Figure 2.4: Far-UV Circular dichroism spectra of $rMOG_{1-117}(His)_6$ (in red) and mMOG (35-55) (in blue) at pH 8.0 (PBS buffer) at 25 °C.

It was previously reported that short synthetic peptides used as immunogenic agents are able to elicit an antibody response against their corresponding sequence on the full-length folded protein.[127,128] Indeed, the peptide MOG(35-55), due to its extreme flexibility, may typically assume a random coil conformation in solution, but can also adopt other conformations like the folded one when interacting with an antibody.

III. Conclusion

A proven animal model, like EAE in the case of Multiple Sclerosis, has many advantages, as it helps us to design experiments aimed to go deeper in understanding pathogenic mechanisms of autoimmune diseases. A limitation of this study is represented by the execution of tests on temporally distinct cohorts, making the data obtained not entirely homogeneous. However, this study prove the lack of evidence of an epitope spreading mechanism related to the MOG sequence as an intense IgG antibody response against both the recombinant protein and the immunogenic peptide MOG(35-55) while no significant response was detected against any other antigen in the case of IgM comparing EAE with naïve mice. Even if future developments of this work are needed to disclose the putative pathologic role of the anti-MOG immunological response, the results we obtained boost the interest in using recombinant MOG to assess the presence of antibodies in the mice model of Multiple Sclerosis.

IV. Experimental part

IV.1. Sera samples

47 EAE induced mice serum samples (provided by Dr. Rina Aharoni, Weizmann Institute, Rehovot, Israel) were analyzed and divided according to disease status. 9 naïve mice serum samples were used as healthy control group. Samples were tested in triplicate with a single dilution (1:100) in FBS Buffer.

IV.2. Antigens

Recombinant MOG(1-117) protein was produced and refolded according to the protocol published by Gori *et al.*[136] at PeptLab-NEUROFARBA (Section of Pharmaceutical Sciences, University of Florence, Italy). Peptide probes were synthesized following the general protocol of the high-efficiency Solid Phase Peptide Synthesis (HE-SPPS) using a Liberty Blue™ automated microwave synthesizer (CEM) following the Fmoc/tBu methodology (see Chapter 4, I). Crude peptides were purified to homogeneity (final HPLC purity >95%) and characterized by analytical RP-HPLC with UV detection at 215 nm, coupled with ESI-MS (see Annexe II, III). The methods followed for cleavage of the peptides from the resin as well as their purification and characterizations are described below (see Chapter 4, I). The analytical data are reported in Table 2.2. Data were acquired and processed using MassLynx software (Waters, Milford, Massachusetts, USA).

Table 2.2. Analytical data of the synthetic peptide antigens.

No	Antigen	HPLC Rt (min)	ESI-MS $[M + 2H]^{2+}$ (m/z) found (calcd)
2	MOG(1-34)	4.02[a]	1770.2 (1769.9)
3	MOG(35-55)	3.88[a]	1291.0 (1291.1)
4	MOG(56-75)	3.23[b]	1175.2 (1175.1)
5	MOG(76-95)	3.53[b]	1103.3 (1103.1)
6a	MOG(96-117)	3.60[a]	1348.1 (1348.1)
6b	MOG(96-117)KKKK	3.17[c]	1604.3 (1604.3)

Analytical HPLC conditions: column, Kinetex C_{18} (2.6µm × 100mm); solvent systems, A: 0.1% TFA in H_2O, B: 0.1% TFA in CH_3CN; flow rate 0.6 mL min^{-1}.
Gradient [a]20–70% B in 5 min, [b]10–60% B in 5 min, [c]25–70% B in 5 min.

IV.3. Animal model

EAE was induced as previously described.[129,130] Briefly, C57BL/6 female mice, 8-12 weeks of age, were immunized with a peptide encompassing the sequence 35-55 of MOG. Mice were injected subcutaneously at the flank, with a 100 µl emulsion containing 300 µg of MOG peptide in complete Freund's adjuvant enriched with 4 mg/ml of heat-inactivated *Mycobacterium tuberculosis*. Pertussis toxin (Sigma), 250 ng/mouse, was injected intravenously immediately after the encephalitogenic injection and 48 h later. Mice were examined daily. EAE was scored as follows: 0—no disease, 1— loss of tail tonicity, 2—hind limb paralysis, 3— hind leg paralysis with hind body paresis, 4— hind and foreleg paralysis, and 5—death. Mice showing definite EAE manifestations were bled 2-4 weeks after disease induction and their sera were analyzed.

IV.4. Recombinant MOG(1-117) expression and refolding **(PeptLab-**NEUROFARBA, Section of Pharmaceutical Sciences, University of Florence, Italy)

MOG(1-117) cDNA was subcloned into the His-tag expression vector pET-22. Recombinant MOG(1-117) protein was produced and refolded according to the protocol

published by Gori *et al*.[65] ER2566 electrocompetent cells were transformed with pET-22rMOG(1-117)$(His)_6$ plasmid. The protein was overexpressed in inclusion bodies (IBs). For this reason, cells were disrupted by sonication and IBs were purified by repetitive steps of centrifugation and resuspension in 50 mM Tris, 0.5 M NaCl, 0.5% lauryldimethylamine oxide, pH 8.0. IBs were then solubilized in a denaturating buffer (100 mM NaH_2PO_4, 10 mM Tris, 6 M guanidine·HCl, 40 mM mercaptoethanol, pH 8.0). The protein purification and refolding were performed using an Ni-NTA affinity chromatography in the ÄKTA protein purification system under a gradient of denaturating buffer (100 mM NaH_2PO_4, 10 mM Tris, 6 M guanidine·HCl, pH 8.0) versus nondenaturating solution (100 mM NaH_2PO_4, 10 mM Tris, 3 mM reduced glutathione, pH 8.0) over 10 h. Subsequently, the properly folded protein was eluted with 0.5 M imidazole in 100 mM NaH_2PO_4, 10 mM Tris, 0.2 M NaCl (pH 8.0). Finally, protein fractions obtained were pooled and checked by 12% SDS PAGE, then dialyzed against PBS (pH 8).

IV.5. Enzyme Linked ImunoSorbent Assays (ELISA)

1 µg/well of antigen (peptide or protein) was dissolved in Coating Buffer (12 mM Na_2CO_3, 35 mM $NaHCO_3$, pH 9.6), then 100 µL of solution were dispensed in each well of 96-well Maxisorp plates (NUNC Maxisorp; Sigma-Aldrich, Milano, Italy). Plates were incubated at 4 °C overnight. The plates were washed 3 times with Washing Buffer (0.9% NaCl, 0,01% Tween 20), and blocked 1 h at room temperature with 100 µL/well of fetal bovine serum (FBS) Buffer (10% FBS in Washing Buffer). Subsequently, FBS Buffer was removed, and 100 µL/well of diluted sera sample (1:100 in FBS Buffer) were dispensed. In all the plates, blank wells were included, obtained using FBS Buffer instead of serum. Plates were incubated at 4 °C overnight, and then washed 3 times with Washing Buffer. 100 µL/well of secondary antibodies diluted in FBS Buffer (anti-mouse IgG 1:30000 and anti-mouse IgM 1:7500) were dispensed, and plates were incubated 3 h at room temperature. Plates were washed 3 times with Washing Buffer and 100 µL/well of p-NitroPhenyl Phosphate Substrate Solution (1mg/mL p-NPP in Substrate Buffer: 1 M diethanolamine, 1 mM $MgCl_2$, pH 9.8) were dispensed. The incubation of the plates was for 15-40 min at room temperature, and then the absorbance (ABS) of each well was read with a multichannel

ELISA reader (Tecan Sunrise, Männedorf, Switzerland) at 405 nm. ABS value for each serum was calculated as (mean ABS of triplicate) – (mean ABS of blank triplicate).

IV.6. Circular Dichroism Studies

CD spectra were recorded on a Jasco J-810 spectropolarimeter equipped with a thermostated cell holder and connected to a PC for signal averaging and processing. All spectra were recorded between 190-250 nm employing quartz cuvette of 0.1 cm optical path length. Recombinant MOG(1-117) and MOG(35-55) were analyzed at 0.2 mg/ml in PBS. Far-UV CD spectra were recorded at 25 °C, with a cell path length of 0.1 cm. Scans were acquired using a 50 nm/min scanning speed and 1 nm data pitch. Each curve is the mean of ten spectra. Measurements were performed with peptides in buffer of PBS buffer, pH=8.

CHAPTER 3

Structure-Activity Relationship Studies: SPR Affinity Characterization and Conformational Analysis of Peptides Mimicking the HNK-1 Carbohydrate Epitope

I. Introduction

The role of disease biomarkers for chronic immune-mediated neuropathies is significant for the disease classification, patient stratification, and prediction of patient response to therapy. Patients affected by autoimmune neurological disorders such as IgM monoclonal gammopathy and demyelinating polyneuropathy often develop anti-MAG antibodies specifically targeting the HNK-1 epitope.[131,132] Therefore determination of these antibodies is clinically relevant as it may help to target also a specific immunotherapy.[133]

Taking into account that the HNK-1 epitope is substantial in the formation and maintenance of myelin sheath in the peripheral nervous system, as previously extensively mentioned, we focused our study on this carbohydrate epitope and on the detection of anti-HNK-1 autoantibodies by immunoassays for setting up alternative diagnostic techniques of these neuropathies.

Since both the chemical synthesis and the isolation from natural sources of HNK-1 appear to be difficult, the development of glycomimetics of this carbohydrate is a desirable goal pursued during this thesis. In the literature, several carbohydrate-based glycomimetics have been reported,[134,135,136,137] but only a few examples of peptides mimicking glycans are presented.[138] The majority of the reported peptides mimic carbohydrate epitopes and have been selected using monoclonal antibodies to screen phage displayed random peptide libraries.[139,140,141]

In this context, we focused our research on peptide-based mimetics of the trisaccharide human natural killer cell-1 epitope (HNK-1) with the aim of identifying a simple synthetic diagnostic tool for practical clinical use able to recognize antibodies in neurogammopathy patient sera. Specifically, this thesis reports a structure-activity relationship (SAR) study of one of these previously reported HNK-1 mimetic peptide, c-(LSETTdL*), based on the measurement of binding affinities by surface plasmon resonance (SPR) experiments (see Annexe V.2). Our objective was the optimization in terms of binding affinity of a peptide that is able to mimic the minimal carbohydrate and to be recognized by the commercially available monoclonal antibody. Subsequently this peptide could be used for the development of a novel and reliable diagnostic tool for

* dL refers to D-Leu

anti-HNK-1 antibody identification in sera of patients affected by autoimmune neurological disorders.

SPR is a technique used for the evaluation and quantification of antigen-antibody interactions, enabling direct visualization of biomolecular interactions in real-time (see Annexe V.2).[133,142] Lastly, in our laboratory, many studies have been performed by SPR for the detection of specific antibodies in sera of patients affected by multiple sclerosis, using the glycopeptide-based SPR biosensor[134] as well as for the kinetic characterization of different antibody families in rheumatoid arthritis patient sera using a panel of citrullinated peptides.[143]

II. Results and Discussion

II.1. Antigen design and SPR experiments

We focus our study on the rational design of a high affinity peptide mimicking the HNK-1 carbohydrate epitope recognized by the anti-HNK1 monoclonal antibody, starting from the previously described cyclic hexapeptide c-(LSETTdL) (**1**).[144]

The cyclic sequence of the reference, c-(LSETTdL), contains polar amino acids (Ser, Thr) with hydroxylated side chains, as expected for carbohydrate mimetics. Additionally, the backbone amine groups of the peptide possibly act as intermolecular hydrogen-bond donors and acceptors. Unpolar amino acids are present to establish hydrophobic interactions with the monoclonal antibody and a residue bearing a negative charge (Glu). Therefore, we synthesized the cyclic hexapeptide reported in the literature, c-(LSETTdL) (**1**) in order to evaluate in our hands its binding affinity. Moreover, we prepared its linear precursor LSETTdL (**2**) to investigate possible differences in binding affinity value between the linear and cyclic structures. Indeed, the SPR experiments showed that the K_D measured (1.09 x 10^{-5} M) is comparable to the previously published data[156] (K_D = 6.7 x 10^{-5} M) while the corresponding linear sequence LSETTdL (**2**) appears to be a much weaker binder (K_D = 2.18 x 10^{-2} M). Moreover, as the HNK-1 epitope bears two negatively charged functional groups, the carboxylic function at the position C1 and the sulfate group at position C3 (Figure 1.13), we envisaged the synthesis of a series of peptides characterized by net charge -2.

Accordingly, a second Glu residue was inserted to the previous sequence to obtain the linear sequence LSETETdL (**3**) bearing two negative net charges. Tested in SPR, this peptide had a higher affinity to the anti-HNK-1 monoclonal antibody, with K_D = 1.04 x 10^{-7} M, confirming the hypothesis that the increase in net negative charges increases significantly the affinity for the antibody. Afterwards, a Lys residue was also inserted in the sequence, with the aim of introducing a further functional group to be eventually used to covalently anchor this peptide to a solid support, for further SP-ELISA studies. In this context and having in mind to maintain a net charge of -2 we synthesized the peptides LSETETK(Ac)dL (**4**) and the corresponding cyclic c-(LSETETK(Ac)dL) (**5**). The fact that the increase in the net negative charge increases the affinity for the antibody was

further confirmed by the analysis of the affinities registered for peptides c-(LSETKTdL) (**7**), K_D = 4.33 x 10^{-2} M, c-(LSETETKdL) (**6**), K_D = 1.73 x 10^{-5} M, and c-(LSETETK(Ac)dL) (**5**), K_D = 1.09 x 10^{-7} M, displaying net negative charges of 0, 1, and 2, respectively, corresponding to an affinity increase of almost 5 log units. It is interesting to be highlighted that the linear analogue LSETETK(Ac)dL (**4**) presented a slightly lower affinity as compared to the corresponding cyclic analog (**5**), but their K_D values were in the same range (K_D = 4.62 x 10^{-7} and 1.09 x 10^{-7} M, respectively), in contrast to the important difference observed in the case of the parent peptides **1** and **2**. Taking into account that the HNK-1 trisaccharide contains a sulfate group (Figure 1.13), we replaced the second Glu residue with a sulfated tyrosine, Tyr(OSO_3), synthesizing the linear peptide LSETY(OSO_3)TKdL (**8**) and the corresponding cyclic one c-(LSETY(OSO_3)TKdL) (**9**). The two peptides, linear and cyclic with non-sulfated Tyr were also prepared (linear **10** and cyclic **11**). Despite the presence of the sulfate moiety which is also present in the native carbohydrate epitope the peptides **8** and **9** did not interact with the immobilized monoclonal anti-HNK-1 antibody, possibly because the bulky side-chain of the tyrosine residue does not fit into the antibody. On the other hand, the corresponding non sulfated peptides LSETYTKdL (**10**) and c-(LSETYTKdL) (**11**) showed a weak, but significant binding interaction with the antibody (K_D = 1.92 x 10^{-4} and 6.90 x 10^{-5} M, respectively). Finally, the linear peptide bearing L-Leu instead of D-Leu, e.g. LSETETL (**11**) was also prepared and SPR experiments showed an affinity roughly one order of magnitude lower than that of the unmodified peptide **3** (K_D = 1.89 x 10^{-6} M). This result could confirm the beneficial effect of a D-Leu residue in the antibody interaction.[156]

Table 3.1. Sequences of the synthetic peptides and affinity binding constants[a] to the anti-HNK1 monoclonal antibody determined by SPR.

No	Sequence	k_a (1/Ms)	k_d(1/s)	K_D (M)
1	c-(LSETTdL)	$1.41 \cdot 10^{2}$	$1.55 \cdot 10^{-3}$	$1.09 \cdot 10^{-5}$
2	LSETTdL	$1.99 \cdot 10^{1}$	$43.6 \cdot 10^{-2}$	$2.18 \cdot 10^{-2}$
3	LSETETdL	$8.6 \cdot 10^{4}$	$0.9 \cdot 10^{-2}$	$1.04 \cdot 10^{-7}$
4	LSETETK(Ac)dL	$1.09 \cdot 10^{3}$	$50.2 \cdot 10^{-5}$	$4.62 \cdot 10^{-7}$
5	c-(LSETETK(Ac)dL)	$3.72 \cdot 10^{5}$	$40.7 \cdot 10^{-3}$	$1.09 \cdot 10^{-7}$
6	c-(LSETETKdL)	$1.05 \cdot 10^{2}$	$1.82 \cdot 10^{-3}$	$1.73 \cdot 10^{-5}$
7	c-(LSETKTdL)	$1.46 \cdot 10^{1}$	$6.30 \cdot 10^{-1}$	$4.33 \cdot 10^{-2}$
8	LSETY(OSO_3)TKdL	no interaction		
9	c-(LSETY(OSO_3)TKdL)	no interaction		
10	LSETYTKdL	$1.20 \cdot 10^{3}$	$23.0 \cdot 10^{-2}$	$1.92 \cdot 10^{-4}$
11	c-(LSETYTKdL)	$1.45 \cdot 10^{2}$	$1.0 \cdot 10^{-2}$	$6.90 \cdot 10^{-5}$
12	LSETETL	$5.16 \cdot 10^{2}$	$9.6 \cdot 10^{-4}$	$1.89 \cdot 10^{-6}$
13	Ttds-LSETETdL [b]	$8.5 \cdot 10^{2}$	$5.4 \cdot 10^{-4}$	$6.32 \cdot 10^{-7}$

[a] k_a: association rate constant, k_d: dissociation rate constant; K_D: equilibrium dissociation constant. [b] Ttds: 4,7,10-trioxa-1,13-tridecanediamino succinic acid.

The SPR affinity characterization of the synthetic peptides with the anti-HNK1 monoclonal antibody produced in mouse gave us the possibility to associate the structural motifs with the antibody recognition. Considering the results presented above, the linear sequence LSETETdL (**3**), a 7-mer peptide bearing 2 net negative charges, was selected as an optimized HNK-1 epitope mimetic, showing higher affinity than the peptides reported in prior studies.[156] It is noteworthy that the cyclic peptide c-(LSETETK(Ac)dL) (**5**), showed almost the same K_D values as compared to **3** (1.04 x 10^{-7} M and 1.09 x 10^{-7} M, respectively). This cyclic peptide, which bears also 2 net negative charges, contains an additional acetylated Lys residue, which may allow further

functionalization with spacers for being efficiently adsorbed on plastic plates in a solid-phase immunoenzymatic assay (SP-ELISA) (see Annexe V.1) in a future development of novel anti-HNK-1 antibody detection tools. For this reason, the peptide **5** could be considered as the cyclic counterpart of linear peptide **3**, since the simple head-to-tail cyclization of **3** would yield a peptide without a functional group available for subsequent covalent immobilization.

To sum up, the peptide probes **3** and **5** were selected by affinity and kinetics experiments in SPR as the best candidates to mimic the trisaccharide HNK-1**.** Moreover, in order to obtain a molecule with the best physico-chemical properties and because the fact that peptide **3** appear to be too short for an efficient adsorption on the SP-ELISA plastic plates[145], was modified by insertion in N-terminal position with a flexible and hydrophilic moiety, such as the PEG chain 4,7,10-trioxa-1,13-tridecanediamino succinic acid linker (Ttds, Figure 3.1).

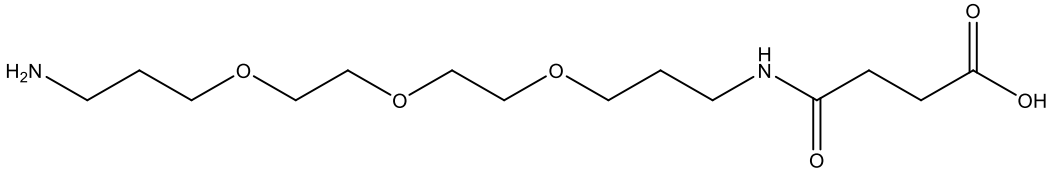

Figure 3.1: Structure of the spacer 4,7,10-trioxa-1,13-tridecanediamino succinic acid (Ttds).

The modified peptide Ttds-LSETETdL (**13**) was firstly tested in SPR experiments to verify if the introduced spacer affects the binding affinity to the antibody. Indeed, the K_D value (6.32×10^{-7} M) of the peptide **13** despite the presence of the N-terminal modification showed a negligible loss of affinity compared to the original sequence (**3**). Our research group had previously observed a weak decrease in affinity of antigenic peptides due to N-terminal modifications.[146] This could be explained by the introduction of a quite long chain that lead to the increase of steric hindrance, which however did not trouble the use of these peptides in ELISA. Thus, we tested in SP-ELISA the peptide Ttds-LSETETdL (**13**), which can be directly adsorbed on plastic plates.

II.2. SP-ELISA experiments

The properly modified peptide, Ttds-LSETETdL (**13**) was tested for its ability to detect the commercial anti-HNK-1 monoclonal antibody produced in mouse in SP-ELISA in an attempt to develop a novel anti-HNK-1 antibody detection tool (see Annexe V.1). In order to determine the optimal SP-ELISA conditions for the identification of anti-HNK-1 antibodies, using the monoclonal antibody, various conditions in terms of the type of the polymeric support of the ELISA plate, the amount of peptide per well, the coating buffer, the blocking buffer, and the concentration of the secondary antibody were evaluated. In particularly, we used the polyvinylchloride (PVC) plates at which the material used is polyvinyl and can be used to a wide variety of experiments. Furthermore, to select the appropriate blocking buffer we tested bovine serum albumin (BSA) buffer with concentration 1, 2.5, 5 and 10% in washing buffer and fetal bovine serum (FBS) with concentration 5%. The dilution of the secondary antibody in the washing buffer was tried 1:7500 and 1:4000. Two concentrations of the peptide antigen were tested: 1 μg/well and 5 μg/well. Once these series of experiments were completed, the considered as optimal conditions were: PVC plates using 1 μg/well peptide probe, 5% BSA as blocking buffer and 1:7500 dilution of the secondary antibody. Subsequently, the anti-HNK-1 monoclonal antibody was titrated by SP-ELISA at the established conditions. Titration results using the modified peptide **13**, shown in Figure 3.2, suggest that the peptide-based ELISA is able to identify commercial anti-HNK1 antibodies in a good range of concentrations. Moreover, when the same test was repeated using in parallel a BSA-coated plate the specificity of the signal obtained was confirmed but unfortunately the BSA gave a not negligible signal (Figure 3.3). For this reason, we tested two more different types of plates; the Polysorp® and Maxisorp® with polystyrene the polymeric support. The non-modified polystyrene surfaces are hydrophobic in nature and can only bind biomolecules through passive interactions. One drawback of hydrophobic immobilization is the denaturing effect it has on biomolecules as the unfold to expose hydrophobic regions that can interact with the interface. Specifically, he Polysorp® plates present high affinity to molecules with a hydrophobic nature while the Maxisorp® are adapted to mixed hydrophobic and hydrophilic domains. Using these plates the signal of

BSA was decreased but we were not able to repeat successfully the titration using the modified peptide **13** and the anti-HNK-1 monoclonal antibody.

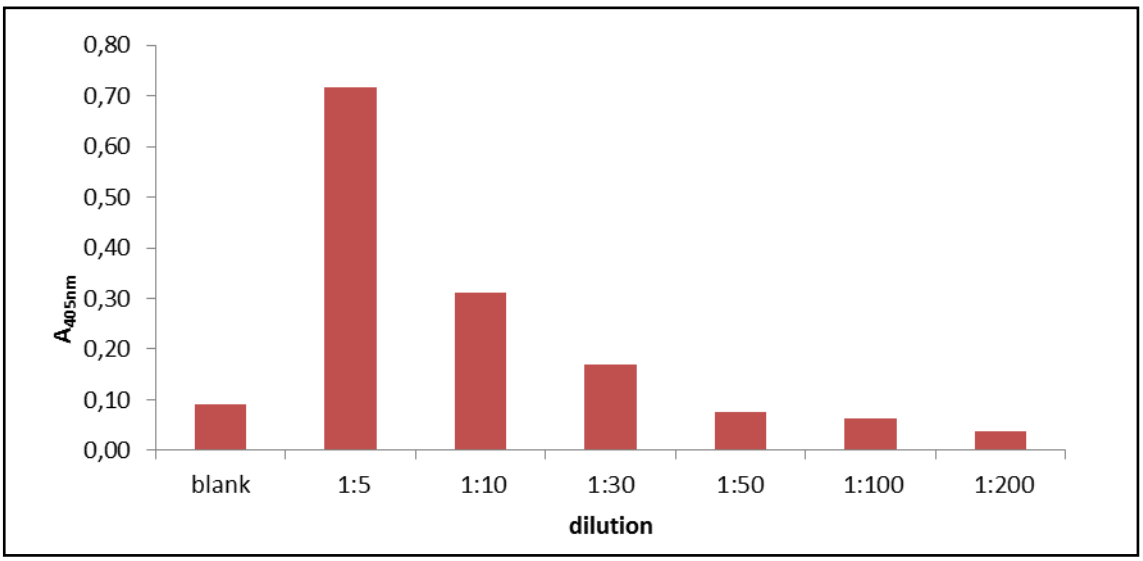

Figure 3.2: Anti-HNK1 monoclonal antibody titration in SP-ELISA with coated peptide 13. Blank is obtained using BSA buffer instead of the monoclonal antibody.

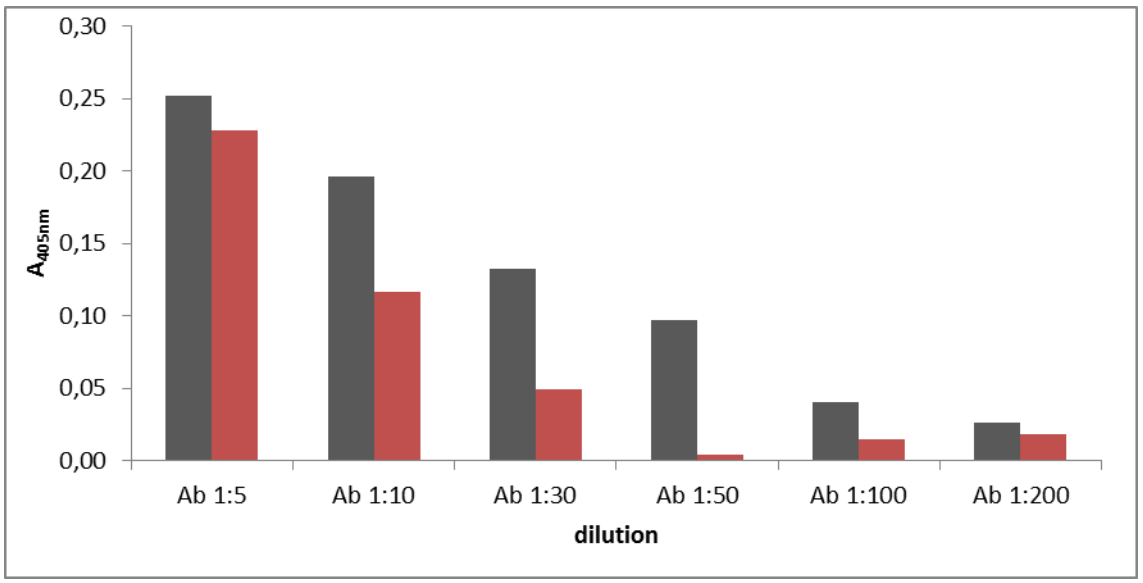

Figure 3.3: SP-ELISA with coated peptide 13. Blank is obtained using BSA buffer instead of the monoclonal antibody. ABS values of anti-HNK-1 monoclonal antibody (in grey), ABS values of anti-HNK1 monoclonal antibody – ABS values of blank (in red).

The final aim of this work is the development of a diagnostic tool for patients affected by autoimmune neurological disorders, characterized by the circulating anti-HNK-1 antibodies, such as IgM monoclonal gammopathy. Therefore, having in mind that this

simple synthetic peptide probe appears to be able to recognize specific anti-HNK-1 antibodies produced in mouse in SP-ELISA, we decided to go forward testing patient sera. Using the optimized conditions, we investigated the presence of Ab response against the synthetic antigen probe (peptide **13**) in 9 sera of patients affected by polyneuropathies with IgM monoclonal gammopathy showing high IgM level against HNK-1 in immunohistochemistry assay and 4 normal blood donors (NBD) sera. The preliminary results didn't show any specificity as the peptide was able to detect Abs also in NBD sera (Figure 3.4).

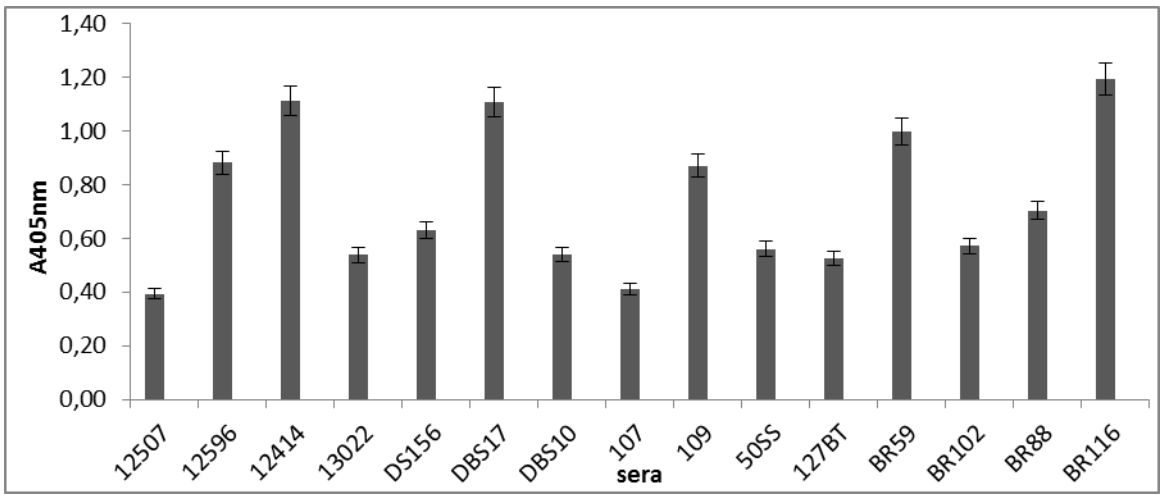

Figure 3.4: IgM response against the peptide 13 in 9 sera of patients affected by polyneuropathies with IgM monoclonal gammopathy and 4 NBD sera.

In the same time, the Ab response against peptide **13** was investigated in patients affected by other diseases like multiple sclerosis and type II diabetes. The results confirmed the non-specificity of the synthetic probe as high titers of Abs were measured independently from the patient (data not shown). The fact that the epitope recognition is not the same between mice and humans could be a possible explanation for these results.

II.3. Peptide Synthesis

All linear peptides were synthesized by a high-efficiency Solid Phase Peptide Synthesis (HE-SPPS) strategy, using a Liberty Blue™ automated microwave synthesizer (CEM) following the Fmoc/tBu methodology (see chapter 4, I). The syntheses were performed

on Fmoc-dLeu-Wang resin (0.7 mmol/g) for the linear peptides **2**, **3**, **4**, **8**, **10**, **13**, and Fmoc-Leu-Wang resin (0.7 mmol/g) for the peptide **12**. Peptides were cleaved from the resin and crude peptides obtained in a high yield of purity. To use them in SPR and ELISA experiments a final purity ≥95% was requested. For this reason, peptides were purified by semi-preparative RP-HPLC characterized by electrospray ionization mass spectrometry (ESI-MS) (see Annexes II, III). Analytical HPLC methods, retention times, and observed mass peaks for each peptide are summarized in the experimental part (Table 3.2).

Cyclic peptides were synthesized following the most common mode of cyclization, called head-to-tail on-resin cyclization. In this cyclization, the ring closure occurs by lactamisation via amide bond formation between the N-terminal amino group and the C-terminal carboxy group. Cyclic peptides have been under intense investigation by different research groups and for diverse purposes due to their reduced conformational flexibility and their resulting turn topology. In principle, cyclization can be performed in solution and on solid support (on-resin cyclization). Generally, peptides prepared in solution could be also cyclized in solution, whereas peptides prepared by SPPS may be cyclized either attached on the resin or in solution after cleavage of their linear precursors from the resin. There are no many significant differences between the two approaches and the choice of the method is a matter of opinion. Although, with the on resin approach one purification step is spared, resulting probably to a higher final yield. In both strategies the important principle that has to be applied is high dilution in order to avoid oligomerization reactions, as at higher concentration bimolecular reactions such as dimerization, trimerization or polymerization can occur. During a cyclization, side chain reactions may be formed. There are two possibilities to avoid these reactions. Firstly, when the cyclization step is performed on fully protected peptides the only site where cyclization can occur is between the N-terminal amino group and the C-terminal carboxy group. Secondly, the cyclization step can be performed by a selective chemical reaction such as disulfide bond formation or chemical ligation, where other functionalities present in the peptide do not interfere. In this case, the cyclization may be performed even on a deprotected peptide. Cyclization reaction is a quite demanding reaction and its yield depends on many factors like the ring size, the site of cyclization,

the number and the position of modified amino acids (D-amino acids, Pro residues etc.), the sequence characteristics of the linear precursor, and the nature of the side-chain protection. The ring size is a limiting factor for the reaction; the cyclization of heptapeptides or even larger precursors is straightforward while in shorter peptides the cyclization remains difficult and epimerization frequently occurs. Moreover, structure inducing elements, such as D-amino acids, can favor cyclization. Cyclization is usually a relatively slow process, and thus long reaction times are required. Reaction time as well as the coupling reagents used influence the degree of side-chain reactions and epimerization. Taking into account all the above mentioned problems, we decided to perform the cyclization reaction of the hexa- and hepta-peptides bearing a D-Leu residue on-resin using a three-dimensional strategy. Therefore, a special low loading resin Fmoc-Glu(Wang Resin)-OAll (0.33 mmol/g) was used to avoid dimerization problems. The resin and the permanent protections present on the amino-acid side chains offer the first dimension of orthogonality for which deprotection will be performed under acidic conditions. The base-labile Fmoc temporary group represents the second dimension, and the third one is provided by the allyl group. For the removal of the allyl group two different strategies were tested; either with 0.25 eq $Pd(PPh_3)_4$ in anhydrous DCM and 24eq Ph_3SiH as allyl-group scavengers[147,148] for 40 min (repeated twice with fresh solutions) or with 3 eq. $Pd(PPh_3)_4$ in 15 mL/g_{resin} mixture of DCM (dry)/ AcOH/ NMM (37:2:1) for 2 h under N_2. Allyl deprotection had to be performed before the deprotection of the N-terminal amino group[149]. Afterwards, the head-to-tail cyclization was possible after activation by HATU (5 eq), and then the linear peptide was cyclized on-resin with the use of Oxyma (5 eq) and NMM (5 eq). The end of the reaction was verified by Kaiser test after 1 h. The Dde protection of the side chain of Lys was removed with a solution of 2% hydrazine in DMF. For the peptides **4** and **5** the acetylation of the free side chain of Lys was performed with a solution of 10 eq acetic anhydride and 10 eq NMM. At the end, after cleavage from the resin and deprotection the desired cyclopeptides were obtained. The best method of allyl deprotection was the first one, where minimum quantity of the linear peptide remained allyl protected but without creating troubles during the purification process.

II.4. Conformational studies

The peptides **3** and **5** considered by SPR as the best candidates to mimic the cardohydrate HNK-1 by affinity and kinetics experiments were selected for further conformational studies (see Annexe IV). A CD analysis in water and HFA/water 30% solutions was performed. The figures below show the CD spectra of peptide **5** in the two solutions: both are very similar presenting a minimum at 204 nm and a shoulder at 222 nm characteristic of turn-helix structures (Figure 3.5a). This is an indication that the environment has little influence on the cyclic peptide structure. In contrast, the CD spectra of peptide **3** (Figure 3.5b) is different in HFA/water solution indicating an increase of the folded structure in the last medium. Spectra of peptides **3** and **5** in HFA/water solution are qualitatively comparable (Figure 3.5c) showing a similar conformation of the two peptides but dichroic intensity was reduced for peptide **3** pointing to a lower conformational stability.

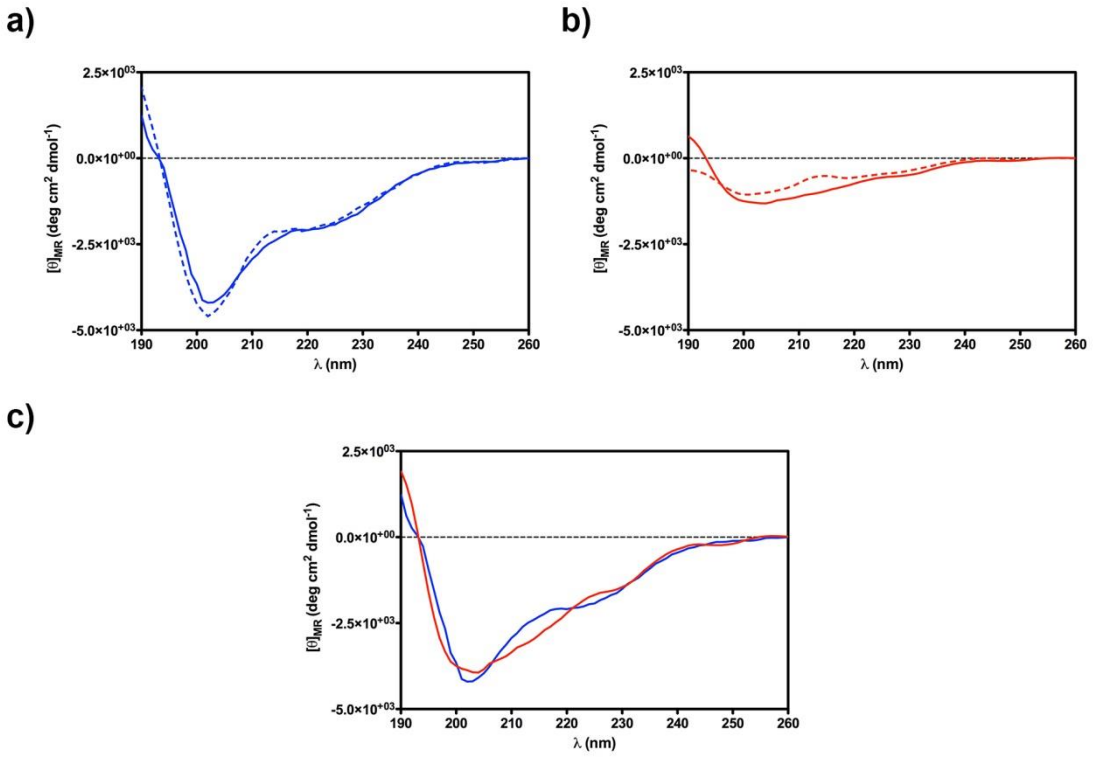

Figure 3.5: CD spectra of peptide 5 (a) and 3 (b) in water (dashed lines) or 30% HFA/water solution (solid lines) respectively. (c) Overlap of the CD spectra in HFA/water solution of 5 (blue) and 3 (red). For qualitative comparison, the last spectrum intensity was multiplied by three.

We then followed up with a detailed NMR conformational analysis of peptide **5** in HFA/water solution. Several NOE dipolar couplings observed in the NOESY spectrum of **5** pointed to the presence of turn-helical structures. In particular strong $d_{NN}(i,i+1)$ between Glu^3 and Thr^4 and between Thr^6 and $DLeu^8$, $d_{\alpha N}(i,i+2)$ between Ser^2 and Thr^4, and between Thr^4 and Thr^6, $d_{\beta N}(i,i+3)$ between Leu^1 and Glu^3, $d_{\beta N}(i,i+4)$ between Leu^1 and Thr^4, $d\gamma_N(i,i+3)$ between Thr^4 and Lys^7 were observed. Also, side chain to side chain NOEs were observed between Ser^2 and Glu^5. Using the NOE derived data as input, structure calculations by restrained simulated annealing gave the conformers of peptide **5** shown in Figure 3.7. Structures are well defined (backbone rmsd is 0.20 Å), and analysis of the ensemble dihedral angles provides the presence of four β-turns along residues 1-4 (type III), 2-5 (distorted type VIII), 4-7 (type III), and 5-8 (distorted type VIII). Interestingly, side chains of residues Ser^2 and Glu^5 are spatially close and, in many cases, an H-bond is observed between Ser^2 hydroxyl and Glu^5 carboxyl groups. Previous conformational studies on parent peptide **1**, revealed the existence of a β-turn around Ser^2-Glu^3-Thr^4-Thr^5 sequence.[150] In our peptide **5** (and **3**) a Glu residue replaced Thr^5 and the stable H-bond between the side chains of residues 2 and 5 (not reported for peptide **1**) could be one of the reasons for the increased affinity of peptide **5** (and **3**) for the antibody. Moreover, the other secondary structural elements of peptide **5**, not observed in peptide **1**, could be responsible of such binding improvement.

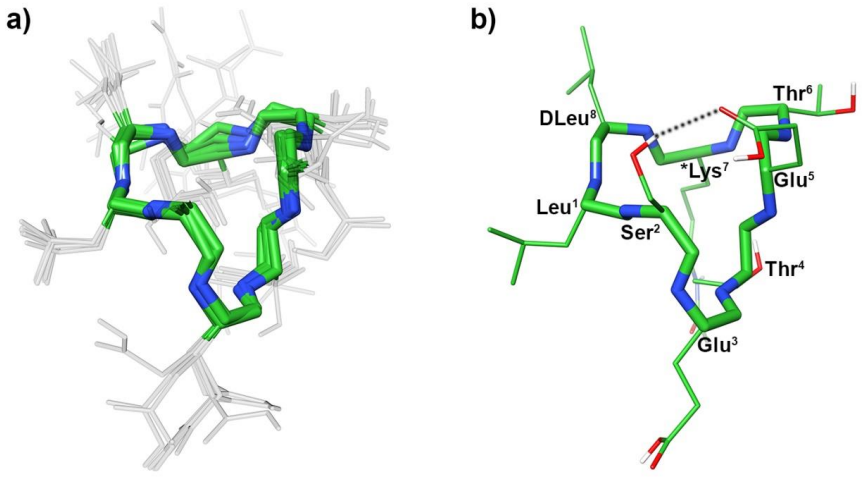

Figure 3.6: (a) Superposition of the ten lowest energy conformers of peptide 5. Structures were superimposed using the backbone heavy atoms. Side chains are shown in light grey. (b) Lowest energy conformer of 5: hydrogen bond between Ser^2 hydroxyl and Glu^5 carboxyl groups is shown as black dotted line. Heavy atoms have different colors (carbon, green; nitrogen, blue; oxygen, red; sulfur, yellow). Hydrogen atoms are hidden for a better view. *Lys: Acetyl-lysine.

III. Conclusions

Nowadays, identification and reproduction of conformational epitopes involved in antibody recognition, especially sugars, are more and more under investigation by different research groups. In this context, peptide molecules, mimicking carbohydrates, have to be designed to improve antibody affinity and specificity. Anti-MAG and anti-SGPG antibodies are already used in clinical practice to support the diagnosis of patients affected by PNS disorders. The trisaccharide HNK-1 epitope is present to both MAG and SGPS protein and substantial in the formation and maintenance of myelin sheath in the peripheral nervous system. Herein, HNK-1 is considered as the putative target of these antibodies circulating in patient sera. As the synthesis of the thisaccharide is not straightforward, we focused our study on the synthesis of a simple synthetic minimal peptide epitope mimicking this carbohydrate, which could be useful for the detection of anti-HNK-1 autoantibodies by immunoassays and setting up alternative diagnostic techniques for practical clinical use in PNS neuropathies. Therefore, we rationally designed a series of peptides mimicking the HNK-1 molecule that could be sufficient to ensure the specificity of antibody recognition. After screening a peptide library over the immobilized commercial monoclonal anti-HNK-1 antibody by SPR, we selected a cyclic heptapeptide bearing 2 net negative charges as the best mimetic of the HNK-1 epitope. Biological experiments by ELISA were performed to evaluate the effects of this analogue in the detection of autoantibodies in the sera of patients with IgM monoclonal gammopathy. The results confirmed the non-specificity of the synthetic probe as high titers of Abs were measured independently the patient. Moreover, conformational analysis gave possible explanations of the increased antibody affinity displayed by some novel analogues. This study even if the results we obtained are preliminary may hold promise in the development of novel diagnostic tools.

IV. Experimental part

IV.1. Synthesis of the antigens

The figure below describes step by step the synthetic strategy followed for the corresponding cyclic peptide of **13** with an acetylated Lys residue, i.e. **5**, or with the Ttds group. Firstly, the peptide was synthesized on a Fmoc-Glu(Wang resin)-OAll by a high-efficiency Solid Phase Peptide Synthesis (HE-SPPS) strategy, using a Liberty Blue™ automated microwave synthesizer (CEM) following the Fmoc/tBu methodology. Lys was protected with the Dde protecting group. After the Allyl and then the Fmoc-deprotection, the peptide was cyclized on the resin. Subsequently, the Dde was removed from the Lys and it was substituted by the Ttds or the Ac group. At the end, the side chain protection of the cyclic peptide was removed and the peptide was cleaved from the resin. Each step will be precisely described in the next paragraphs.

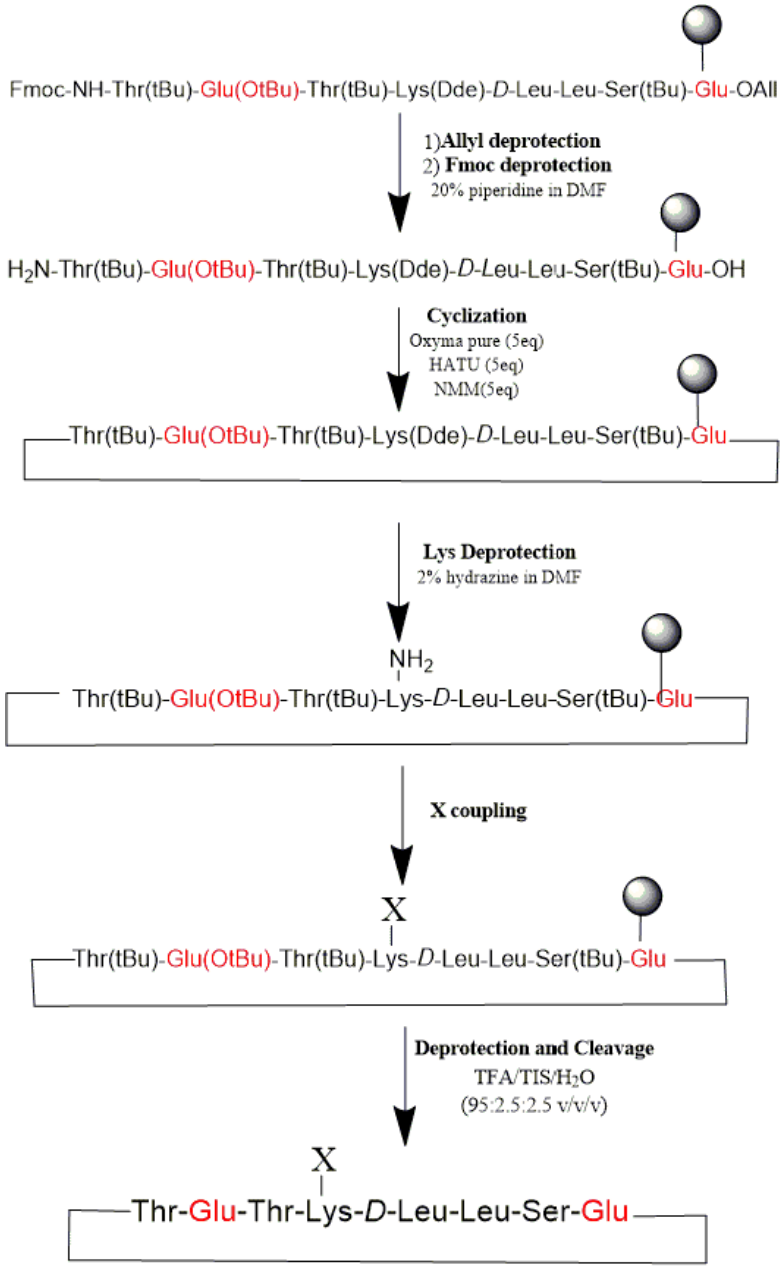

Figure 3.8: Synthetic scheme of the cyclic antigen (5) or the c(TETK(Ttds)dLLSE) using head-to-tail on resin cyclization, X refers to Ttds or Ac

IV.1.1. MW-assisted Solid Phase Peptide Synthesis (see Chapter 4.I)

The linear peptides were synthesized on a 0.1 mmol scale (5 eq of activator and amino acid) by a high-efficiency Solid Phase Peptide Synthesis (HE-SPPS) strategy, using a Liberty Blue^{TM} automated microwave synthesizer (CEM) following the Fmoc/tBu methodology. The syntheses were performed on Fmoc-Ile-Wang resin (0.7 mmol/g) for the linear peptide **3**, Fmoc-dLeu-Wang resin (0.7 mmol/g) for the linear peptides **1**, **6**, **8**, **10**, **13**, Fmoc-Glu(Wang resin)-OAll (0.21 mmol/g) for the cyclic peptides **2**, **4**, **5**, **7**, **9**, **12** and Fmoc-Leu-Wang resin (0.7 mmol/g) for the peptide **11**. The resins were swelled with DMF (1mL/100mg of resin) for 20 min.

A general protocol for the MW-assisted Solid Phase Peptide Synthesis as well as for the cleavage of the peptides from the resin and their purification is described in Materials and Methods (see Chapter 4.I). The spacer Fmoc-Ttds-OH was coupled with the MW synthesizer as a normal amino acid.

IV.1.2. Cyclization on the resin

Removal of allyl protecting group

Protocol N^{o}1

Peptide-resin bearing the allyl protecting group was swollen in anhydrous DCM under atmosphere for 20 min. Then $Pd(PPh_3)_4$ (3 eq) in a solution of dry DCM/AcOH/NMM (37:2:1) was added (15 mg/g of resin) and the resin was shaken for 2 h at room temperature. The reaction is air-sensitive and all manipulations were carried out under Ar. Finally, the resin was transferred to a syringe and was filtered and washed consecutively with 0.5% *N,N*-Diisopropylethylamine (DIPEA) in DMF and 0.5% sodium diethyldithiocarbamate in DMF to remove the catalyst.

Protocol N^{o}2

Peptide-resin containing the allyl protecting group was swollen in anhydrous DCM under argon atmosphere for 20 min. The resin was shaken for 5 min with a solution of $PhSiH_3$ (24 eq) in dry DCM. Then a solution of $Pd(PPh_3)_4$ (0.25 eq) in dry DCM was added for the allyl group cleavage (1mL of total volume for 100mg of resin). After 40 min the resin was

filtered and washed with dry DCM. The treatment with $PhSiH_3$/ $Pd(PPh_3)_4$ was repeated once again. Finally the resin was filtered and washed successively with DCM, a solution of 0.5% sodium diethyldithiocarbamate in DMF, DMF and DCM.

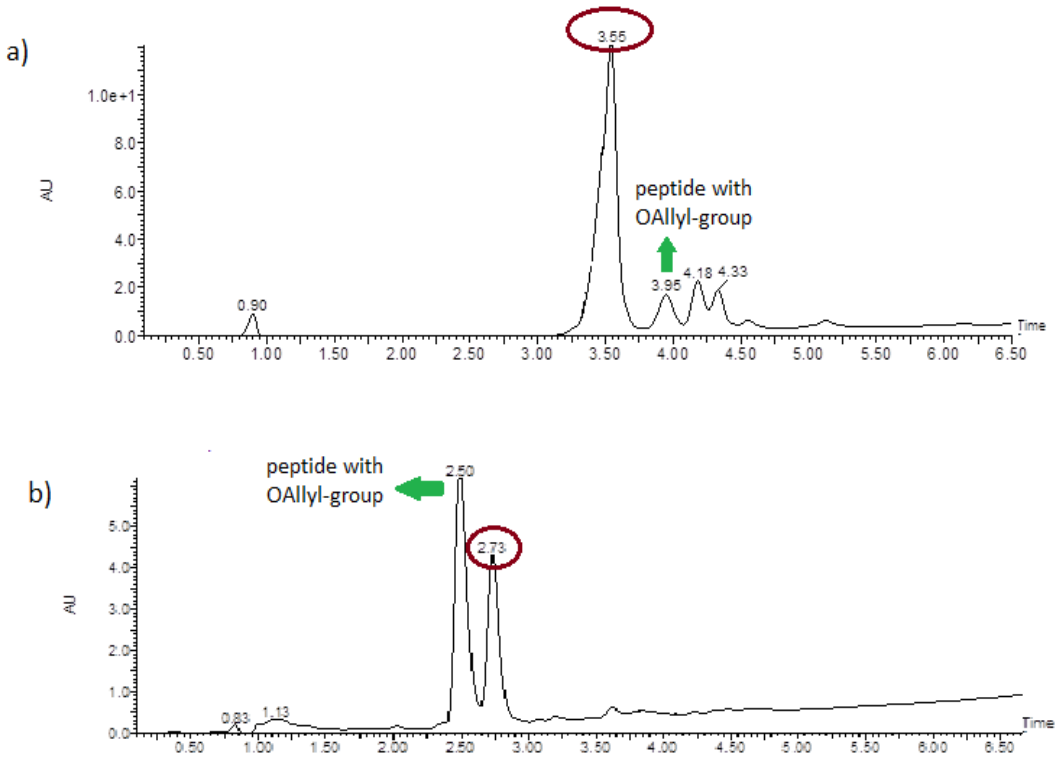

Figure 3.7: HPLC chromatograms after the Allyl deprotection of the TETK(Dde)dLLSE, precursor of c(TETK(Ttds)dLLSE). a) protocol N°1, b) protocol N°2. The desired peptide peaks are indicated in red cycle.

Analytical HPLC conditions: column, BIOshell™ A160 Peptide C18 (2.7µm, 10cm × 30mm); solvent systems, A: 0.1% TFA in H_2O, B: 0.1% TFA in CH_3CN; flow rate 0.6 mL min $^{-1}$.

Gradient a) 35–70% B in 5 min, b) 30–70% B in 5 min

As we can observe in the Figure 3.7, the best results for allyl deprotection were obtained when the first protocol was followed. Even if the reaction using the second protocol was repeated two more times, a percentage of the protected peptide with the Allyl group remained.

Cyclization

Previously (see Chapter 3, II.3) we extensively discussed the reason why the on-resin head-to-tail cyclization has to be preferred. Although attempts of cyclization in solution with the use of the 2-chlorotrityl chloride resin were performed, the yield of the reaction was low and the monitoring and the work up difficult. In both cases the final Fmoc-deprotection was achieved.

Cyclization on solid phase

The resin was swollen in DMF and coupled with Oxyma (5 eq), HATU (5 eq) and NMM (5 eq). After shaken for 1.5 h, the resin was filtered and washed successively with DMF and DCM. The reaction completion was verified by Kaiser Test.

Cyclization in solution

Peptides were firstly cleaved from resin with a solution of TFE/DCM (3:7) at r.t. for 3 h. The solution was evaporated and the peptide was lyophilized. In the case of the head-to-tail cyclization in solution different reagents were tried in different dilutions in order to avoid the formation of the dimer. Here are reported the optimized conditions. A solution of the side-chain protected peptide diluted in the minimum quantity of DMF and TBTU (3 eq) was added dropwise in a solution of collidine (6 eq), HOAt (3 eq) and DCM (~ 5 mL/mg peptide). The reaction was stirred overnight at r.t.. Finally the solution was evaporated and the peptide was lyophilized.

Acetylation and coupling of Ttds group

Firstly the Dde protecting group was removed from the side chain of Lys with a solution of 2% hydrazine in DMF (25 mL/g resin) at r.t. for 3min. The resin was filtered and the treatment with hydrazine was repeated two more times. At the end the partially protected resin was washed several times with DMF and DCM. For the peptide **13** and the corresponding cyclic one, i.e c(TETK(Ttds)dLLSE), which were modified with a Ttds group, the coupling reaction was performed adding on the peptide-resin a solution of 5 eq Fmoc-Ttds-OH, 5 eq HATU and 7 eq NMM in DMF. The reaction was stirred for 40 min at r.t.. While for the peptides **4, 5**, modified with an acetyl group at the side chain of Lys,

the acetylation was performed adding on the peptide-resin a solution of acetic anhydrite (10 eq) and NMM (10 eq) in DMF. After shaken for 1 h, the resin was filtered and washed successively with DMF and DCM. The completion of both reactions was verified by Kaiser Test.

The following figure describes step by step the synthesis of a corresponding cyclic peptide of **13** with an acetylated Lys residue or with the Ttds group. Firstly, the peptide was synthesized on a Fmoc-Glu(Wang resin)-OAll, as descrided above having the Lys protected with the Dde protecting group. After the Allyl and the Fmoc-deprotection, the peptide was cyclized on the resin. Furthermore, the Dde was removed from the Lys and it was substituted by the Ttds or the Ac group. At the end, the side chain protection of the cyclic peptide was removed and the peptide was cleaved from the resin.

Subsequently, the peptides were cleaved from the resin and their purification and characterization (see Annexes II, III) were followed. The analytical data are reported in Table 3.2. Data were acquired and processed using MassLynx software (Waters, Milford, Massachusetts, USA).

Table 3.2. Sequences of the synthetic antigens and analytical data

No	Antigen	HPLC Rt (min)	ESI-MS $[M + H]^{2+}$ (m/z) found (calcd)
1	**LSETTdL**	3.37[a]	663.42 (663.75)
2	**c-(LSETTdL)**	4.71[b]	645.53 (645.75)
3	**LSETTI**	3.37[a]	663.42 (663.75)
4	**c-(LSETTI)**	4.71[b]	645.52 (645.75)
5	**c-(LSETKTdL)**	4.26[b]	773.67 (773.93)
6	**LSETYTKdL**	4.14[b]	955.02 (955,10)
7	**c-(LSETYTKdL)**	4.77[b]	937.02 (937.10)
8	**LSETY(OSO3)TKdL**	4.32[b]	1035.04 (1035.10)
9	**c-(LSETY(OSO3)TKdL)**	4.43[b]	1017.04 (1017.10)
10	**LSETETdL**	3.37[c]	792.13 (792.36)
11	**LSETETL**	3.98[c]	744.26 (744.36)
12	**c-(LSETETKdL)**	4.15[b]	902.82 (903.04)
13	**LSETETK(Ac)dL**	3.63[c]	962.35 (961.5)
14	**c-(LSETETK(Ac)dL)**	3.15[d]	944.36 (944.5)

Analytical HPLC conditions: column, BIOshell™ A160 Peptide C18 (2.7µm, 10cm × 30mm) and Phenomenex Kinetex C-18 column 2.6µm (100 × 3.0 mm); solvent systems, A: 0.1% TFA in H_2O, B: 0.1% TFA in CH_3CN; flow rate 0.6 mL min^{-1}. Gradient [a]20–60% B in 5 min, [b]10–60% B in 5 min, [c]15–50% B in 5 min , [d]25-50% B in 5 min, [e]isocratic 23%B in 5 min, [f]75–95% B in 5 min.

IV.2. SPR studies

IV.2.1. Anti-HNK-1 antibody immobilization

Antibody was covalently linked according to the amine-coupling strategy. Immobilization buffer was selected to obtain the electrostatic pre-concentration of the antibody on CM5 chip surface, using the following buffers: D-PBS buffer pH 6 and 7.2, AcNa 5 mM pH 6 and 5, AcNa 0.5 mM pH 5.5 and 6.5, AcNa 0.1 mM pH 6 and 7, NaCl 5 mM pH 6. Chip surface was activated with two injections of *N*-hydroxysuccinimide (NHS 0.1 M) and 1-ethyl-3-(3-dimethylaminopropyl)-carbodiimide (EDC 0.4 M) 50:50 for 420 and 60 seconds at a flow rate of 10µl/min to give reactive succinimide esters; antibody solubilized in the previously selected immobilization buffer [5 µg/mL], was injected for 420 seconds at a flow rate of 5 µl/min. Immobilization was continued in manual mode by changing ligand concentration and contact time to reaching a satisfactory immobilization level around 730RU. Non-reacted sites on sensor chip surface were blocked with ethanolamine-HCl 1 M pH 8.5 for 420 and 60 seconds at a flow rate of 30 µL/min. Reference channel was activated injecting NHS/EDC 50:50 and directly blocked with ethanolamine-HCl.

IV.2.2. Kinetic and affinity experiments

Once the antibody was immobilized on the chip, kinetic studies were started. Peptides were tested at 3 different concentrations (2.0, 3.0 and 3.5 mM) in running buffer and injected in a different cycle of analysis. Each diluted peptide was injected over the immobilized antibody for 80 seconds at a flow rate of 30µl/min, dissociation was followed for 120 seconds by injecting running buffer and finally the chip surface was regenerated with an injection of NaOH 0.1 M for 60 seconds. Experimental data were recorded and further elaborated with Bia Evaluation Software 2.0 and the kinetic parameters and the affinity constants were calculated according to a 1:1 binding model optimized for small analytes.

IV.3. ELISA experiments

1 µg/well of antigen (peptide or protein) was dissolved in EtOH, then 100µL of solution were dispensed in each well of 96-well PVC plates were incubated overnight at room temperature. Subsequently, plates were washed 3 times with 0.9% NaCl, and blocked 1 h at room temperature with 100 µL/well of bovine serum albumin (BSA) Buffer [5% BSA in Washing Buffer (0.9% NaCl, 0,01% Tween 20)]. BSA Buffer was removed, and 100 µL/well of diluted monoclonal anti-HNK1 antibody in BSA Buffer were dispensed. Blank wells were included in all the plates, and were obtained using BSA Buffer instead of the monoclonal Ab. Plates were incubated at 4 °C overnight, then washed 3 times with Washing Buffer. 100 µL/well of secondary antibodies diluted in 2,5% BSA Buffer (goat anti-mouse IgM 1:7500) were dispensed, and plates were incubated 3 h at room temperature. Plates were washed 3 times with Washing Buffer, then 100 µL/well of p-NitroPhenyl Phosphate Substrate Solution (1mg/mL p-NPP in Substrate Buffer: 10 mM $MgCl_2$, 12 mM Na_2CO_3, 35 mM $NaHCO_3$, pH 9.6) were dispensed. Plates were incubated at room temperature, and then the absorbance (ABS) of each well was red with a multichannel ELISA reader (Tecan Sunrise, Männedorf, Switzerland) at 405 nm. ABS value for each serum was calculated as (mean ABS of triplicate) – (mean ABS of blank triplicate).

IV.4. Conformational Studies

All conformational studies for the peptides **3** and **5** were performed at "Università degli Studi di Napoli Federico II", Department of Pharmacy in cooperation with Prof. Alfonso Carotenuto.

IV.4.1. Circular Dichroism Studies

CD spectra (Figure 3.5) were recorded using a JASCO J710 spectropolarimeter at 20 °C between λ=260–190 nm (1mm path, 1 nm bandwidth, 4 accumulations, and 100 nm min^{-1} scanning speed). Measurements were performed with peptides in H_2O (0.100 mM, pH 7.4) or in HFA/water 30% solution.

IV.4.2. NMR Studies

The samples for NMR spectroscopy were prepared by dissolving the appropriate amount of peptide **5** in 0.30ml of ^1H_2O (pH 5.5), 0.05ml of ^2H_2O and 0.15ml of HFA to obtain a 2mM concentration of peptide. NMR spectra were recorded on a Varian INOVA 700 MHz spectrometer equipped with a z-gradient 5 mm triple-resonance probe head. All the spectra were acquired at a temperature of 25 °C. The spectra were calibrated relative to TSP (0.00 ppm) as internal standard. One-dimensional (1D) NMR spectra were recorded in the Fourier mode with quadrature detection. The water signal was abolished by gradient echo[151]. 2D DQF-COSY,[152,153] TOCSY,[154] and NOESY[155] spectra were recorded in the phase-sensitive mode using the method from States[156]. Data block sizes were 2048 addresses in t_2 and 512 equidistant t_1 values. Before Fourier transformation, the time domain data matrices were multiplied by shifted sin^2 functions in both dimensions. A mixing time of 70 ms was used for the TOCSY experiments. NOESY experiments were run with mixing times in the range of 100-200 ms. The qualitative and quantitative analyses of DQF-COSY, TOCSY, and NOESY spectra, were obtained using the interactive program package XEASY[157]. $^3J_{HN\text{-}H\alpha}$ coupling constants were obtained from 1D ^1H NMR and 2D DQF-COSY spectra. ^1H NMR chemical shift assignments were effectively achieved according to the Wüthrich procedure.[158]

IV.4.3. Structure Calculation

The NOE-based distance restraints were obtained from NOESY spectra acquired with a mixing time of 200 ms. The NOE cross peaks were integrated with the CARA program and were converted into upper distance bounds using the CALIBA program incorporated into the program package DYANA[159]. Only NOE derived constraints were considered in the annealing procedures. NMR-derived upper bounds were imposed as semiparabolic penalty functions with force constants of 16 Kcal mol-1 $Å^{-2}$. A distance maximum force constant of 1000 Kcal/ mol^{-1} $Å^{-2}$ was used. Cyclic peptide **5** was built using the Insight Builder module (Accelrys Software Inc., San Diego). Atomic potentials and charges were assigned using the consistent valence force field (CVFF)[160]. The conformational space of compound was sampled through 100 cycles of restrained simulated annealing (ε = 1r). In simulated annealing, the temperature is altered in time increments from an initial temperature to a final temperature by adjusting the kinetic energy of the structure (by rescaling the velocities of the atoms). The following protocol was applied: the system was heated up to 1500 K over 2000 fs (time step = 1.0 fs); the temperature of 1500 K was applied to the system for 2000 fs (time step = 1.0 fs) with the aim of surmounting torsional barriers; successively, temperature was linearly reduced to 300 K in 1000 fs (time step = 1.0 fs). Resulting conformations were then subjected to restrained Molecular Mechanics (MM) energy minimization within Insight Discover module (ε = 1r) until the maximum RMS derivative was less than 0.001 kcal/Å, using Conjugate Gradient as minimization algorithm. Finally, conformations were subjected to 1000 steps of unrestrained MM Conjugate Gradient energy minimization. From the produced 100 conformations, 10 structures, whose interproton distances best fitted NOE derived distances, were chosen for statistical analysis. The final structures were analyzed using the InsightII program (Accelrys, San Diego, CA). Molecular graphics images of the complexes were realized using the UCSF Chimera package

CHAPTER 4

Materials and methods: General Protocols

I. General Protocols

I.1. Microwave Solid Phase Peptide Synthesis

The peptides were synthesized on a 0.1 mmol scale (5 eq. of activator and amino acids) by a high-efficiency Solid Phase Peptide Synthesis (HE-SPPS) strategy, using a Liberty Blue™ automated microwave synthesizer (CEM) following the Fmoc/tBu methodology. The reactions were performed in a Teflon vessel and mixed by N_2 bubbling. Reaction temperatures were monitored by an internal fiber-optic sensor.

Figure 4.1: Liberty Blue™ automated microwave synthesizer (CEM).

At the beginning of the synthesis the resins were swelled with DMF (1 mL/100mg of resin) for 20 min.

A general coupling cycle was initiated with a double deprotection step with 20% piperidine in DMF, for 15 sec at 75 °C using 155W followed by 50 sec with a fresh deprotection solution at 90 °C reached with 30W. Three washes with DMF and N_2 bubbling were performed. Fresh stock solutions of the Fmoc-protected amino acids (0.2 M), Oxyma (1 M) and DIC (0.5 M) in DMF were prepared in separated bottles and used as reagents during the SPPS. The MW-SPPS protocol, consisted of two coupling steps (standard coupling), performed firstly at 75 °C for 15 sec using 170W and then at 90 °C for 110 sec using 30W. The same coupling conditions were used for all amino acids except from Arg, His and Cys residues for which specific parameters were required. Arg double coupling MW method comprised a 25 min at 25 °C coupling step and afterwards a second one for 2 min at 75 °C using 30 W. For the His and Cys couplings a longer coupling time (7 min) was utilized, at room temperature for the first 2 min followed by 5

min at 50 °C using 35W. One wash was performed after the coupling step with DMF and N_2 bubbling. A standard cycle time (deprotection, washes DMF (3x), coupling, wash DMF (1x)) was slightly longer than 4 min.

Table 4.1. MW-assisted SPPS protocol

	Power (W)	Time (sec)	Temperature (°C)
Standard coupling	170 30	15 110	75 90
Cys, His coupling	0 35	120 300	25 50
Arg coupling	0 30	1500 120	25 75
Deprotection	155 30	15 50	75 90

I.2. Deprotection and Cleavage

Cleavage from the resin and side-chain deprotection were achieved by treatment with a TFA/TIS/EDT/water solution (94:1:2:2 v/v/v/v, 1mL/100 mg of resin-bound peptide) for the peptides containing Met and Cys residues and with a TFA/TIS/water solution (95:2.5:2.5 v/v/v, 1 mL/100 mg of resin-bound peptide) for the rest. The cleavage was carried out approximately for 5 h with vigorous shaking at room temperature. The resin was filtered and the filtrate was concentrated by flushing with N_2. The crude peptides were precipitated from the cleavage mixture by addition of ice-cold Et_2O, centrifuged, washed with ice-cold Et_2O (x3), dried and lyophilized.

I.3. Purification and characterization of the peptide antigens

Lyophilized crude peptides were pre-purified by solid-phase extraction with a RP-18 LiChroprep silica column from Merck (Darmstadt, Germany) via Armen system (ARMEN GLIDER FLASH AGF/IMbO6, Saint-Avé, France) working at 20mL/min using as solvent system H_2O (MiliQ) (A)/CH_3CN (B). The final purification of the peptides was performed by semi-preparative Waters RP-HPLC on a Phenomenex Jupiter C18 (10µm, 250mm × 10mm) column (Phenomenex, Castel Maggiore, Italy) at 4 mL/min. The solvent systems used were 0.1% TFA in H_2O (A) and 0.1% TFA in CH_3CN (B) combined with different gradients. All peptides were obtained with a purity >95%.

Characterization of the peptides was performed by analytical Waters Alliance RP-HPLC (model 2695) with UV detection at 215 nm, coupled with an ESI-MS detector (Micromass ZQ, Waters, Milford Massachusetts, USA) using a Kinetex C18 (2.6µm × 100mm) column at 35 °C, with a flow rate of 0.6 mL/min. The total run time of the analysis was 5 min and the solvent systems used were: 0.1% TFA in H_2O (A) and 0.1% TFA in ACN (B). Data were acquired and processed using MassLynx software (Waters, Milford, Massachusetts, USA).

II. Materials

II. 1. Materials for Peptide Synthesis and Purification

All Fmoc-protected amino acids, Fmoc-Wang resins, DIC and Oxyma were purchased from Iris Biotech GmbH (Marktredwitz, Germany). The following amino acid side-chain-protecting groups were used: OtBu (Asp, Glu), tBu (Ser,Thr), Pbf (Arg), Trt (Gln, His) and Boc (Lys). Peptide-synthesis grade *N,N*-dimethylformamide (DMF) was purchased from Scharlau (Barcelona, Spain); acetonitrile (ACN) from Carlo Erba (Milan, Italy); dichloromethane (DCM), trifluoroacetic acid (TFA), piperidine were purchased from Sigma-Aldrich (Milan,Italy). The scavengers for cleavage of peptides from resin, 1,2-ethanedithiol (EDT) and triisopropylsilane (TIS) were purchased from Acros Organics (Geel, Belgium).

II.2. Materials for biological tests

SP-ELISA experiments were performed using 96 wells plates NUNC Maxisorp and Polysorp (Sigma-Aldrich, St. Louis, USA). Washing steps were performed with Hydroflex Microplate Washer (Tecan, Männedorf, Switzerland). Fetal bovine serum was purchased by Euroclone (Milan, Italy). Anti-mouse IgG and IgM alkaline phosphatase conjugates were purchased from Sigma Aldrich (Milano, Italy). BSA Anti-mouse IgG and IgM alkaline phosphatase conjugates were purchased from Sigma Aldrich (Milan, Italy). p-Nitrophenyl phosphate was purchased from Fluka (Milano, Italy). Absorbance values were measured on a Sunrise Tecan ELISA plate reader purchased from Tecan (Tecan Italia, Milano, Italy). Electrocompetent ER2566 *E.coli* cells were purchased from New England Biolabs (Ipswich, MA, USA). Plasmid pET-22 was purchased from Novagen (Madison, WI, USA). Protein purification and refolding were performed using a Chelating Sepharose Fast Flow column on ÄktaBasic chromatography system (GE Healthcare, Milano, Italy). The far-UV circular dichroism spectra were recorded by using a J-810 Jasco spectropolarimeter (JASCO, Easton, MD). C57BL/6 mice were purchased from Harlan (Jerusalem, Israel).

ANNEXES

I. Principles of Peptide Synthesis

During the past decades, peptide chemistry was considerably developed due to the significant involvement of the peptides into the physiological and biochemical functions of life. Nowadays, more than one hundred peptides, having a crucial role in the central and peripheral nervous systems, in immunological processes, in the cardiovascular system, and in the intestine, are known. Peptides are involved in a number of biochemical processes, like metabolism, pain, reproduction and immune response and their interaction with receptors influence cell-cell communication.[161] Furthermore, peptides could not only serve as antigens to raise antibodies from sera as it was already mentioned above but also as enzyme substrates to map the active site requirements of an enzyme under investigation, or as enzyme inhibitors to influence signaling pathways in biochemical research or pathologic processes in medical research. According to an approach called "peptide dissection approach" short peptide fragments that are part of a protein could be used and their ability to fold independently could be investigated providing us information about the folding of the protein. Despite the abundance of peptide functionalities, their isolation from natural sources is still problematic; a fact that led to the development of the peptide chemistry.

The methods of peptide synthesis could be divided conveniently into two categories: solution and solid-phase. Classical solution peptide chemistry involves the preparation of fully protected peptide segments and their subsequent condensation in organic solvents for the convergent synthesis of large polypeptides. In solid-phase peptide synthesis (SPPS), suitably *Nα*- and side-chain protected amino acids are coupled sequentially to a growing peptide chain attached to a solid support (resin) in the C--> N direction. The desirable peptide is then cleaved from the resin, typically under acidic conditions. SPPS has numerous advantages over the classical solution procedure, such as automation of the elongation reaction, independence from solubility problems, and minimization of side product formation. On the other hand, in the classical solution procedure, the products can be monitored and purified at each step in the reaction, potentially leading to easier isolation of the desired final peptide. The synthesis of the peptides described during this thesis was performed by SPPS.[162]

The term “orthogonal” was coined by Barany and Merrifield in 1977[163] to designate “classes of protecting groups which are removed by differing chemical mechanisms. Therefore, they can be removed in any order and in the presence of the other classes. Orthogonal protection schemes allow milder overall reaction conditions as well as the synthesis of partially protected peptides”. The most popular and truly orthogonal combination of protecting groups is the Fmoc/tBu methodology. The (9H-fluoren-9-ylmethoxy)carbonyl (Fmoc) protecting group is usually removed in basic conditions (20% piperidine in DMF) at room temperature while deprotection of the side chain protecting groups is performed in acidic conditions (TFA). During the Fmoc-deprotection of the amino function with piperidine, the released byproduct dibenzofulvene-piperidine has a distinct absorbance detectable at 301 nm. Thus, the synthesis can be well monitored by reading the UV absorbance of the piperidine-dibenzofulvene adduct in solution.[39,40]

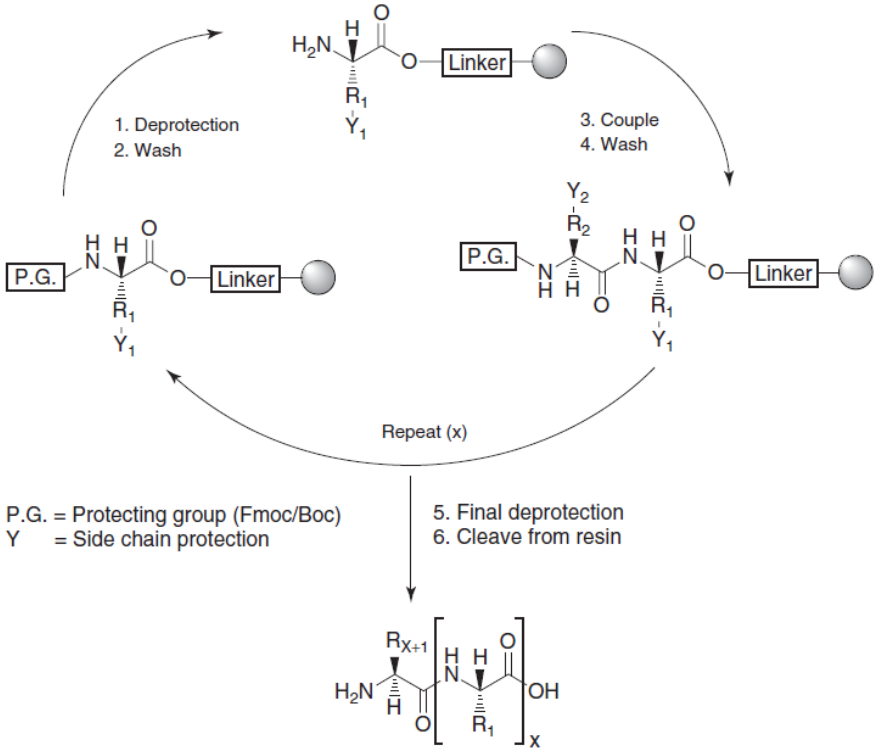

Figure A.1: Solid-phase peptide synthesis cycle.

The formation of an amide bond between a carboxylic acid moiety and an amino function of two amino acids is the basic reaction in peptide synthesis. Over the years, many activation methods have been developed, such as the carboxylic azides, symmetrical or mixed anhydrides or the use of carbodiimides (DCC, DIC, EDC) with or

without additives. Carbodiimides have been used as activators for decades in solid-phase and solution peptide synthesis. Though in recent years two classes of coupling reagents are used more and more, the phosphonium- and the aminium-(imonium-) type reagents such as BOP, PyBOP, PyBrOP, oxyma pure, TBTU, HBTU, HATU and COMU. The advantages of these compounds are the high coupling rates accompanied by few undesired side reactions. In contrast to activation by carbodiimides, peptide couplings using the latter compounds require the presence of a base. Diisopropylethylamine (DIPEA) and N-methylmorpholine (NMM) are the most frequently used ones in Fmoc/tBu-based solid-phase synthesis.

During the SPPS several problems could be raised associated with the amino acids and the peptide sequence, the choice of the strategy to be followed (Fmoc / tBu or Boc / Bzl), the selection of the individual protecting groups of the side chains and the cleavage of the peptide from the resin. Some of them are studied below:

- Racemization

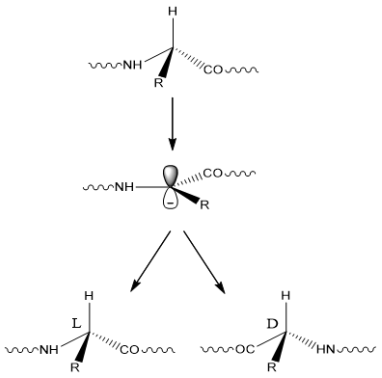

Figure A.2: Schematic configuration of racemization of an alpha-carbon atom.

The alpha-carbon atom of natural amino acids is optically active (L-amino acids). The preservation of the stereochemical arrangement of amino acids during peptide synthesis is very important as long as the function of peptides is completely dependent on their stereochemistry. Unfortunately, the optical purity of the Cα-atom is not easily maintained, resulting in each coupling reaction to produce two products. Many efforts aim to keep the steric arrangement of the Cα-atom of the amino acids during peptide synthesis in order to improve the peptide synthesis. The racemization of the amino acids

is affected by posting the Hα proton to form a carbanion in the presence of base. Aromatic amino acids such as phenylalanine, tyrosine and also histidine, valine and cysteine are particularly susceptible to racemization.[164,165]

To limit as much as possible the racemization some general rules have to be followed:

- Avoid using large excess of base. Use of tertiary amines with high steric hindrance.
- Avoid use of solvents with high polarity.
- Acceleration of the coupling reaction.

➢ Formation of diketopiperazine[166]

Sometimes the coupling of an amino acid or a peptide to a dipeptide can create troubles. The esters of dipeptides undergo spontaneous cyclization and produce 2,5-diketopiperazines. On diketopiperazines both amide bonds are *cis* while, as previously reported for the peptide bond, the C-N bond is mainly *trans*. The driving force for this reaction is the formation of the highly stable diketopiperazine ring. The reaction is especially favored in the peptides containing glycine and proline and is also the case where an amino acid is L and the other D. High concentrations of reactants increase the speed of the desired coupling reaction and reduce the degree of cyclization.

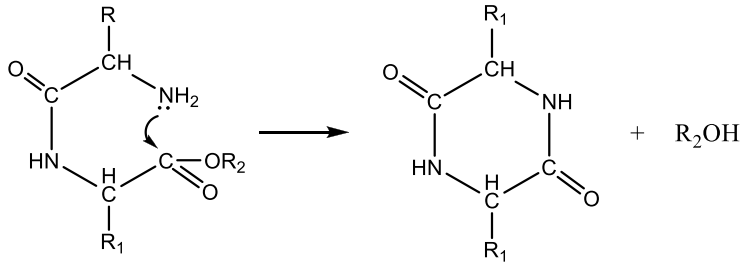

Figure A.3: Schematic configuration of diketopiperazine formation.

➢ Formation of Nitrile

Upon activation of Asn and when it is not protected at the side amide nitrile may be formed. To avoid it, preactivated esters, such as Fmoc-Asn-OPfp, are used.

- Formation of S-lactam

During activation, it is possible that the N^{δ} of Arg attacks the activated carboxyl group and forms a S-lactam (especially when we use a symmetrical anhydride, while HOBt prevents this formation).

- Formation of aspartimide

The most common side reaction that occurs once we use Asp(OtBu) is the formation of aspartimide. When the nitrogen which is bonded with α carboxyl group of Asp attacks the side ester bond it leads to a cyclic five carbon pentamer imide derivative. This intermediate leads to ring opening during the deprotection with piperidine to successively form the corresponding alpha- and beta-aspartylamides or to remain until the cleavage of the peptide from the resin and to be subsequently hydrolyzed to the corresponding alpha- and beta-aspartyl peptides. This secondary reaction depends on the sequence of the peptide, but is common especially with the motif Asp (OtBu)-X, wherein X is Asn(Trt), Gly, Ser, Thr, or Arg(Pmc). In such cases, it is suggested to use N-Hmb or Dmb as temporary protection of the amino acid before Asp, and/or the addition of 0.1 M HOBt or 1M Oxyma pure in the piperidine solution and/or the use of sterically hindered protecting groups of the side chain of the Asp residue, such as Mpe.

- Oxidation of Met[167]

The main side reaction of Met is the acid catalyzed oxidation of thioether into sulfoxide during deprotection, or even by the oxygen of air. The conversion of the sulfoxide to thioether is achieved using NH_4I / TFA.

- Alkylations upon deprotection

The cations that are generated upon removal of the side-chain protective groups attack the reactive side-chain groups of amino acids such as in Trp, Tyr and Met. To avoid these side reactions, suitable compounds (scavengers) are used in the deprotection solution binding the produced electrophilic moieties.

I.1. Microwave energy

Over the last decades, microwave energy is increasingly used for many chemical reactions. The direct heating, which is provided by the microwaves to the reaction mixture, results in reducing the reaction time from hours to a few minutes. Furthermore, the side reactions are reduced, increasing the yield and improving the repeatability of results.

Microwaves are a form of energy, relatively low in the electromagnetic range. In the energy spectrum this form of radiation is below the X-radiation, the UV, visible and infrared domain, with a frequency between 300 and 300.000 MHz. Due to their low frequency, the microwaves cause the rotation of the molecules bonds without breaking them.

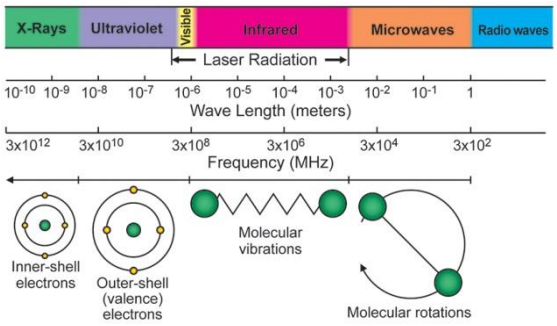

Figure A.4: The spectrum of electromagnetic radiation.

The way that a solvent or a reagent absorb microwave energy is different. Each of them has different degree of polarity within the molecule and therefore sometimes the influence of the microwave field is more or less intense. For example, a more polar solvent will cause stronger rotational movement in its attempt to align with the alternating field. Conversely, a less polar solvent will not be so affected by the changes of the field and therefore will not absorb much energy. The polarity of the solvent is not the only factor determining the actual absorption of the microwave energy but is, however, a good reference point. Most of the organic solvents can be divided into three categories: low, medium and high absorption. The hydrocarbons are generally considered as low absorption, while polar substances have high absorption.

The microwave applications have been extended to many fields of chemistry including synthetic organic chemistry, inorganic chemistry, pharmaceutical research, chemistry of polymers, and even the synthesis of nanomaterials.

I.1.1. Key factors for creating microwave method

There are many factors to be taken into account when creating a microwave method. Below are listed the most basic of them:

A) The power

The microwave system allows the selection of a power between 0 and 300 Watts. Increasing the power, more energy is transferred to the reaction and its temperature is raised rapidly. However, if power is excessive it is more likely that side reactions shall take place.

B) The temperature

Each molecule dipole moment absorbs energy. As a result, its kinetic energy increases. However, through collisions with other molecules that energy can be transferred to the system. The temperature measured is the average temperature of each molecule in the system, including the solvent, providing information on the overall energy situation of the entire system.

C) Time

The longer is the time, the more the molecules will collide and react. It has to be taken into account both the time of application of microwaves and the total reaction time. If a polar solvent is used, such as DMF, low power is needed to raise the temperature to the desired level. Thus, the microwave power must be used only for a very short time, as the system will remain at the desired temperature using only minimal additional force, so that the reaction proceeds only with heating.

I.2. Microwave energy in SPPS

SPPS synthesis was improved by the use of microwave-assisted SPPS especially for the synthesis of long peptide sequences.[168] As the N-terminal amino group and peptide backbone are polar, they constantly try to align with the alternating electric field of the microwave; this helps in breaking up the chain aggregation and permits the synthesis of peptides in high yields and low degrees of racemization.[169] Various peptides were synthesized in a shorter time when microwave-assisted SPPS was applied instead of the traditional SPPS.[170,171]

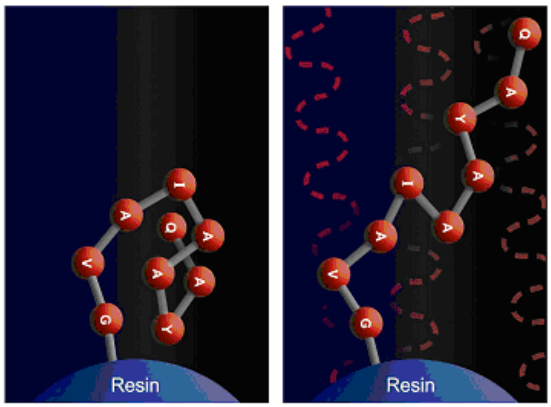

Figure A.5: Aggregation through dipole rotation of the polar peptide backbone is hindered by microwave energy.

II. Principles of High Performance Liquid Chromatography (HPLC)

After the completion of the peptide synthesis follows the characterization of the products and the purification from byproducts that have been occurred either during the synthesis or during the cleavage reaction.[172] The most widely used method for the purification of synthetic peptides, which was used also for this thesis, is the *Reverse Phase High Performance Chromatography* (Reverse Phase- High Performance Liquid Chromatography, RP-HPLC). The stationary phase in the Reversed Phase chromatographic columns is a hydrophobic support that is consisted mainly of porous particles of silica gel in various shapes (spheric or irregular) at various diameters and at various pore sizes. The surface of these particles is covered with various chemical entities, such as hydrocarbons (C1, C6, C4, C8, C18, etc). In most methods used currently to separate medicinal materials, C18 columns are used. The more hydrophobic are the sample components the longer they stay in the column thus they are separated. The mobile phases are mixtures of water and organic polar solvents mostly acetonitrile (AcN) and methanol (MeOH). Lastly, very often in the mobile phase strong acids are added in small concentrations in order to increase the solubility of the products.

Apart from HPLC chromatography column, the pumps that regulate the flow and the detectors are very important. The pumps must be highly accurate in the elution rate even at high pressures. The detector that usually used for the characterization of the peptides is ultraviolet. The width of the wavelength wherein is detected the higher absorption of the peptide bond, is between 214 and 220nm and 254nm for the detection of the amino acids bearing aromatic groups. Moreover RP-HPLC offers the possibility to calculate the purity of product and to characterize and identify it based on its retention time (t_R), which depends on the device, the column and the system used for detection of the molecule. Generally the RP-HPLC chromatography is now widely used for the certification of the final products of peptide synthesis and their puritication.

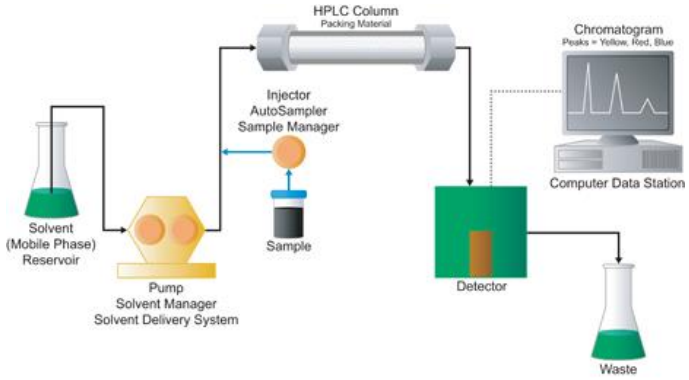

Figure A.6: Scheme of an HPLC System.

III. Principles of Mass Spectrometry (MS)[173]

Mass spectrometry is an analytical tool used for measuring the molecular mass of a sample. Mass spectrometers can be divided into three fundamental parts, namely the *ionisation source*, the *analyser*, and the detector**.** The sample is introduced into the ionisation source of the instrument. The sample molecules are ionised, because ions are easier to be manipulated than neutral molecules. These ions are extracted into the analyser region of the mass spectrometer where they are separated according to their mass(m)-to-charge(z) ratios (m/z). The separated ions are sent to the detector and this signal is read to a data system where the m/z ratios are stored together with their relative abundance for presentation in the format of a m/z spectrum. The analyser and detector of the mass spectrometer, and often the ionisation source too, are maintained under high vacuum to give to the ions a reasonable chance of travelling from the one end of the instrument to the other without any hindrance from air molecules.

For the majority of biochemical analyses the methods for the ionisation used are **Electrospray Ionisation *(ESI)***[174] and ***Matrix Assisted*** **Laser Desorption Ionisation (MALDI)**. ESI, which is used for the present thesis, is used for the analysis of polar molecules ranging from less than 100 Da to more than 1,000,000 Da in molecular mass. During standard electrospray ionization,[175] the sample is dissolved in a polar, volatile solvent and pumped through a narrow, stainless steel capillary. A high voltage is applied to the tip of the capillary and as a consequence the sample emerging from the tip is dispersed into an aerosol of highly charged droplets, a process that is aided by a co-axially introduced nebulizing gas flowing around the outside of the capillary. This gas, usually nitrogen, helps to direct the spray emerging from the capillary tip towards the mass spectrometer. Eventually charged sample ions, free from solvent, are released from the droplets, some of which pass through a sampling cone or orifice into an intermediate vacuum region, and from there through a small aperture into the analyser of the mass spectrometer, which is held under high vacuum**.** The lens voltages are optimized individually for each sample.

IV. Circular Dichroism[176,177,178,179]

Chiral molecules are molecules that exist as pair of mirror-image isomers. These mirror image isomers are not super-imposable and are known as enantiomers. The physical and chemical properties of a pair of enantiomers are almost identical. The exceptions are the way that they interact with the polarized light and the way that they interact with other chiral molecules. Circular dichroism (CD) only occurs at wavelength that could be absorbed from chiral molecules. At these wavelengths left- and right-polarized light will be absorbed to different extents. Measurements carried out in the visible and ultra-violet region of the electro-magnetic spectrum monitor electronic transitions, and, if the molecule under study contains chiral chromophores then one CPL (circular polarized light) state will be absorbed to a greater extent than the other and the CD signal over the corresponding wavelengths will be non-zero. A circular dichroism signal can be positive or negative, depending on whether L-CPL is absorbed to a greater extent than R- CPL (CD signal positive) or to a lesser extent (CD signal negative). For example, a chiral chromophore may absorb 88% of left-handed circularly polarized light (L-CPL) and 90% of right-handed circularly polarized light (R-CPL). This effect is called circular dichroism; it is the difference in the absorption of L-CPL and R-CPL and occurs when a molecule contains one or more chiral chromophores (light-absorbing groups). CD measured as function of wavelength is termed CD spectroscopy. CD spectroscopy is used extensively to analyse the secondary structure or the conformation of chiral biological macromolecules, particularly proteins as 19 of the 20 natural amino acids that form proteins are themselves chiral. Each molecule has its own CD signature. The most widely studied CD signatures are the different secondary structural elements of proteins such as the α-helix and the β-sheet. As their secondary structure is sensitive to their environment, temperature or pH, circular dichroism can be used to observe how secondary structure is affected by environmental changes or by interacting with other molecules. Structural, kinetic and thermodynamic information about macromolecules can be derived from circular dichroism spectroscopy.

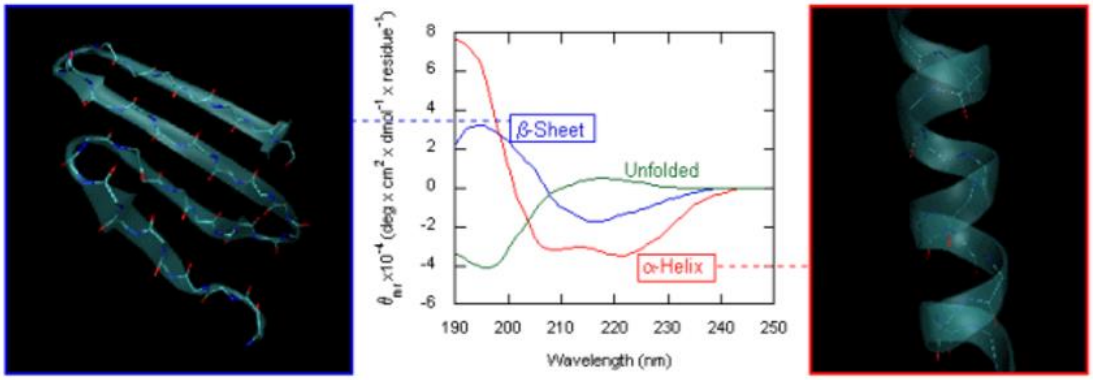

Figure A.7: The secondary structure conformation and the CD spectra of protein structural elements. Right: a backbone conformation of a peptide in an α-helix. Left: a backbone conformation of a peptide in a β-sheet. Center: the associated CD spectra for these different conformations.

V. Immunological assays

V.1 ELISA[180]

The enzyme-linked immunosorbent assay (ELISA) is a usual laboratory technique for the measurement of the concentration of an analyte (usually antibodies or antigens) in a solution. This technique has been introduced some years ago by Engvall and Perlmann.[181] Examples in which ELISA is used, include the diagnosis of HIV infection, pregnancy tests, and measurement of cytokines or soluble receptors in cell supernatant or serum. The antibodies used in an ELISA can be either monoclonal (derived from unique antibody producing cells called hybridomas and capable of specific binding to a single unique epitope) or polyclonal (a pool of antibodies purified from animal sera that are capable of binding to multiple epitopes).

There are four basic ELISA formats (Direct ELISA, Indirect ELISA, Sandwich ELISA, Competition or Inhibition ELISA), which can be adjusted based on the antibodies available, the results required, or the complexity of the samples.

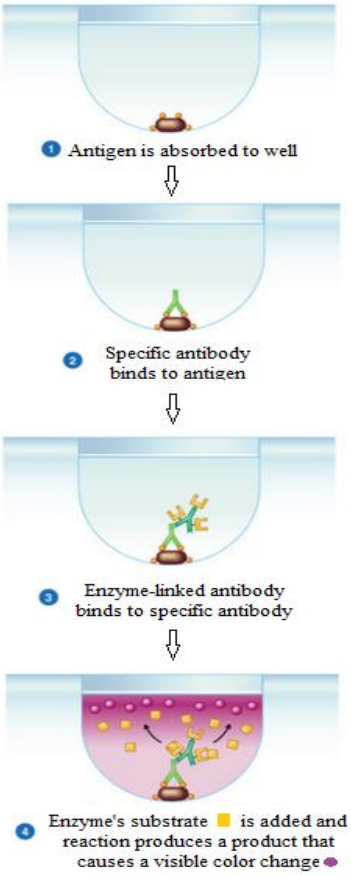

In the present thesis was used the Indirect ELISA technique in which an antigen is coated to a multiwell plate is detected. Afterwards an unlabeled primary antibody, which is specific for the antigen, is applied. At the end an enzyme-labeled secondary antibody is bound to the first antibody. This method was selected as it has several advantages like sensitivity, since more than one labeled antibody is bound per primary antibody, flexibility, since different primary detection antibodies can be used with a single labeled secondary antibody and also its cost is low comparing to other methods.

V.2. Surface Plasmon Resonance (SPR)

SPR immunoassay has been developed a couple of decades ago and nowadays is a really powerful technique to monitoring biomolecular interactions in real-time in a label-free environment.[182,183] One of the reactants (called ligand) is immobilized to the sensor surface while the other (called analyte) is free in solution and passed over the surface. This technique is based on the SPR phenomenon which occurs when plane-polarized light strikes a thin metal film at the interface between media with different Reflective Index (RI). In condition of total internal reflection the reflected photons create an electric field (evanescent field) on the opposite side of the interface. At a particular critical angle, the resonance angle, the evanescent wave resonates with the oscillation in the electrons (plasmons) on the surface of the metal film and this causes a drop in the reflected light. When the ligand and the analyte interact to form a complex, this causes a change in the refractive index and thus a shift of the resonance angle. This response is measured in Resonance Units (RU) and is reported in a graph called sensorgram (Figure A.8). The SPR response is directly proportional to the change in mass concentration close to the surface.

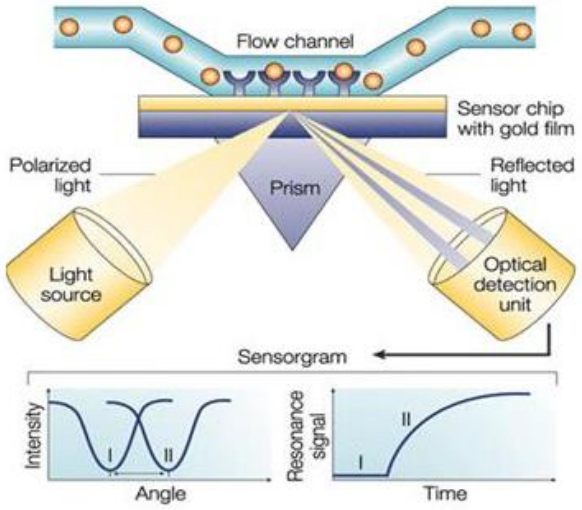

Figure A.8: Schematic representation of the Surface Plasmon Resonance.

Biacore is the most common used optical biosensor that uses SPR for affinity measurements and binding kinetics, concentration determinations, binding specificity analyses and epitope mapping. In Biacore system, the two media are the glass of the

sensor chip (high reflective index) and the flowing solution (low reflective index), and the conducting film is a thin layer of gold on the sensor chip surface. The wavelength of the incident light and the reflective index of the inner surface are constant, so the SPR phenomenon is used to monitor the change of reflective index in the flowing solution close to the sensor chip surface.

The sensor chip is the most important part in a Biacore system as it maintains the physical conditions necessary to generate the SPR signal from the interactions studied on its surface. The sensor chip consists of a glass slide coated with a thin layer of gold which is covered by a linker layer and a matrix of modified dextran providing a means for attaching ligand. The specificity of the analysis depends from the nature and the properties of the molecule that is attaches to the dextran. There are three different approaches that could be used for the immobilization of the ligand; a covalent immobilization, where the biomolecule is attached to the surface through a covalent chemical link, a high affinity capture, where it is attached by noncovalent but high specific interaction with another molecule and a hydrophobic adsorption, which exploits more or less specific hydrophobic interactions to attach either the molecule of interest or a hydrophobic carrier, such as a lipid monolayer or bilayer, to the sensor chip surface (Figure A.9).

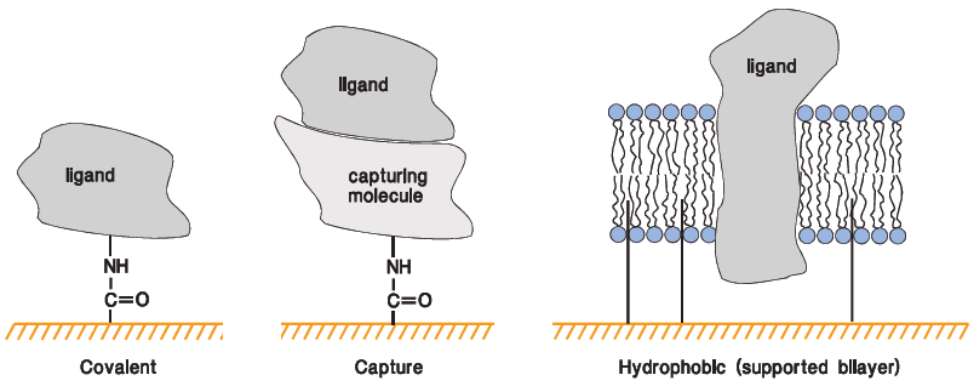

Figure A.9: Three most common approaches for attaching biomolecules to the sensor chip surface.

There is a wide variety of sensor chips designed for different application requirements. One of the most commonly used Biacore sensor that is also used for this thesis, is the CM5 type which carries a matrix of carboxymethylated dextran covalently attached to

the gold surface (Figure A.10). The dextran matrix is flexible, allowing relatively free movement of attached biomolecules within the surface layer. This kind of sensor chip provides a high surface capacity for immobilizing a wide range of ligands (small organic molecules, nucleic acids, proteins, carbohydrates).

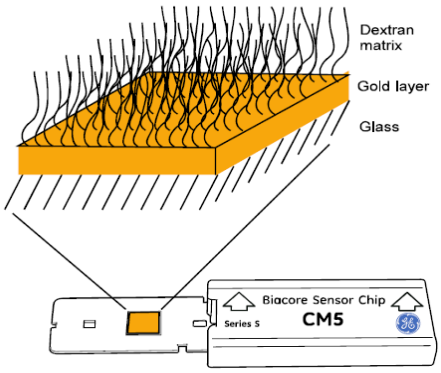

Figure A.10: Schematic illustration of the structure of a CM5 sensor chip.

The main immobilization chemistries for the CM5 sensor are:

- amine coupling, exploiting primary amine groups of the ligand after activation of the surface;
- thiol coupling, exploiting thiol-disulfide exchange between thiol groups and active disulfides introduced on either the ligand (surface thiol coupling) or the surface matrix (ligand thiol coupling);
- aldehyde coupling, using the reaction between hydrazine or carbohydrazide groups introduced on the surface and aldehyde groups obtained by oxidation of carbohydrates in the ligand.

On purpose of this study, antibody was covalently linked according to the amine coupling strategy (Figure A.11).

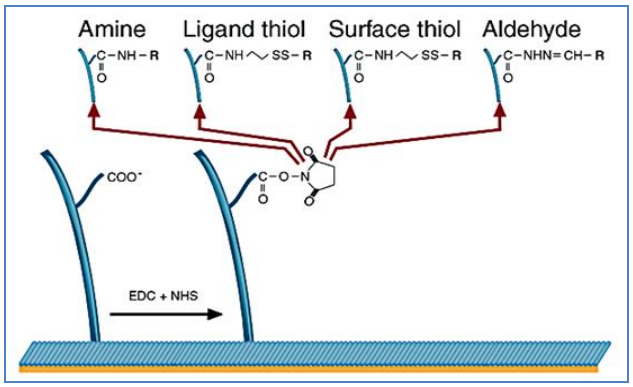

Figure A.11: Schematic illustration of the immobilized ligand (R) linked to the surface through a covalent chemical bond.

To obtain a good immobilization level, the electrostatic pre-concentration of ligands in the dextran matrix must be achieved. At pH values above 3.5 the carboxymethylated dextran on the sensor chip surface is negatively charged, so the primary requirement for the electrostatic pre-concentration on the surface is that the pH of the ligand solution should be between 3.5 and the isoelectric point of the ligand, so that the surface and the ligand carry opposite net charges. Moreover, the electrostatic interactions involved in pre-concentration are favored by low ionic strength in the coupling buffer. With the pH scouting performed for each ligand, the optimum values of pH and ionic strength can be determined experimentally; this procedure consists of: injecting the ligand in different buffers over the non-activated surface of the chip and evaluating the instrumental response at the end of the injection which depends only on the electrostatic interactions between the chip surface and the ligand and that consequently will give an indication of whether the conditions are suitable.

V.2.1. Binding Studies

Once the ligand is immobilized on the surface of the sensor chip, the binding experiment consists of different steps. During the association phase the analyte binds to the ligand. This binding generates a change in the reflective index and is detected as an increase of the signal (Resonance Units) that is directly related to the change in mass concentration on the surface, so that molar response are proportional to the size of the molecule involved. The given response of the small molecules is represented by higher molar concentration than the larger ones; conversely, a given number of molecules binding to the surface will give a lower response if the molecule is small. After a certain period of time all the binding sites are occupied that's mean that saturation is reached and the signal remains stable. At the end of the injection, the buffer flew at the surface of the sensor chip to obtain a partial dissociation. The analyte gets desorbed from the ligand, which is detected with a decrease to the response. The phases of a Biacore experiment is graphically expressed by a sensorgam (Figure A.12).

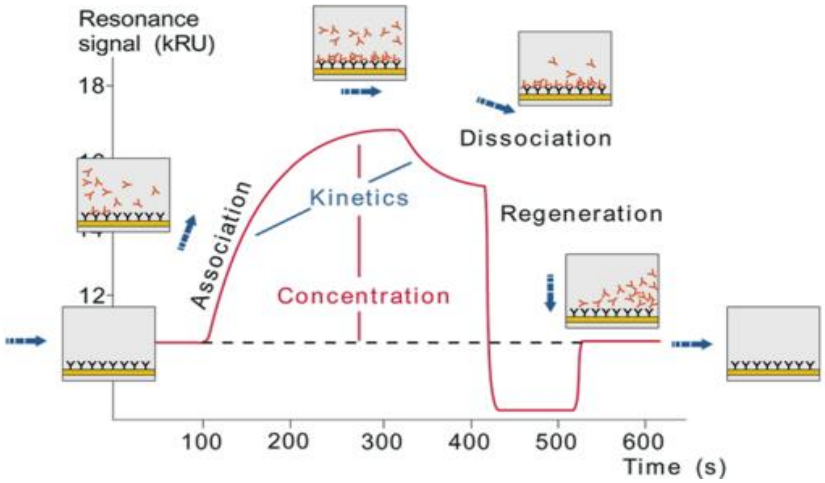

Figure A.12: Sensorgram from a binding experiment; the signal in Resonance Units is direclty related to the quantity of the analyte that binds to the ligand.

V.2.2. Kinetic and affinity studies

A kinetic analysis experiment using a Biacore system could be set up with two different ways. A series of analyte concentration could be injected either in separated cycles with, regenerating the surface after each sample injection (multi-cycle analysis) or on one cycle with no regeneration between sample injections (single-cycle analysis). The data from the monitoring of the interaction as a function of time over a range of analyte concentration are then fitted to mathematical models. The association phase during sample injection contains information on both association and dissociation processes and allows the calculation of the association rate ka ($M^{-1}s^{-1}$), from the dissociation phase when buffer flow removes dissociated analyte molecules, the dissociation rate kd (s^{-1}) can be obtained. For the simple 1:1 binding model provided by a Biacore system, the affinity constant KD (M) is equal to the ratio of the rate constants (kd/ka) and can therefore be derived from kinetic measurements.

$$A + B \underset{k_d}{\overset{k_a}{\rightleftharpoons}} AB$$

The dissociation rate constants can be obtained for samples with unknown concentration as it is independent of the analyte concentration in the injected sample. It is important to be mentioned that fitting the data to a mathematical model does not provide evidence of the interaction mechanism.

ABBREVIATIONS

The abbreviations used in this thesis have been proposed by the Biochemical Nomenclature Committee of the International Union of Pure and Applied Chemistry (IUPAC) and the International Union of Biochemistry (IUD). These proposals were announced in 1972 and gradually completed until 1989.[184,185]

Aa	Amino acid
Ab	Antibody
Ac	Acetyl
CAN	Acetonitrile
Ag	Antigen
Boc	tert-butoxycarbonyl
Bz	Benzoyl
CD	Circular Dichroism
CIDP	Chronic inflammatory demyelinating polyneuropathy
CNS	Central Nervous System
DCM	Dichloromethane
Dde	1-[(4,4 - dimethyl - 2,6 - dioxocyclohex -1-ylidine)ethyl]
DIC	*N,N'*-Diisopropylcarbodiimide
DIPEA	Diisopropylethylamine
DMAP	4-(Dimethylamino) pyridine
DMF	*N,N*-dimethylformamide
DMSO	Dimethylsulfoxide
EAE	Experimental Autoimmune Encephalomyelitis
EDT	1,2-ethanedithiole
ELISA	Enzyme-linked immunosorbent assay
ESI-MS	Electrospray Ionization Mass Spectrometry
FBS	Fatal Bovine Serum
Fmoc	9-H-fluoren-9-ylmethoxycarbonyl
GBS	Guillian Barré syndrome
HOBt	1-Hydroxybenzotriazole
HPLC	High performance liquid chromatography
Ig	Immunoglobulin (IgE, IgG, etc.)
MAG	Myelin associated glycoproteins
MBP	Myelin Basic Protein
MGUS	Monoclonal gammopathy of undetermined significance
MMN	Multifocal motor neuropathy with conduction blocks
MOG	Myelin Oligodedrocyte Glycoprotein
MRI	Magnetic Resonance Imaging
MW	Microwaves
NBD	Normal Blood Donors

NMM	*N*-Methyl morpholine
NMR	Nuclear magnetic resonance
ON	Overnight
PNS	Peripheral nervous system
PPN	Paraproteinemic Polyneuropathies
RP-HPLC	reverse phase-high performance liquid chromatography
RT	room temperature
Rt	Retention time
SGPG	Sulfated glucuronosyl paragloboside
SPPS	Solid phase peptide synthesis
SPR	Surface plasmon resonace
TBTU	2 - (1H-Benzotriazole-1-yl) - 1,1,3,3 – tetramethyluronium tetrafluoroborate
TCR	T-cell receptor
TFA	Trifluoroacetic acid
THF	Tetrahydrofurane
TLC	Thin layer chromatography
UPLC	Ultra Performance Liquid Chromatography
UV	Ultraviolet

BIBLIOGRAPHY

[1] MacPherson G. & Austyn J. Exploring Immunology: Concepts and Evidence, 1st ed. Wiley-Blackwell, 2012.

[2] Abbas, A., Lichtman, A., Pillai, S. Basic Immunology: Functions and Disorders of the Immune System. 4th ed. Elsevier Saunders, 2014.

[3] Abbas, A. and Lichtman. A. Basic Immunology: Functions and Disorders of the Immune System. 3rd ed. Philadelphia, PA: Saunders Elsevier, 2009.

[4] Parham, P. The Immune System. 5th ed. Garland Science, Taylor & Francis Group, 2015.

[5] Campell, N. and Reee, J. Biology. 8th ed. AP® Edition, 2008.

[6] Fairweather, D. Autoimmune Disease: Mechanisms. Encyclopedia Of Life Science, John Wiley & Sons, 2007.

[7] Davidson, A., Diamond, B. General Features of Autoimmune Disease. *In: Rose, R., Mackay, R. The Autoimmune Diseases.* Elsevier, St Louis, 2006.

[8] von Mühlen, A., Tan, M. Autoantibodies in the diagnosis of systemic rheumatic diseases. *Semin Arthritis Rheum*, **24** (1995): 323-3583.

[9] Arbuckle, R., McClain, T., Rubertone, V., Scofield, H., Dennis, J. Development of autoantibodies before the clinical onset of systemic lupus erythematosus. *N Engl J Med* **349** (2003): 1526-1533.

[10] Rosenblum M., Remedios, K., Abbas A., Mechanisms of human autoimmunity. *J Clin Invest.* **125(6)** (2015): 2228–2233.

[11] Ray, S., Sonthalia, N., Kundu, S., Ganguly, S. Autoimmune Disorders: An Overview of Molecular and Cellular Basis in Today's Perspective. *J Clin Cell Immunol* (2012).

[12] Temajo, N., Howard, N. The mosaic of environment involvement in autoimmunity: the abrogation of viral latency by stress, a non-infectious environmental agent, is an intrinsic prerequisite prelude before viruses can rank as infectious environmental agent that trigger autoimmune diseases, *Autoimmunity Reviews* **13**, (2014): 605–610.

[13] Karen, C., Steffen, G., Marta, A.-R., Luca, I., Andrea D. Genes, Epigenetic regulation and Environmental Factors: Which is the most relevant in developing autoimmune diseases? *Autoimmunity Reviews* **11**, (2012): 635–609.

[14] Morahan, G. & Morel, L. Genetics of autoimmune diseases in humans and in animal models. *Curr Opin Immunol* **14** (2002): 803-811.

[15] Adorini, L., Gregori, S., Harrison, L.C. Understanding autoimmune diabetes: insights from mouse models. *Trends Mol Med* **8** (2002): 31-38.

[16] Ray, S., Sonthalia, N., Kundu, S., Ganguly S. Autoimmune Disorders: An Overview of Molecular and Cellular Basis in Today's Perspective. *J Clin Cell Immunol* S10 (2012).

[17] de Carvaho, F., Pereira, M., Shoenfeld, Y. The mosaic of autoimmunity : the role of environmental factors. *Fronti Biosci. (Elit. Ed.)* **1** (2009): 501-9

[18] Agma-Levin, N., Theodor, E., Segal, M., Shoenfeld, Y. Vitamin D in systemic and organ-specific autoimmune diseases. *Clin Rev Allergy Immunol* **45(2)** (2013): 256-66

[19] Breuer, J., Schwab, N., Schneider-Hohendorf, T., Marziniak, M., Mohan, H., Bhatia, U., Gross, C., Clausen, B., Weishaupt, D., Luger, T., Meuth, S., Loser K., Wiendl, H. UVB Light Attenuates the Systemic Immune Response in CNS Autoimmunity. *Annals of Neurology* (2014): 739–758.

[20] Bach J.F. Infections and autoimmune diseases. *Journal of Autoimmunity* **25** (2005): 74-80.

[21] Benros, M., Mortensen, P., Eaton, W. Autoimmune diseases and infections as risk factors for schizophrenia. *Ann. N.Y. Acad. Sci.* **1262** (2012): 56–66.

[22] Whitacre, C. Sex differences in autoimmune disease. *Nat Immunol* **2** (2001): 777-780.

[23] Ahmed, A., Hissong, BD., Verthelyi, D., Donner, K., Becker, K. Gender and risk of autoimmune diseases: possible role of estrogenic compounds. *Environ Health Perspect* **107** (1999): 681-686.

[24] Progress in Autoimmune Disease Research. Report to Congress The Autoimmune Diseases Coordinating Committee, National Institute of Allergy and Infectious Diseases, National Institutes of Health (2005).

[25] Ermann, J. and Fathman, G. Autoimmune diseases: genes, bugs and failed regulation. *Nature Immunology* **2** (2001): 751-756.

[26] Bonsor, D., Grishkovskaya, I., Dodson, E., Kleanthous, C. Molecular mimicry enables competitive recruitment by a natively disordered protein. *J Am Chem Soc* **129** (2007): 4800-4807.

[27] Rose, N. The adjuvant effect in infection and autoimmunity. *Clin Rev Allergy Immunol* **34(3)** (2008): 279-82.

[28] Torres, A., Johnson, M. Modulation of disease by superantigens. *Curr Opin Immunol* **10** (1998): 465-470.

[29] Grant, C., Liberal, R., Mieli-Vergani, G., Vergani, D., Longhi M.S. Regulatory T-cells in autoimmune diseases: Challenges, controversies and—yet—unanswered questions. *Autoimmunity Reviews* **14** (2015): 105–116.

[30] Vignali, A., Collison, W., Workman, J. How regulatory T cells work. *Nat Rev Immunol* **8** (2008): 523–32.

[31] Yang, M., Rui, K., Wang, S., Lu, L. Regulatory B cells in autoimmune diseases. *Cellular & Molecular Immunology* **10**, (2013): 122–132.

[32] Mizoguchi, A., Bhan, A. A case for regulatory B cells. *J Immunol* **176** (2006): 705–710.

[33] Doyle, H., Mamula, M. Autoantiogenesis: the evolution of protein modifications in autoimmune disease. *Current Opinion in Immunology* **24** (2012): 112-118.

[34] Doyle, H., Mamula, M. Post-translational protein modifications in antigen recognition and autoimmunity. *TRENDS in Immunology* **22(8)** (2001): 443-449.

[35] Spiro,G. Protein glycosylation: Nature, distribution, enzymatic formation, and disease implications of glycopeptide bonds. *Glycobiology* **12** (2002): 43R-56R.

[36] Cohen, I. Biomarkers, self-antigens and the immunological homunculus. *Journal of Autoimmunity* **29** (2007): 246-249.

[37] Leslie, D., Lipsky, P., Natkins, A.L. Autoantibodies as predictors of disease. *J. Clin. Invest.* **108** (2001): 1417-1422.

[38] Biolynicki-Birula, R. The 100th anniversary of Wassermann-Neisser-Bruck reaction. *Clin. Dermatol.* **26** (2008): 79-88.

[39] Van Gaalen, F.A., Linn-Rasker, S., van Venrooij, W.J., de Jong, B.A., Breedveld, F.C., Verweij, C.L. Autoantibodies to cyclic citrullinated peptides predict progression to rheumatoid arthritis in patients with undifferentiated arthritis. *Autoimmunity* **50** (2004): 1238-1241.

[40] Bizzano, N. Autoantibodies as predictors of disease: The clinical and experimental evidence. *Autoimmunity Reviews* **6** (2007): 325-333.

[41] Alcaro, M.C., Lolli, F., Migliorini, P., Chelli, M., Rovero, P., Papini, A.M. Peptides as autoimmune diseases antigenic probes. *Chem. Today* **25** (2007): 14-16.

[42] Papini, A.M. The use of post-translational modified peptides for detection of biomarkers of immune-mediated diseases. *J. Pept. Sci.* **15** (2009): 621-628.

[43] Simon, M., Girbal, E., Sabbag, M., Gomés-Daudrix, V., Vincent, C., Salema, G., serre, G. The cytokeratin filament-aggregation protein filaggrin is tha target of the so-called 'antikeratin antibodies'. Autoantibodies specific for rheumatoid arthritis. *J. Clin. Invest.* **92** (1995): 2672-2679.

[44] Mazzucco, D., Matà, S., Vergelli, M., Fioresi, R., Nardi, E., Mazzanti, B., Chelli, M., Lolli, F., Ginanneschi, M., Pinto, F., Massacesi, L., Papini, A.M. A synthetic glycopeptide of human myelon oligodendrocyte glycoprotein to detect antibody response in multiple sclerosis and other neurological diseases. *Bioorg. Med. Chem. Let.* **9** (1999): 167-172.

[45] Carotenuto, A., D'Ursi, A. M., Nardi, E., Papini, A. M. & Rovero, P. Conformational analysis of a glycosylated human myelin oligodendrocyte glycoprotein peptide epitope able to detect antibody response in multiple sclerosis. *J. Med. Chem.* **44** (2001): 2378–2381.

[46] Lolli, F. et al. An N-glucosylated peptide detecting disease-specific autoantibodies, biomarkers of multiple sclerosis. *Proc. Natl. Acad. Sci. U. S. A.* **102** (2005): 10273–10278.

[47] Lolli, F. et al. The glycopeptide CSF114(Glc) detects serum antibodies in multiple sclerosis. *J. Neuroimmunol.* **167** (2005): 131–137.

[48] Papini, A. M. Simple test for multiple sclerosis. *Nat. Med.* **11** (2005): 13.

[49] Real-Fernández, F., Colson, A., Bayardon, J., Nuti, F., Peroni, E. Ferrocenyl glycopeptides as electrochemical probes to detect autoantibodies in multiple sclerosis patients' sera. *Biopolymers* **90** (2008): 488-495.

[50] Lublin, F., Reingold, S. Defining the clinical course of multiple sclerosis. *Neurology* **46(4)** (1996): 907-911.

[51] Cottrell, DA, Kremenchutzky, M, Rice, GP, et al. The natural history of multiple sclerosis: a geographically based study. 5. The clinical features and natural history of primary progressive multiple sclerosis. *Brain* **122** (1999): 625–639.

[52] Vincent, A., Bien, C. G., Irani, S. R., Waters, P., Autoantibodies associated with diseases of the CNS: new developments and future challenges. *Lancet Neurol.* **10** (2011): 759–772.

[53] Lancaster, E. and J. Dalmau, Neuronal autoantigens—pathogenesis, associated disorders and antibody testing. *Nat. Rev. Neurol*. **8** (2012): 380–390.

[54] Iorio, R. and Lennon V. A. Neural antigen-specific autoimmune disorders. *Immunol. Rev.* **248** (2012): 104–121.

[55] Srivastava, R., Aslam, M., Kalluri, S. R., Schirmer, L., Buck, D., Tackenberg, B., Rothhammer, V., Chan, A., Gold, R., Berthele, A. Potassium Channel KIR4.1 as an Immune Target in Multiple Sclerosis. *N. Engl. J. Med.* **367** (2012): 115– 123.

[56] Compston A., Coles A. Multiple Sclerosis. Lancet **372** (2008): 1502–17.

[57] Brunner, C., Lassmann H., Waehneldt T. V., Matthieu J. M., Linington C. Differential ultrastructural localization of myelin basic protein, myelin/oligodendroglial glycoprotein, and 2',3'-cyclic nucleotide 3'-phosphodiesterase in the CNS of adult rats. *J. Neurochem.* **52(1)** (1989): 296–304.

[58] Mayer, M. C., Breithaupt, C., Reindl, M., Schanda, K., Rostásy, K., Berger, T., Dale, R.C., Brilot, F., Olsson, T., Jenne, D., Pröbstel A-K., Dornmair, K., Wekerle H., Hohlfeld, R., Banwell, B., Bar-Or,xx, A., Meinl, E. Distinction and Temporal Stability of Conformational Epitopes on Myelin Oligodendrocyte Glycoprotein Recognized by Patients with Different Inflammatory Central Nervous System Diseases. *J. Immunol.* **191** (2013): 3594–3604.

[59] Schluesener, H. J., Sobel, R. A., Linington, C., Weiner, H. L., Schluesener, H.J., Sobel, R.A., Linington, C. & Weiner, H.L. A monoclonal antibody against a myelin oligodendrocyte glycoprotein induces relapses and demyelination in central nervous system autoimmune disease. *J. Immunol.* **139** (1987): 4016–4021.

[60] Genain, C. P., Nguyen, M. H., Letvin, N. L., Pearl, R., Davis, R. L., Adelman, M., Lees, M. B., Linington, C., Hause, S. L. Antibody facilitation of multiple sclerosis-like lesions in a nonhuman primate. *J. Clin. Invest.* **96** (1995): 2966–2974.

[61] Linnington, C., Lasssmann, H. Antibody responses in chronic relapsing experimental allergic encephalomyelitis: Correlation of serum demyelinating activity with antibody titre to the myelin/oligodendrocyte glycoprotein. *J. Neuroimmunol.* **17** (1987): 61–69.

[62] Mayer, M. C., Meinl, E. Glycoproteins as targets of autoantibodies in CNS inflammation: MOG and more. *Ther. Adv. Neurol. Disord.* **5(3)** (2012): 147 –159.

[63] Johns, T. G., Kerlero de Roslo, N., Menon, K. K., Abo, S., Gonzales, M. F., Bernard, C. C. Myelin oligodendrocyte glycoprotein induces a demyelinating encephalomyelitis resembling multiple sclerosis. *J. Immunol.* **154** (1995): 5536–5541.

[64] Von Budingen, C., Hauser, L., Fuhrmann, A., Nabavi, B., Lee, I., Genain, P. Molecular characterization of antibody specificities against myelin oligodendrocyte glycoprotein in autoimmune demyelination. *Proc. Natl. Acad. Sci. U.S.A.* **99** (2002): 8207-8212.

[65] Von Budingen, C., Hauser, L., Quallet, C., Tanuma, N., Menge, T., Genain, P. Frontline: Epitope recognition on the myelin/oligodendrocyte glycoprotein differentially influences disease phenotype and antibody effector functions in autoimmune demyelination. *Eur. J. Immunol.* **34** (2004): 2072-2083.

[66] Breithaupt, C., Schubart, A., Zander, H., Skerra, A., Huber, R., Linington, C., Jacob, U. Structural insights into the antigenicity of myelin oligodendrocyte glycoprotein. *Proc. Natl. Acad. Sci*. U.S.A. **100** (2003): 9446–51.

[67] De Graaf, L., Albert, M., Weissert, R. Autoantigen Conformation Influences Both B- and T-cell Responses and Encephalitogenicity. *J. Biol. Chem.* **287** (2012): 17206-17213.

[68] Ohtani, S., Kohyama, K., Matsumoto, Y. Autoantibodies recognizing native MOG are closely associated with active demyelination but not with neuroinflammation in chronic EAE. *Neuropathology* **31** (2011): 101-111.

[69] Marta, B., Oliver, R., Sweet, A., Pfeiffer, E., Ruddle, H. Pathogenic myelin oligodendrocyte glycoprotein antibodies recognize glycosylated epitopes and perturb oligodendrocyte physiology. *Proc. Natl. Acad. Sci. U.S.A.* **102** (2005): 13992–13997.

[70] Egg, R., Reindl, M., Deisenhammer, F., Linington, C., Berger, T. Anti-MOG and anti-MBP antibody subclasses in multiple sclerosis. *Mult. Scler.* **7** (2001): 28-289.

[71] Gaertner, S., de Graaf, I., Greve, B., Weissert, R., J. Neurol. Sci. 211, (2004): 67-73.

[72] Lim, T., Berger, T., Reindl, M., Dalton, M., Fernando, K., Keir, G. Anti-myelin antibodies do not allow earlier diagnosis of multiple sclerosis. *Mult. Scler.* **11** (2005): 492-495.

[73] Kuhle, J., Pohl, C., Mehling, M., Edan, G., Freedman, S., Hartung, P. Lack of association between antimyelin antibodies and progression to multiple sclerosis. *N. Engl. J. Med.* **356** (2007): 371-378.

[74] Wang, H., Munger, L., Reindl, M., O'Reilly, J., Levin, I., Berger, T. Myelin oligodendrocyte glycoprotein antibodies and multiple sclerosis in healthy young adults. *Neurology* **71** (2008): 1142-1146.

[75] Waters, P., Woodhall, M., O'Connor, C., Reindl, M., Lang, B., Sato, K. MOG cell-based assay detects non-MS patients with inflammatory neurologic disease. *Neurol. Neuroimmunol. Neuroinflamm.* **1351** (2015): 22-38.

[76] Dale, C., Tantsis, E., Merheb, V., Kumaran R.-A., Sinman, N., Pathmanandavel, K. Antibodies to MOG have a demyelination phenotype and affect oligodendrocyte cytoskeleton. *Neurol. Neuroimmunol. Neuroinflamm.* **2(e89)** (2014).

[77] Probstel, K., Dornmair, K., Bittner, R., Sperl, P., Jenne, D., Magalhaes, S. Antibodies to MOG are transient in childhood acute disseminated encephalomyelitis. *Neurology* **77** (2011): 580-588.

[78] Zhou, D., Srivastava, R., Nessler, S., Grummel, V., Sommer, N., Bruck, W. Identification of a pathogenic antibody response to native myelin oligodendrocyte glycoprotein in multiple sclerosis. *Proc. Natl. Acad. Sci. U.S.A.* **103** (2006): 2280–2283.

[79] Mader, S., Gredler, V., Schanda, K., Rostasy, K., Dujmovic, I., Pfaller, K. Complement activating antibodies to myelin oligodendrocyte glycoprotein in neuromyelitis optica and related disorders. *J. Neuroinflammation* **8** (2011): 184.

[80] O'Connor, C., McLaughlin, D., Da Jager, L., Chitnis, T., Bettelli, E., Xu, C. Self-antigen tetramers discriminate between myelin autoantibodies to native or denatured protein. *Nat. Med.* **13** (2007): 211-217.

[81] Fernandez-Carbonell, C., Vargas-Lowy, D., Musallam, A., Healy, B., McLaughlin, K., Wucherpfenning, W. Clinical and MRI phenotype of children with MOG antibodies. *Mult. Scler.* **2015.**

[82] Ketelslegers, A., Van Pelt, E., Bryde, S., Neuteboom, F., Catsman-Berrevoets, E., Hamann, D. Anti-MOG antibodies plead against MS diagnosis in an Acquired Demyelinating Syndromes cohort*. Mult. Scler*. **1(e40)** (2014).

[83] Reindle, M., Di Pauli, F., Rostasy, K., Berger, T. The spectrum of MOG antibody-associated demyelinating diseases. Nat. Rev. Neurol. **9** (2013): 455-461.

[84] Ramanatan, S., Reddel, W., Henderson, A., Parratt, E., Barnett, M., Gatt, N. Antibodies to myelin oligodendrocyte glycoprotein are uncommon in Japanese opticospinal multiple sclerosis. *Neurol. Neuroimmunol. Neuroinflamm.* **1351** (2015) : 22-38.

[85] Kroepfl, F., Viise, R., Charron, J., Linington, C., Gardinier,V. Investigation of myelin/oligodendrocyte glycoprotein membrane topology. *J. Neurochem.* **67(5)**, (1996): 2219–2222.

[86] Clements, C.,Reid, H., Beddoe, T., Tynan, F., Perugini, M., Johns, T., Bernard, C., Rossjohn, J. The crystal structure of myelin oligodendrocyte glycoprotein, a key autoantigen in multiple sclerosis Proc. Natl. Acad. Sci. U.S.A. **100** (2003): 11059–11064.

[87] Johns, G., Bernard, C.A. The Structure and Function of Myelin Oligodendrocyte GlycoproteinJ. Neurochem. **72** (1999): 1–9.

[88] Steck, A.J., Stalder, A.K., Renaud, S. Anti-myelin-associated glycoprotein neuropathy. *Curr. Opin. Neurol*. 19 (2006): 458-463.

[89] Kyle, R. A., Rajkumar, S. V. Long-term follow-up of IgM monoclonal gammopathy of undetermined significance. *Immunol. Rev.* **194** (2003): 112–13.

[90] Smith, I. The natural history of chronic demyelinating neuropathy associated with benign IgM paraproteinaemia: a clinical and neurophysiological study. *Brain* **117(5)** (1994): 949–957.

[91] Nemni R., Gerosa, E., Piccolo, G., Merlini, G. Neuropathies Associated With Monoclonal Gammopathies. *Haematologica* **79** (1994): 557-566.

[92] Kuijf, M.L., Eurelings, M., Tio-Gillen, A.P., van Door, P.A., van den Berg, L.H., Hooijkaas, H., Strork, J., Notermans, N.C., Jacods, B.C. Detection of anti-MAG antibodies in polyneuropathy associated with IgM monoclonal gammopathy. *Neurology* **73** (2009): 688-695.

[93] Eurelings, M., Moons, K.G.M., Notermans, N.C., Sasker, L.D., De Jager, A.E., Wintzen, A.R., Wokke, J.H.J., Van den Berg, L.H. Neuropathy and IgM M-proteins. Prognostic value of antibodies to MAG, SGPG, and sulfatide. *Neurology* **56** (2001): 228-233

[94] Abo, T.; Balch, C. M. A differentiation antigen of human NK and K cells identified by a nonoclonal antibody (HNK-1). *J. Immunol.* **127** (1981): 1024-1029.

[95] Murray, N.; Steck, A. Indication of a possible role in a demyelinating neuropathy for an antigen shared between myelin and NK cells. J. *Lancet* 1 (1984): 711-713.

[96] Morita, I., Kizuka, Y., Kakuda, S., Oka, S. Expression and Function of the HNK-1 Cardohydrate. *J.Biochem.* **143** (2008): 719-724.

[97] Engels, L., Henze, M., Hummel, W., Elling, L. Enzyme Module Systems for the Synthesis of Uridine 5'-Diphospho-α-*D*-glucuronic Acid and Non–Sulfated Human Natural Killer Cel-1 (HNK-1) Epitope. *Adv. Synth. Catal.* **357** (2015): 1751-1762.

[98] Quarles, R. Glycoproteins in Myelin and Myelin-Related Membranes. In *Complex Carbohydrates of Nervous Tissue*, 209-233. New York: Springer US, 1979.

[99] Quarles, R. Myelin-associated glycoprotein (MAG): past-, present, and beyond. *J. Neurochemistry* **100** (2007): 1431-1448.

[100] Georgiou, J., Tropak, M., Roder, J. Myelin Associated Glycoprotein Gene. In *Myelin Biology and Disorders*, 421-467. New York: Springer US, 2004.

[101] Focosi, D., Bestagno, M., Burrone, O., Petrini, M. CD57+ T lymphocytes and functional immume deficiency. *J. Leukoc Biol.* **87** (2010): 107-116.

[102] Oka, S., Terayama, K., Kawashima, C., Kawasaki, T. A novel glucuronyltransferase in nervous system presumably associated with the biosynthesis of HNK-1 carbohydrate epitope on glycoproteins. *J. Biol. Chem.* **267(32)** (1992): 22711-22714.

[103] Tagawa, H., Kizuka, Y., Ikeda, T., Itoh, S., Kawasaki, N., Kurihara, H., Onozato, M.L., Tojo, A., Sakai, T., Kawasaki, T., Oka, S. A Non-sulfated Form of the HNK-1 Carbohydrate Is Expressed in Mouse Kidney. J. Biolog. Chem. 280(25) (2005): 23876–23883.

[104] Voshol, H.; van Zuylen, C. W.; Orberger, G.; Vliegenthart, J. F.; Schachner, M. Stucture of the HNK-1 carbohydrate epitope on Bovine Peripheral Myelin Glycoprotein P0. *J. Biol. Chem.* **271(38)** (1996): 22957–22960.

[105] Kleene, R., Schachner, M. Glycans and neural cell interactions. *Nat. Rev. Neurosci.* **5** (2004): 195-208.

[106] Inoue, M., Kato, K., Matsuhashi, H., Kizuka, Y., Kawasaki, T., Oka, S. Distributions of glucuronyltransferases, GlcAT-P and GlcAT-S, and their target substrate, the HNK-1 carbohydrate epitope in the adult mouse brain with or without a targeted deletion of the GlcAT-P gene. *Brain Res.* **1179** (2007): 1-15.

[107] Suzuki-Anekoji, M.,Suzuki, M., Kobayashi, T., Sato, Y.; Nakayama, J., Suzuki, A., Bao, X., Angata, K., Fukuda.M. HNK-1 glycan functions as a tumor suppressor for astrocytic tumor. *J. Biol. Chem*. **286** (2011): 32824–32833

[108] Abo, T., Balch, C. A differentiation antigen of human NK and K cells identified by a monoclonal antibody (HNK-1). *J. Immun*. **127(3)** (1981): 1024-1029.

[109] Nohonha, A., Ilyas, A., Antonicek, H., Schachner, M., Quarles, H. Molecular specificity of L2 monoclonal antibodies that bind to cardohydrate determinants of neural cell adhesion molecules and their resemblance to other monoclonal antibodies recognizing the Myelin-Associated Glycoprotein. *Brain Research* **385** (1986): 237-244.

[110] Schmitz, B., Schachner, M., Ito, Y., Nakano, T., Ogawa, T. Determination of structural elements of the L2/HNK-1 carbohydrate epitope required for its function. *Glycoconjugate J.* **11 (**1994): 345-352.

[111] McCluskey, J., Farris, D., Keech, L., Purcell, W., Rischmueller, M., Kinoshita, G., Reynolds, P., Gordon, P. Determinant spreading: lessons from animal models and human disease. *Immunol Rev* **164** (1998): 209–229.

[112] Vanderlugt, L., Miller, D. Epitope spreading in immune-mediated diseases:implications for immunotherapy. *Nat Rev Immunol* **2 (**2002): 85–95.

[113] Kidd, A., Ho, P., Sharpe, O., Zhao, X., Tomooka, H., Kanter, L., Steinman, L., Robinson, H. Epitope spreading to citrullinated antigens in mouse models of autoimmune arthritis anddemyelination. *Arthritis Res Ther* **10 (**2008): R119.

[114] Pollinger, B., Krishnamoorthy, G., Berer, K., Lassmann, H., Bosl, M.R., Dunn, R., Domingues, H.S., Holz, A., Kurschus, F.C., Wekerle, H. Spontaneous relapsing-remitting EAE in the SJL/J mouse: MOG-reactive transgenic T cells recruit endogenous MOG-specific B cells. *J Exp Med* **206** (2009): 1303–1316.

[115] Steinman, L. Multiple sclerosis. Presenting an odd autoantigen. *Nature* **375 (**1995): 739–740.

[116] Bernard, C.C., Johns, T.G., Slavin, A., Ichikawa, M., Ewing, C., Liu J., Bettadapura, J. Myelin oligo-dendrocyte glycoprotein: a novel candidate autoantigen in multiple sclerosis. *J Mol Med* **75** (1997): 77–88.

[117] Gori F, Mulinacci B, Massai L, Avolio C, Caragnano M, Peroni E, Lori S, Chelli M, Papini AM, Rovero P, Lolli F. IgG and IgM antibodies to the refolded MOG(1-125) extracellular domain in humans. *J Neuroimmunol.* **233** (2011): 216-220.

[118] Mendel, I., Kelero de Rosbo, N., Ben-Nun, A. A myelin oligodendrocyte glycoprotein peptide induces typical chronic experimental autoimmune encephalomyelitis in H-2b mice: fine

specificity and T cell receptor V beta expression of encephalitogenic T cells. *Eur J Immunol*. **25** (7) (1995): 1951-1959.

[119] Rizzolo, F., Testa, C., Lambardi, D., Chorev, M., Chelli, M., Rovero, P., Papini, A.M. Conventional and microwave-assisted SPPS approach: a comparative synthesis of PTHrP(1-34)NH(2). *J Pept Sci* **17 (10)** *(*2011): 708-714.

[120] Kaiser T, Nicholson G, Kohlbau H, Voelter W, Racemization studies of Fmoc-Cys(Trt)-OH during stepwise Fmoc-solid phase peptide synthesis. *Tetrahedron Lett* **37** (1996): 1187-1190.

[121] Musiol H.-J, Siedler F, Quarzago D, Moroder L. Redox-active bis-cysteinyl-peptides. I. Synthesis of cyclic cystinyl-peptides by conventional methods in solution and on solid supports. *Biopolymers* **34 (**1994): 1553-1562.

[122] Angell YM, Alsina J, Baranu G, Albericio F, Practical protocols for stepwise solid-phase synthesis of cysteine-containing peptides. *J Pept Res* **60** (2002): 292–299.

[123] Louis A. Carpino and Aymanel El-Faham, The Diisopropylcarbodiimide /1-Hydroxy-7-azabenzotriazole system: segment coupling and stepwise peptide assemply. *Tetraedron* **55 (**1999): 6813-6830.

[124] Subirós-Funosas, R., Prohens, R., Barbas, R., El-Faham, A., Albericio, F. Oxyma: an efficient additive for peptide synthesis to replace the benzotriazole-based HOBt and HOAt with a lower risk of explosion. *Chemistry*. **15(37)** (2009): 9394-9403.

[125] Rentier, C., Pacini, G., Nuti, F., Peroni, E., Rovero, P., Papini, AM. Synthesis of diastereomerically pure Lys(Nε -lipoyl) building blocks and their use in Fmoc/tBu solid phase synthesis of lipoyl-containing peptides for diagnosis of primary biliary cirrhosis. *J Pept Sci*. **21** (2015): 408-414.

[126] Gori F., Mulinacci, B., Massai, L., Avolio, C., Caragnano, M., Peroni, E., Lori, S., Chelli, M., Papini, A.M., Rovero, P., Lolli, F. IgG and IgM antibodies to the refolded MOG(1-125) extracellular domain in humans. *J Neuroimmunol.* **233** (2011): 216-220.

[127] Dyson, J., Cross, J., Houghten, A., Wilson, A., Wright, E., Lerner, A. The immunodominant site of a synthetic immunogen has a conformational preference in water for a type-II reverse turn. *Nature*.; **318 (6045)** (1985): 480-483.

[128] Dyson, J., Lerner, A., Wright, E. The physical basis for induction of protein-reactive antipeptide antibodies. *Annu Rev Biophys Biophys Chem*. **17** 1988): 305-324.

[129] Aharoni, R., Vainshtein, A., Stock, A., Eilam, R., From, R., Shinder, V., Arnon, R. Distinct pathological patterns in relapsing-remitting and chronic models of experimental autoimmune enchephalomyelitis and the neuroprotective effect of glatiramer acetate. *J. Autoimmun*. **37** (2011): 228-241.

[130] Mendel, I., Kelero de Rosbo, N., Ben-Nun, A. A myelin oligodendrocyte glycoprotein peptide induces typical chronic experimental autoimmune encephalomyelitis in H-2b mice: fine

specificity and T cell receptor V beta expression of encephalitogenic T cells. *Eur J Immunol*. **25 (7)** (1995): 1951-1959.

[131] Ilyas, A., Quarles, H., MacIntosh, D., Dobersen, J., Trapp, D., Dalakas, C., Brady,O. IgM in a human neuropathy related to paraproteinemia binds to a carbohydrate determinant in the myelin-associated glycoprotein and to a ganglioside. *Proc. Natl. Acad. Sci. USA* **81** (1984): 1225–1229.

[132] Burger, D., Perruisseau, G., Simon, M., Steck, A.K. Comparison of the N-linked oligosaccharide structures of the two major human myelin glycoproteins MAG and P0: assessment of the structures bearing the epitope for HNK-1 and human monoclonal immunoglobulin M found in demyelinating neuropathy. *J. Neurochem.* **58** (1992): 854–861.

[133] Matà, S., Ambrosini, S., Mello, T., Lelli, F., Minciacchi, D. Anti-myelin associated glycoprotein antibodies recognize HNK-1 epitope on CNS. *J. Neuroimmunol.* **236 (**2011): 99-105.

[134] Rao, N., Anderson, M.B., Musser, J.H., Gilbert, J., Schaefer, M., Foxall, C., Brandley, B. Sialyl LewisX mimics derived from a pharmacophore search are selectin inhibitors with anti-inflammatory activity. *J. Biol. Chem.* **269** (1994): 19663–19666.

[135] Mikkelsen, L.M., Hernáiz, M.J., Martín-Pastor, M., Skrydstrup, T., Jiménez-, J. Conformation of glycomimetics in the free and protein-bound state: structural and binding features of the C-glycosyl analogue of the core trisaccharide alpha-D-Man-(1-3)-[alpha-D-Man-(1-6)]-D-Man. *J Am. Chem. Soc*. **124** (2002): 14940-51.

[136] Magnani, J.L., Ernst, B. Glucomimetic drugs – A new source of therapeutic opportunities. *Nat. Rev. Drug Discov.* **8** (2009): 247-252.

[137] Fernández-Tejada, A., Cañada, F.J., Jiménez-Barbero, J. Recent Developments in Synthetic Carbohydrate-Based Diagnostics, Vaccines, and Therapeutics. *Chemistry* **21** (2015): 10616-10628.

[138]Johnson, M.A., Pinto, B.M. Molecular mimicry of carbohydrate by peptides. *Aust. J. Chem.* **35** (2002): 13-25.

[139] Torregrossa, P., Buhl, L., Bancila, M., Durbec, P., Schafer, C., Schachner, M., Rougon, G. Selection of Poly-α 2,8-Sialic Acid Mimotopes from a Random Phage Peptide Library and Analysis of Their Bioactivity. *J. Biol. Chem.* **29** (2004): 30707-30714.

[140] Mehanna, A., Mishra, B., Kurschat, N., Schulze C., Bian, S., Loers, G., Irintchev, A., Schachner, M. Polusialic acid glycomimetics promote myelination and functional recovery after peripheral nerve injury in mice. *Brain* 132 (2009): 1449-1462.

[141] Katagihallimath, N., Mehanna, A., Guseva, D., Kleene, R., Schachner, M. Identification and validation of a Lewis x glycomimetic peptide. *J. Cell Biol.* **89** (2010): 77-86.

[142] Gomes, P., Giralt, E., Andreu D. Direct single-step surface plasmon resonance analysis of interactions between small peptides and immobilized monoclonal antibodies*J. Immunol. Methods* **235** (2000): 101–111.

[143] Rossi, G.; Real Fernandez, F.; Panza, F., Barbetti, F., Pratesi, F., Rovero P., Migliorini, P. Biosensor analysis of anti-citrullinated protein/peptide antibody affinity. *Analytical Biochemistry* **465** (2014): 96-101.

[144] Bächle, D., Loers, G., Guthöhrlein, E.W., Schachner, M., Sewald. Glycomimetic Cyclic Peptides Stimulate Neurity Outgrowth. N. *Angew. Chem. Int. Ed.* **45** (2006): 6582 –6585.

[145] Van Regenmortel, M.H.V., Muller, S. Synthetic Peptides as Antigens. Elsevier, Amsterdam (1999): 1–381.

[146] Real Fernández, F., Di Pisa, M., Rossi, G., Auberger, N., Lequin, O., Larregola, M., Benchohra, A., Mansuy, C., Chassaing, G., Lolli, F., Hayek, J., Lavielle, S., Rovero, P., Mallet, J.M., Papini,. AM. Antibody Recognition in Multiple Sclerosis and Rett Syndrome Using a Collection of Linear and Cyclic N-Glucosylated Antigenic Probes. *Biopolymers* **104 (**2015): 560-576.

[147]Loffet, A., Zhang, H.X. Allyl-based groups for side-chain protection of amino-acids. *Int. J. Peptide Protein Res.* 42 (1993): 346-351.

[148] Grieco, P., Gitu, P.M., Hruby, V.J. Preparation of 'side-chain-to-side-chain' cyclic peptides by Allyl and Alloc strategy: potential for library synthesis. *J. Peptide Res.* 57 (2001): 250-256.

[149] Royo, M., van Den Nest, W., del Fresno, M., Frieden, A., Yahalom, D., Rosenblatt, M., Chorev, M., Albericio, F. Solidphase syntheses of constrained RGD scaffolds and their binding to the α vβ 3 integrin receptor. *Tetrahedron Lett.* 42 (2001): 7387-7391.

[150] Bhunia, A., Vivekanandan, S., Eckert, T., Burg-Roderfeld, M, Wechselberger, R., Romanuka, J., Bächle, D., Kornilov, A.V, von der Lieth, C-W, Jimenez-Barbero, J., Nifantiev, N.E., Schachner, M., Sewald, N., Lütteke, T., Siebert, H-C. Why structurally different cyclic peptides can be glycomimetics of the HNK-1 carbohydrate antigen. *J. Am. Chem. Soc.* ***132*** (2010): 96–105.

[151] Hwang, T. L., Shaka, A. J. Water suppression that works. Excitation sculpting using arbitrary wave-forms and pulsed-field gradients. *J. Magn. Res.* **112** (1995): 275-279.

[152] Piantini, U., Sorensen, O.W., Ernst, R.R. Multiple quantum filters for elucidating NMR coupling network. *J. Am. Chem. Soc*. **104** (1982): 6800-6801.

[153] Marion, D., Wüthrich, K. Application of phase sensitive two-dimensional correlated spectroscopy (COSY) for measurements of 1H-1H spin-spin coupling constants in proteins. *Biochem. Biophys. Res. Commun*. ***113*** (1983): 967-974.

[154] Braunschweiler, L., Ernst, R. R. Coherence transfer by isotropic mixing: application to proton correlation spectroscopy. *J. Magn. Reson*. **53** (1983): 521–528.

[155]Jenner, J.; Meyer, B.H.; Bachman, P.; Ernst, R.R. Investigation of exchange processes by two-dimensional NMR spectroscopy. *J. Chem. Phys*. **71** (1979): 4546-4553.

[156] States, D.J., Haberkorn, R.A., Ruben, D.J. A two-dimensional nuclear overhauser experiment with pure absorption phase in four quadrants. *J. Magn. Reson*. ***48*** (1982): 286-292.

[157] Bartels, C., Xia, T., Billeter, M., Guentert, P., Wüthrich, K. The program XEASY for computer-supported NMR spectral analysis of biological macromolecules. *J. Biomol. NMR* **6** (1995): 1-10.

[158] Wüthrich, K. In *NMR of Proteins and Nucleic Acids*; John Wiley & Sons: New York, 1986.

[159] Güntert, P.; Mumenthaler C.; Wüthrich, K.; Torsion angle dynamics for NMR structure calculation with the new program DYANA. *J. Mol. Biol*. **273** (1997): 283-298.

[160] Maple, J.; Dinur, U.; Hagler, A.T. Derivation of force fields for molecular mechanics and dynamics from Ab Initio energy surface. *Proc. Natl. Acad. Sci. U.S.A*. **85** (1988): 5350-5354.

[161] Sewald, N., Jakubke, H-D. *Peptides: Chemistry and Biology.* Wiley-VCH Verlag GmbH & Co, 2002.

[162] Benoiton, L. *Chemistry of Peptide Synthesis*. Taylor & Francis Group, LLC, 2006.

[163] Barany, G., Merrifield, R. B. A new amino protecting group removable by reduction. Chemistry of the dithiasuccinoyl (Dts) function. *J Am Chem Soc **99*** **(22)** (1977): 7363–7365.

[164] Carpino, L.A., Ionescu, D., El-Faham, A. Peptide Coupling in the Presence of Highly Hindered Tertiary Amines. *J Org Chem* **61** (1996): 2460-2465.

[165] Williams, A.W., Young, G.T. The effect of solvent on the rates of racemisation and coupling of some acylamino-acid p-nitrophenyl esters; the base strengths of some amines in organic solvents, and related investigations. *J Chem Soc* **9** (1972): 1194-1200.

[166] Fischer, P. M. Diketopiperazines in Peptide and Combinatorial Chemistry, *J. Pept. Sci*, **9** (2003): 9-35.

[167] Huang, H. and Rabenstein, D.L. A cleavage cocktail for methionine-containing peptides. *J Pept Res.* 53(5) (1999): 548-53.

[168] Alewood, P.; Alewood, D.; Miranda, L.; Love, S.; Meutermans, W.; Wilson, D. Rapid in situ neutralization protocols for boc and fmoc solid-phase chemistries. *Methods Enzymol.* **289** (1997): 14–29.

[169] Palasek, S. A., Cox, Z. J., Collins, J. M. Limiting racemization and aspartimide formation in microwave-enhanced Fmoc solid phase peptide synthesis. *J. Pept. Sci.* **13** (2007): 143.

[170] Rizzolo, F., Testa, C., Lambardi, D., Chorev, M., Chelli, M., Rovero, P., Papini, A.M. Conventional and microwave-assisted SPPS approach: a comparative synthesis of PTHrP(1–34)NH_2. *J. Pept. Sci.* **17(10)** (2011): 708–714.

[171] Friligou, I., Rizzolo, F., Nuti, F., Tselios, T., Evangelidou, M., Emmanouil, M., Karamita, M., Matsoukas, J., Chelli, M., Rovero, P., Papini, A. M. Divergent and convergent synthesis of polymannosylated dibranched antigenic peptide of the immunodominant epitope MBP(83–99). *Bioorg. Med. Chem.* **21** (2013): 6718–6725.

[172] Chan, W., White, P., *Fmoc Solid Phase Peptide Synthesis. A practical Approach*. Oxford University Press, 2000**.**

[173] Downard, K. Mass Spectrometry: A Foundation Course", Royal Society of Chemistry, 2004.

[174] Fenn, J.B., Mann, M., Meng, C.K., Wong, S.F., Whitehouse, C.M. Electrospray ionization–principles and practice. *Mass Spectrometry Reviews*. 9(1) (1990): 37-70.

[175] Masamichi Yamashita, John B. Fenn Electrospray ion source. Another variation on the free-jet theme. *J. Phys. Chem.* 88 (20) (1984): 4451–4459.

[176] Alder, A.J., Greenfield, N.J., Fasman, G.D. Circular Dichroism and Optital Rotatory Dispersion of Proteins and Polypeptides. Methods *Enzymol 27 (1973): 675-735.*

[177] Nakanishi, K., Berova, N., Woody, R. Circular dichroism: principles and applications. 2nd ed. Wiley-VCH, 2000.

[178] Fasman, G.D. Circular dichroism and the conformational analysis of biomolecules. 1st ed. *Springer Science+Business Media,* 1996.

[179] Greenfield, N.J. Using circular dichroism spectra to estimate protein secondary structure. Nature protocols 1(6) (2006): 2876–90.

[180] Crowther, J. The ELISA Guidebook, New York: Humana Press, a part of Springer Science+Business Media, 2009.

[181] Engvall, E.; Perlmann, P. Enzyme-Linked Immunosorbent Assay, Elisa III. Quantitation of Specific Antibodies by Enzyme-Labeled Anti-Immunoglobulin in Antigen-Coated Tubes. *J. Immunol* **109** (1972): 129-135.

[182] Gomara, M. J. Ercilla, G. Alsina, M. A.; Haro, I. Assessment of synthetic peptides for hepatitis A diagnosis using biosensor technology. *J. Immunol. Methods* **246** (2000): 13-24.

[183] Real-Fernández, F., Passalacqua, I., Peroni, E., Chelli, M., Lolli, F., Papini, A-M., Rovero, P. Glycopeptide-Based Antibody Detection in Multiple Sclerosis by Surface Plasmon Resonance. *Sensors* **12** (2012): 5596-5607.

[184] IUPAC-IUB Joint Commission on Biochemical Nomenclature (JCBN), Nomenclature and Symbolism for Amino Acids and Peptides, Recommendations. *Eur J Biochem* **138** (1984): 9.

[185] Jones, H. A revised guide to abbreviations in peptide science and a plea for conformity. *J Pep Sci* **9** (2003): 1-8.

SUPPORTING INFORMATION

SYNTHETIC STRATEGIES TO CYCLIC PEPTIDE MIMICS OF HNK-1, A POSSIBLE SYNTHETIC ANTIGENIC PROBES FOR CHRONIC DEMYELINATION DISEASE DIAGNOSTICS

M. Ieronymaki,[a,b] E. Peroni,[a,b] F. Nuti,[a,d] G. Rossi,[a,c], P. Rovero,[a,c] and A.-M. Papini[a,b,d]

[a]*French-Italian Laboratory of Peptide & Protein Chemistry & Biology ,University of Cergy-Pontoise & University of Florence (www.peptlab.eu)*, [b]*SOSCO - EA4505, University of Cergy-Pontoise, 5 mail Gay-Lussac, Neuville-sur-Oise, 95031 Cergy-Pontoise, France,* [c]*Department NEUROFARBA, Section of Pharmaceutical Sciences, Via Ugo Schiff 6, University of Florence, I-50019 Sesto Fiorentino, Italy,* [d]*Department of Chemistry "Ugo Schiff", Via della Lastruccia 3/13, Polo Scientifico e Tecnologico, University of Florence, I-50019 Sesto Fiorentino, Italy*

Abstract

Monoclonal gammopathy of undetermined significance (MGUS) is a common age-related demyelinating sensor-motor polyneuropathy [1]. MGUS has been shown to be associated with antibodies against myelin-associated glycoproteins (MAG) and sulfated glucuronosyl paragloboside (SGPG). The HNK-1 carbohydrate epitope is a terminal 3-sulfo-glucuronyl residue attached to lactosamine structures and it is present both in MAG and SGPG [2,3]. HNK-1 plays an important role in preferential motor reinnervation [4,5] but it is difficult to be isolated and synthesized. The aim of this study is to identify a simple synthetic diagnostic tool: a mimetic of the HNK-1 epitope possibly able to recognize antibodies in neurogammopathies' sera [6]. Therefore, a series of linear and cyclic peptides, conformationally and/or structurally mimicking HNK-1, have been synthesized in solid phase using different approaches.

[1] Kyle, R. A.; Rajkumar, S. V. Immunol. Rev, **194**, 112–13 (2003)
[2] Dalakas, M.C. Press Med. doi **10**, 1016 (2013)
[3] Nobile-Orazio, E.;et al. J. Neurol. Sci., **266**, 156-163 (2008)
[4] Baumann, N. Clin.Rev.Allergy Immunol., **19**, 31-40 (2000)
[5] Rowland, L.P; Sherman, W.L.; Hays, A.P.;Lange, D.J.;Latov, N.;Trojaborg, W.;Younger, D.S. Neurology, **45**, 827-829 (1995)
[6] A.M. Papini, J. Pept. Sci., **15**, 621 (2009)

SEMI-SYNTHETIC STRATEGY TO OBTAIN ABERRANTLY N-GLUCOSYLATED MYELIN OLIGODENDROCYTE GLYCOPROTEIN: PART I: OPTIMIZATION OF THE SYNTHESIS OF Asn^{31}(Glc)hMOG(1-34)

M. Ieronymaki,[a,b] M. Larregola,[a,b] G. Pacini,[a,c] F. Burlina,[d] S. Lavielle,[d] J. Offer,[e] P. Rovero,[b,c] and A.-M. Papini[a,b,f]

[a]French-Italian Laboratory of Peptide & Protein Chemistry & Biology ,University of Cergy-Pontoise & University of Florence (www.peptlab.eu), [b]SOSCO - EA4505, University of Cergy-Pontoise, 5 mail Gay-Lussac, Neuville-sur-Oise, 95031 Cergy-Pontoise, France, [c]Department NEUROFARBA, Section of Pharmaceutical Sciences, Via Ugo Schiff 6, University of Florence, I-5019 Sesto Fiorentino, Italy, [d]Laboratory of BioMolecules, UPMC - CNRS - ENS, UMR 7203, Paris, France, [e]Division of Physical Biochemistry, MRC NIMR, London, UK, [f]Department of Chemistry "Ugo Schiff", Via della Lastruccia 3/13, Polo Scientifico e Tecnologico, University of Florence, I-50019 Sesto Fiorentino, Italy

Abstract

Multiple sclerosis (MS) is a chronic neuroinflammatory and neurodegenerative disease of the central nervous system (CNS) [1,2]. Sera from MS patients can often contain multiple types of autoantibodies. Some of these are specific for the disease and can thus be used as diagnostic biomarkers [3,4]. We have previously demonstrated that an aberrant *N*-glucosylation in a designed beta-turn peptide structure is able to detect specific autoantibodies in an MS patients' population [5]. In the meanwhile, Myelin Oligodendrocyte Glycoprotein (MOG, expressed in the outermost surface of myelin sheath) is considered to be a putative MS auto-antigen [6,7]. Nevertheless a big debate questions the role of anti-MOG Abs in MS. In order to verify a possible role of an aberrant *N*-glucosylated MOG triggering autoantibodies in MS, the semi-synthesis of the extracellular domain of MOG properly *N*-glucosylated at Asn31 (unique site of glycosylation) will be instrumental to verify our hypothesis. Therefore, we propose a "simplified" native chemical ligation approach [8] to form an amide bond between Asn^{31}(Glc)hMOG(1-34) (synthesized by SPPS) and hMOG(35-117) expressed in *E.coli*. We will report the different synthetic strategies we employed to optimize the peptide synthesis of Asn^{31}(N-Glc)hMOG(1-34).

[1] Pirko I, Lucchinetti CF, Sriram S, Bakshi R, *Neurology* ***68,*** *634* (2007)
[2] Noseworthy JH, Lucchinetti C, Rodriguez M, Weinshenker BG Multiple sclerosis. N Engl J Med. **343,** 938 (2000)
[3] A.M. Papini, *J. Pept. Sci*., ***15***, 621 (2009)
[4] F. Lolli et al. PNAS, **102**(29), 10273 (2005)
[5] F. Lolli et al. J. Neuroimmunol., **167**(1-2), 131 (2005)
[6] T.G. Johns, C.C.A. Bernard, *J. Neurochem*, ***72***, 1 (1999)
[7] Mayer MC and Meinl E, Ther Adv Neurol Disord, ***5[3]****, 147, (*2012)
[8] F. Burlina et al., Chem.Commun., **48**, 2579 (2012)

Journal of PeptideScience

Research Article

Received: 21 September 2015 Revised: 28 October 2015 Accepted: 28 October 2015 Published online in Wiley Online Library

Epitope mapping of anti-myelin oligodendrocyte glycoprotein (MOG) antibodies in a mouse model of multiple sclerosis: microwave-assisted synthesis of the peptideantigens and ELISA screening

Giulia Pacini,[a,b] Matthaia Ieronymaki,[a,b,d] Francesca Nuti,[a,c] Giuseppina Sabatino,[a,c] Maud Larregola,[a,d] Rina Aharoni,[e] Anna Maria Papini[a,c,d] and Paolo Rovero[a,b]*

The role of pathologic auto-antibodies against myelin oligodendrocyte glycoprotein (MOG) in multiple sclerosis is a highly contro-versial matter. As the use of animal models may enable to unravel the molecular mechanisms of the human disorder, numerous studies on multiple sclerosis are carried out using experimental autoimmune encephalomyelitis (EAE). In particular, the most exten-sively used EAE model is obtained by immunizing C57BL/6 mice with the immunodominant peptide MOG(35–55). In this scenario, we analyzed the anti-MOG antibody response in this model using the recombinant refolded extracellular domain of the protein, MOG(1–117). To assess the presence of a B-cell intramolecular epitope spreading mechanism, we tested also five synthetic peptides mapping the 1–117 sequence of MOG, including MOG(35–55). For this purpose, we cloned, expressed in Escherichia coli and on-column refolded MOG(1–117), and we applied an optimized microwave-assisted solid-phase synthetic strategy to obtain the de-signed peptide sequences. Subsequently, we set up a solid-phase immunoenzymatic assay testing both naïve and EAE mice sera and using MOG protein and peptides as antigenic probes. The results obtained disclose an intense IgG antibody response against both the recombinant protein and the immunizing peptide, while no response was observed against the other synthetic fragments, thus excluding the presence of an intramolecular epitope spreading mechanism. Furthermore, as the properly refolded recombinant probe is able to bind antibodies with greater efficiency compared with MOG(35–55), we hypothesize the presence of both linear and conformational epitopes on MOG(35–55) sequence.

Additional Supporting Information may be found in the online version of this article at the publisher's web site.

Keywords: myelin oligodendrocyte glycoprotein; antibodies; experimental autoimmune encephalomyelitis; epitope mapping; microwave-assisted solid-phase synthesis; enzyme-linked immunosorbent assay

Introduction

Multiple sclerosis (MS) is an inflammatory demyelinating disease of the central nervous system (CNS) with unknown etiology, thought to be autoimmune because of a critical involvement of immune response [1,2]. Extensive studies were carried out to elucidate MS immunopathology, and various animal models were developed. As both symptoms and progress of MS are highly heterogeneous [3–5], each model parallels specific aspects answering to detailed research questions. Large part of MS pathophysiology was uncov-ered using experimental autoimmune encephalomyelitis (EAE), which is the most frequently used MS model. EAE is a CD4+ T-cell-mediated inflammatory demyelinating disease of the CNS, obtained by actively immunizing animals with spinal cord

* Correspondence to: Paolo Rovero, Interdepartmental Laboratory of Peptide and Protein Chemistry and Biology – PeptLab, Florence, Italy. E-mail: rovero@unifi.it

‡ These authors contributed equally to the work.

a French-Italian Interdepartmental Laboratory of Peptide and Protein Chemistry and Biology – PeptLab, Florence, Italy and Cergy-Pontoise, France

b Department NeuroFarBa, Section of Pharmaceutical and Nutraceutical Sciences, University of Florence, Via Ugo Schiff 6, Sesto Fiorentino, Florence, I-50019, Italy

c Department of Chemistry “Ugo Schiff”, University of Florence, Via della Lastruccia 3/13, Sesto Fiorentino, Florence, I-50019, Italy

d Laboratoire de Chimie Biologique EA4505, University of Cergy-Pontoise, 5 mail Gay-Lussac Neuville-sur-Oise, Cergy-Pontoise 95000, France

e Department of Immunology, The Weizmann Institute of Science, Rehovot 76100, Israel

Abbreviations: ABS, absorbance; ACN, acetonitrile; CD, circular dichroism; DCM, dichloromethane; DIC, carbodiimmide; EAE, experimental autoimmune encephalomyelitis; EDT, 1,2-ethanedithiol; FBS, fetal bovine serum; IBs, inclusion bodies; MOG, myelin oligodendrocyte glycoprotein; MS, multiple sclerosis; MW, microwave; SP-ELISA, solid-phase enzyme-linked immunosorbent assay; TFA, trifluoroacetic acid; TIS, triisopropylsilane.

homogenates or definite myelin antigens [6–8] and characterized by high versatility [9]. Indeed, different clinical outcomes and pathological manifestations can be obtained depending on the following aspects: (i) species and genetic background of the selected animal, (ii) antigen used for the immunization and (iii) immunization protocol [10]. As far as antigens are concerned, a stepwise reduction of the complexity was obtained, switching from crude brain tissue to myelin proteins such as myelin basic protein, myelin oligodendrocyte glycoprotein (MOG) and proteolipid protein, up to short peptides comprising their encephalitogenic segments. The latter approach, based on well-characterized immunizing agents, enabled to obtain more reproducible models, mirroring specific MS features [9,11]. A prevalent EAE model is obtained by actively immunizing C57BL/6 mice with a 21-mer peptide, representing a partial sequence of mouse MOG, described as the immunodominant epitope of this protein: MOG(35–55) [12]. This protocol leads to a pathology resembling chronic progressive MS disease course [13,14]. While the CD4+ T-cell response in this model is well characterized [15,16], the significance of anti-myelin antibodies and, in particular, anti-MOG antibodies is still a matter of debate [17–19], emphasizing the highly controversial issue of a putative pathogenetic role of anti-MOG antibodies in MS [17,20,21]. Indeed, because both B-cell-deficient and complement-deficient C57BL/6 mice immunized with MOG(35–55) display normal susceptibility to EAE [22,23], it can be assumed that anti-MOG antibodies are not essential to develop the disorder [15,24]. However, the demyelinating activity of anti-MOG antibodies was largely demonstrated both in vitro and in other animal models [25–29], highlighting the possible role of secondary humoral response against MOG in worsening disease severity also in C57BL/6 model.

In this context, we evaluated the presence of anti-MOG antibodies in C57BL/6 EAE mice model testing the antibody response to the extracellular portion of MOG, i.e. MOG(1–117), expressed in Escherichia coli and properly refolded. Moreover, in order to assess the presence of a B-cell epitope spreading mechanism, i.e. the occurrence of a response directed toward epitopes distinct from the disease-inducing agent, we synthesized and tested as antigenic probes also five synthetic peptides covering the 1–117 sequence of MOG.

Experimental Section

Materials and Methods

All Fmoc-protected amino acids, Fmoc-Wang resins, carbodiimmide (DIC) and Oxyma were purchased from Iris Biotech GmbH (Marktredwitz, Germany). The following amino acid side-chain-protecting groups were used: OtBu (Asp, Glu), tBu (Ser, Thr), Pbf (Arg), Trt (Gln, His) and Boc (Lys). Peptide synthesis grade N, N-dimethylformamide (DMF) was purchased from Scharlau (Barcelona, Spain); acetonitrile (ACN) was purchased from Carlo Erba (Milan, Italy); dichloromethane (DCM), trifluoroacetic acid (TFA) and piperidine were purchased from Sigma-Aldrich (Milan, Italy). The scavengers for cleavage of peptides from resin, 1,2-ethanedithiol (EDT) and triisopropylsilane (TIS), were purchased from Acros Organics (Geel, Belgium). Solid-phase ELISA (SP-ELISA) assays were performed using 96-well plates NUNC Maxisorp (Sigma-Aldrich, St. Louis, MO, USA). Washings steps were performed with Hydroflex microplate washer (Tecan, Männedorf, Switzerland). Fetal bovine serum (FBS) was purchased from Euroclone (Milan, Italy). Anti-mouse IgG and IgM alkaline phosphatase conjugates were purchased by Sigma-Aldrich (Milan, Italy). p-Nitrophenyl phosphate was purchased from Fluka (Milano, Italy). Absorbance (ABS) values were measured on a Sunrise Tecan ELISA plate reader purchased from Tecan (Tecan Italia, Milano, Italy). Electrocompetent ER2566 E. coli cells were purchased from New England Biolabs (Ipswich, MA, USA). Plasmid pET-22 was purchased from Novagen (Madison, WI, USA). Protein purification and refolding were performed using a Chelating Sepharose Fast Flow column on ÄktaBasic chromatography system (GE Healthcare, Milan, Italy). The far-UV circular dichroism (CD) spectra were recorded by using a J-810 Jasco spectropolarimeter (JASCO, Easton, MD). C57BL/6 mice were purchased from Harlan (Jerusalem, Israel).

MW-assisted Solid-phase Peptide Synthesis

General protocol

The MOG peptides 2–6 (Table 1) were synthesized on a 0.1-mmol scale (5 eq of activator and amino acid) by a high-efficiency solid-phase peptide synthesis (SPPS) strategy, using a Liberty Blue™ automated microwave (MW) synthesizer (CEM Corporation, Matthews, NC, USA) following the Fmoc/tBu methodology. The reactions were performed in a Teflon vessel and mixed by N_2 bubbling. Reaction temperatures were monitored by an internal fiber optic sensor. The syntheses were performed on Fmoc-Gly-Wang resin (0.44 mmol/g), Fmoc-Lys(Boc)-Wang resin (0.7 mmol/g), Fmoc-Thr (tBu)-Wang resin (0.7 mmol/g), Fmoc-Gly-Wang resin (0.6 mmol/g), Fmoc-Asp(tBu)-Wang resin (0.8 mmol/g) and Fmoc-Lys(Boc)-Wang resin (0.7 mmol/g) for the analogues 1–6, respectively. The resins were swelled with DMF (1 ml/100 mg of resin) for 20 min.

Table 1. Synthetic antigens sequences and analytical data

No.	Antigen	Sequence	HPLC Rt (min)	ESI-MS $[M + 2H]^{2+}$ (m/z) found (calcd)
2	MOG(1–34)	GQFRVIGPGYPIRALVGDEAELPCRISPGKNATG	4.02[a]	1770.2 (1769.9)
3	MOG(35–55)	MEVGWYRSPFSRVVHLYRNGK	3.88[a]	1291.0 (1291.1)
4	MOG(56–75)	DQDAEQAPEYRGRTELLKET	3.23[b]	1175.2 (1175.1)
5	MOG(76–95)	ISEGKVTLRIQNVRFSDEGG	3.53[b]	1103.3 (1103.1)
6a	MOG(96–117)	YTSFFRDHSYQEEAAMELKVED	3.60[a]	1348.1 (1348.1)
6b	MOG(96–117)K_4	YTSFFRDHSYQEEAAMELKVEDKKKK	3.17[c]	1604.3 (1604.3)

Analytical HPLC conditions: column, Kinetex C_{18} (2.6 μm × 100 mm); solvent systems, A: 0.1% TFA in H_2O, B: 0.1% TFA in CH_3CN; flow rate 0.6 ml/min.
[a]Gradient 20–70% B in 5 min.
[b]Gradient 10–60% B in 5 min.
[c]Gradient 25–70% B in 5 min.

Journal of PeptideScience

A general coupling cycle was initiated with a double deprotection step with 20% piperidine in DMF, for 15 s at 75 °C using 155 W, followed by 50 s of a fresh deprotection solution at 90 °C reached with 30 W. Three washes with DMF and N_2 bubbling were performed. Fresh stock solutions of the Fmoc-protected amino acids (0.2 M), Oxyma (1 M) and DIC (0.5 M) in DMF were prepared in separated bottles and used as reagents during the SPPS. The MW-SPPS protocol (Table 2) consisted of two coupling steps (standard coupling), performed firstly at 75 °C for 15 s using 170 W and then at 90 °C for 110 s using 30 W. The same coupling conditions were used for all amino acids except Arg, His and Cys residues for which specific parameters were required. Arg double coupling MW method comprised a 25-min coupling step at 25 °C and afterwards a second one for 2 min at 75 °C using 30 W. For the His and Cys couplings, a longer coupling time (7 min) was utilized at room temperature for the first 2 min followed by 5 min at 50 °C using 35 W. One wash was performed after the coupling step with DMF and N_2 bubbling. A standard cycle time (deprotection, washes DMF (3×); coupling, wash DMF (1×)) was slightly longer than 4 min.

Deprotection, cleavage, purification and characterization of peptides

Cleavage from the resin and side-chain deprotection were achieved by treatment with a TFA/TIS/water solution (95 : 2.5 : 2.5 v/v/v, 1 ml/100 mg of resin-bound peptide) for the peptides 3 and 4 and a TFA/TIS/EDT/water solution (95 : 1 : 2 : 2 v/v/v/v, 1 ml/100 mg of resin-bound peptide) for the others. The cleavage was carried out approximately for 5 h with vigorous shaking at room temperature. The resin was filtered, and the combined filtrates were concentrated by flushing with N_2. The crude peptides were precipitated from the cleavage mixture by addition of ice-cold Et_2O, centrifuged, washed with ice-cold Et_2O (×3), dried and lyophilized.

Lyophilized crude peptides were pre-purified by solid-phase extraction with an RP-18 LiChroprep silica column from Merck (Darmstadt, Germany) via Armen system (ARMEN GLIDER FLASH AGF/IMbO6, Saint-Avé, France) working at 20 ml/min using as solvent system H_2O (MiliQ) (A)/CH_3CN (B) and a gradient of 0–60% of B. The final purification of the peptides was performed by semi-preparative Waters RP-HPLC (Milford, MA, USA) on a Phenomenex Jupiter $^{\circ}_{18}$ (10 μm, 250 mm × 10 mm) column (Phenomenex, Castel Maggiore, Italy) at 4 ml/min. The solvent systems used were 0.1% TFA in H_2O (A) and 0.1% TFA in CH_3CN (B), and the gradients used are presented in Table 1. All peptides were obtained with a purity >95%.

Characterization of the peptides was performed by analytical Waters Alliance RP-HPLC (model 2695) with UV detection at 215 nm, coupled with an ESI-MS detector (Micromass ZQ, Waters) using a Kinetex C18 (2.6 μm × 100 mm) column at 35 °C, with a flow rate of 0.6 ml/min. The total run time of the analysis was 5 min, and the solvent systems used were 0.1% TFA in H_2O (A) and 0.1% TFA in ACN (B). The analytical data are reported in Table 1. Data were acquired and processed using MassLynx software (Waters).

Table 2. MW-assisted SPPS protocol

	Power (W)	Time (s)	Temperature (°C)
Standard coupling	170	15	75
	30	110	90
Cys and His coupling	0	120	25
	35	300	50
Arg coupling	0	1500	25
	30	120	75
Deprotection	155	15	75
	30	50	90

Animal Model

Experimental autoimmune encephalomyelitis was induced as previously described [11,13]. Briefly, C57BL/6 female mice, 8–12 weeks of age, were immunized with a peptide encompassing amino acids 35–55 of MOG. Mice were injected subcutaneously at the flank, with a 100-μl emulsion containing 300 μg of MOG(35-55) peptide in complete Freund's adjuvant enriched with 4 mg/ml of heat-inactivated Mycobacterium tuberculosis. Pertussis toxin (Sigma-Aldrich), 250 ng per mouse, was injected intravenously immediately after the encephalitogenic injection and 48 h later. Mice were examined daily. EAE was scored as follows: 0, no disease; 1, loss of tail tonicity; 2, hind limb paralysis; 3, hind leg paralysis with hind body paresis; 4, hind and foreleg paralysis; and 5, death. Mice showing definite EAE manifestations were bled 2–4 weeks after disease induction, and their sera were analyzed.

Recombinant MOG(1–117) Expression and Refolding

MOG(1–117) cDNA was subcloned into the His-tag expression vector pET-22. Recombinant MOG(1–117) protein was produced and refolded according to the protocol published by Gori et al. [30]. Briefly, ER2566 electrocompetent cells were transformed with pET-22rMOG(1–117)$(His)_6$ plasmid. As the protein was overexpressed in inclusion bodies (IBs), cells were disrupted by sonication, and IBs were purified by repetitive steps of centrifugation and resuspension in 50 mM Tris, 0.5 M NaCl, 0.5% lauryldimethylamine oxide and pH 8.0. IBs were then solubilized in a denaturating buffer (100 mM NaH_2PO_4, 10 mM Tris, 6 M guanidine HCl, 40 mM mercaptoethanol and pH 8.0). Protein refolding was achieved, loading solubilized IBs onto an affinity chromatography column under a gradient of denaturating buffer (100 mM NaH_2PO_4, 10 mM Tris, 6 M guanidine HCl and pH 8.0) versus nondenaturating solution (100 mM NaH_2PO_4, 10 mM Tris, 3 mM reduced glutathione and pH 8.0) over 10 h. Properly folded protein was subsequently eluted with 0.5 M imidazole in 100 mM NaH_2PO_4, 10 mM Tris and 0.2 M NaCl (pH 8.0). Protein fractions obtained were pooled and checked by 12% SDS-PAGE and then dialyzed against phosphate buffered saline (PBS) (pH 8). Identity and integrity of the protein were checked by mass spectrometry (data not shown), as previously described [30].

Circular Dichroism Spectroscopy

Circular dichroism spectra were recorded on a Jasco J-810 spectropolarimeter equipped with a thermostated cell holder and connected to a PC for signal averaging and processing. All spectra were recorded in the 190- to 250-nm range employing quartz cuvette of 0.1-cm optical path length. Recombinant MOG(1–117) and MOG(35–55) were analyzed at 0.2 mg/ml in PBS. Far-UV CD spectra were recorded at 25 °C, with a cell path length of 0.1 cm. Scans were acquired using a 50-nm/min scanning speed and 1-nm data pitch. Each curve is the mean of ten spectra.

ELISA Assays

Serum was obtained from nine naïve C57BL6/J mice and 47 C57BL6/J mice immunized with MOG(35–55) peptide. Samples were stored at −20 °C until use. Recognition of recombinant MOG (1–117) and MOG peptides 2–7 by serum antibodies was evaluated

by SP-ELISA; 1 ug per well of antigen (peptide or protein) was dissolved in coating buffer (12 mM Na_2CO_3, 35 mM $NaHCO_3$ and pH 9.6); then 100 μl of solution was dispensed in each well of 96-well Maxisorp plates (NUNC Maxisorp; Sigma-Aldrich, Milan, Italy). Plates were incubated at 4 °C overnight. Subsequently, plates were washed three times with washing buffer (0.9% NaCl and 0.01% Tween 20) and blocked 1 h at room temperature with 100 μl per well of FBS buffer (10% FBS in washing buffer). FBS buffer was removed, and 100 μl per well of diluted sera sample (1 : 100 in FBS buffer) was dispensed. Blank wells were included in all the plates and were obtained using FBS buffer instead of serum. Plates were incubated at 4 °C overnight and then washed three times with washing buffer; 100 μl per well of secondary antibodies diluted in FBS buffer (anti-mouse IgG 1 : 30000 and anti-mouse IgM 1 : 7500) was dispensed, and plates were incubated 3 h at room temperature. Plates were washed three times with washing buffer; then 100 μl per well of substrate solution (1 mg/ml p-PNP in substrate buffer: 1 M diethanolamine, 1 mM $MgCl_2$ and pH 9.8) was dispensed. Plates were incubated for 15–40 min at room temperature, and then the absorbance (ABS) of each well was red with a multichannel ELISA reader (Tecan, Männedorf, Switzerland) at 405 nm. ABS value for each serum was calculated as (mean ABS of triplicate) minus (mean ABS of blank triplicate).

Results

Animal Model

Humoral response to MOG was investigated using the EAE chronic (non-remitting) model induced by MOG(35 55) peptide. In this model, clinical manifestations, e.g. tail limping, are typically revealed 9 12 days after disease induction and increase in severity, reaching hind limb paralysis or complete limb paralysis by days 14-28. Mice showing definite EAE manifestations were bled 2-4 weeks after disease induction, and antibody response was studied and compared with that of naïve controls.

Antigens Design and Preparation

To obtain recombinant MOG protein, the cDNA of the 1–117 extracellular portion of rat MOG was subcloned into the His-tag expression vector pET-22. The choice to use a shortened protein fragment compared with the canonical extracellular domain 1–125 was inspired by an attempt to avoid the solubility issues characterizing MOG(1–125), which comprises a highly hydrophobic transmembrane portion ($F^{119}YWI^{122}$). The removal of this short sequence leads to a more soluble recombinant product that is more appropriate to be employed as antigen in immunological solid-phase assays. The final product was refolded according to the protocol that we have previously reported [30], using a gradient of denaturating buffer versus nondenaturating buffer over 10 h on a nickel–nitrilotriacetic acid affinity chromatography column.

The choice of the synthetic peptides used to map the sequence of MOG(1–117), reported in Table 1, was guided by the immunizing peptide MOG(35–55), which was previously described as the immunodominant portion of MOG [12] and thus was included among our test peptides.

Next, we decided to split the C-terminal 56–117 in three 20-mer portions and to analyze separately the residual N-terminal fragment, MOG(1–34). As peptide 6a displayed solubility issues, we decided to enhance the solubility of the sequence adding a C-terminal 4-Lys tag (peptide 6b), as previously reported [31]. Although the synthesis of the MOG peptide fragments 2–6b was not expected to be particularly demanding, we decided to use an optimized process for SPPS using MW irradiation combined with the Fmoc/tBu strategy. Crude peptides were purified to homogeneity (final HPLC purity >95%) and characterized by analytical RP-HPLC with UV detection at 215 nm, coupled with ESI-MS. Analytical data are reported in Table 1.

Solid-phase Enzyme-linked Immunosorbent Assay

The presence of antibody response against recombinant refolded MOG(1–117) and MOG peptides in EAE mice sera was evaluated by SP-ELISA strategy, using a method optimized in our lab with both recombinant MOG [30] and synthetic peptides. Briefly, each antigen was adsorbed on 96-well polystyrene plates and incubated first with diluted sera and then with anti-IgG or anti-IgM secondary antibodies to assess the auto-antibody response. Sera from naïve mice were included in each plate as normal controls. The immunological homology between peptides 6a and 6b was preliminarily evaluated on seven representative EAE mice sera (Figure S1). Subsequently, antigens were tested on a cohort of 47 EAE mice sera, together with nine naïve mice sera as control, measuring separately IgG and IgM.

In the case of IgG, strong responses to both the immunizing peptide 3 and the refolded recombinant protein were obtained in sera of all the EAE-induced mice (manifesting clinical scores 2–4) at all the time points tested (2–4 weeks after disease induction), while we were not able to detect antibodies to any of the other peptide fragments (Figure 1). Interestingly, the response against MOG(1–

against the peptide MOG(35–55). Conversely, no significant IgM re-

To estimate the secondary structure of recombinant MOG(1–117) and synthetic MOG(35–55), CD spectra were recorded for both molecules in the far-UV region (240 to 190 nm). Both protein and

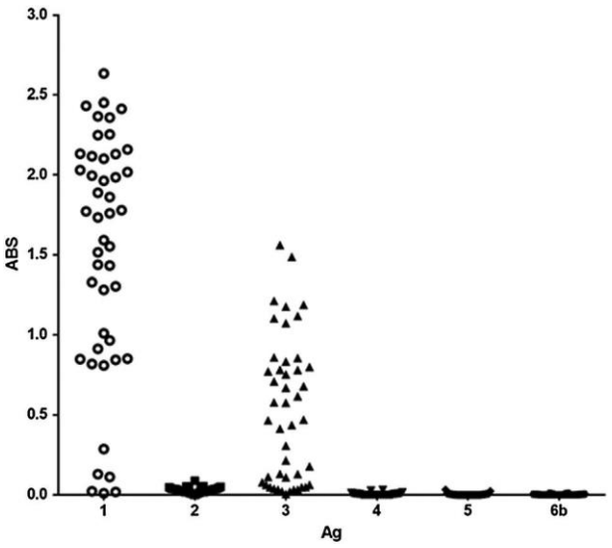

Figure 1. IgG response against recombinant protein MOG(1–117) (1) and peptides mapping the 1–117 sequence (2, 3, 4, 5 and 6b) in EAE mice.

Journal of PeptideScience

peptide were studied at the same concentration in PBS at 25 °C. According to the previously published CD results on MOG(1–125) [30], refolded recombinant MOG(1–117) displays a beta-sheet conformation, characterized by a minimum at 218 nm and a positive peak near 200 nm. Conversely, we have assessed that MOG(35–55) displays a random coil conformation, characterized by a negative peak around 195 nm (data not shown).

Discussion

Myelin oligodendrocyte glycoprotein is one of the most studied candidate antigens in the case of demyelinating autoimmune disorders, especially MS [17–21]. The hypothesis of MOG involvement in MS autoimmune reaction is due to the exposition of its IgG-like extracellular domain on the outermost surface of myelin sheath, allowing the access of potential auto-antibodies to the protein [32]. Despite the numerous studies aimed to characterize the pathological antibody response to MOG in MS, the role of this protein is still highly controversial. To unravel the complexity of MS pathophysiology, several animal models were developed, each of which parallels specific MS aspects [9]. In this context, we attempted to elucidate the anti-MOG antibody response using a widely used MS animal model, i.e. EAE induced by active immunization with MOG(35–55) peptide in C57BL/6 mice, which mirrors aspects of chronic progressive MS. In particular, we analyzed the antibody response to MOG using as antigen the recombinant and properly refolded extracellular domain of the protein, MOG(1–117). The use of a correctly folded antigen enables to characterize both linear and conformational epitopes. In parallel, to accurately map the region recognized by anti-MOG antibodies, we split the sequence into five peptide fragments: MOG(1–34), MOG(35–55), MOG(56–75), MOG(76–95) and MOG(96–117). This approach allowed us to investigate the possible involvement of an intramolecular epitope spreading phenomenon in EAE pathogenesis. Indeed, epitope spreading is physiologically required for an effective adaptive response [33], but its involvement is also documented in many autoimmune disorders [34,35], including MS [36,37] and several EAE models [38,39]. In this context, the significance of T-cell epitope spreading in autoimmunity was extensively evaluated, while the B-cell counterpart is poorly understood [33].

Concerning the recombinant antigens production, we have successfully cloned, expressed in E. coli and refolded the extracellular 1–117 portion of MOG protein, following our previously published protocol [30]. Furthermore, our study reports for the first time the synthesis of MOG peptides performed using an optimized protocol, based on MW irradiation in both coupling and deprotection steps, which enables to obtain peptides with satisfying crude purity (40–65%) in reasonably short time and, most importantly, limiting solvent consumption. In fact, this protocol allows not only a significant reduction (~90%) in total chemical waste but also the completion of a cycle in approximately 4 min. Specifically, the coupling reaction is performed in two short coupling steps at 90 °C and not in one longer step at 75 °C, as previously reported [40]. These conditions were applied to all amino acids except His, Cys and Arg residues, for which specific parameters are required. Racemization of the amino acid residues during the coupling reaction has been extensively documented [41–43]. Various factors, including the electron-withdrawing effect of the amino acid side chain, the temperature and solvent of the reaction and the activator base, could affect the degree of racemization, because an increase of Cys and His epimerization was detected in coupling reactions performed at high temperature. Therefore, the coupling of both Cys and His residues was performed at 50 °C. Once these amino acids are incorporated into the peptide chain, they are protected from epimerization at higher temperatures. Moreover, the nucleophilic side chain of Arg is susceptible to δ-lactam formation during the coupling reaction [41]. In order to protect the activated Arg derivative from MW energy, a first coupling was performed at conventional conditions (25 min at room temperature); then MW energy was applied for 2 min. A second coupling was typically performed to ensure that deletion sequences, resulting from lactam formation, are minimized. The activation was performed with the well-known DIC-based [44] techniques with Oxyma [45], not only because of derivatives like HOBt and HOAt classified as Class 1c explosives but also because of the stability of these reagents at elevated temperatures. The deprotection step was carried out with 20% piperidine in DMF, employing a short initial MW deprotection step for 15 s at 75 °C followed by a second 50-s deprotection at 90 °C. In the end, it is worthy to highlight that the cleavage from the resin of the crude peptides containing more than one Arg residue requested approximately 5 h because of the uncompleted removal of the Pbf side-chain protecting group after 2 h.

Solid-phase ELISA results obtained testing the recombinant protein and its synthetic fragments as antigenic probes on EAE mice sera revealed the presence of a specific IgG response against the immunizing peptide MOG(35–55) and the recombinant protein MOG(1–117), while no response was detected against the other peptide antigens. Notably, the antibody titer revealed against the recombinant protein is higher than the one obtained against the immunizing peptide. The higher antibody titers detected by the refolded protein allow us to hypothesize the presence of both linear and conformational epitopes within the 35–55 region of MOG, recognized by auto-antibodies in EAE mice sera. Indeed, the recombinant refolded protein is able to reproduce both the primary amino acid sequence and the conformation of the native antigen and to correctly expose the latter in the context of the solid-phase ELISA coating phase. Conversely, the MOG(35–55) peptide appears to be able to reproduce only a linear, short portion of the protein but is unable to mimic a conformational epitope on the ELISA plate. Conformational differences between MOG(1–117) and MOG(35–55) were confirmed using CD spectroscopy, which revealed that the recombinant protein has a β-sheet conformation, while the immunizing peptide displays a random coil conformation. It is well known that short synthetic peptides used as immunogenic agents are able to elicit an antibody response against their corresponding sequence on the full-length folded protein [46,47]. Indeed, the peptide in solution typically assumes a random coil conformation but may also adopt other conformations, among which the folded one, because of its extreme flexibility, and thus during the immunization procedure, the peptide can trigger an immunological reaction not only against linear epitopes but also against conformational epitopes. Conversely, the peptide coated on the ELISA plate is more constrained, and it can hardly adopt the original folded conformation. Consequently, the recombinant protein, mimicking both structure and sequence of the native antigen, is able to detect antibodies with greater efficiency, as compared with the peptide. Indeed, the ability of the free peptide to adopt in solution the conformation recognized by the antibody can be tested using more elaborate experiments, such as competition ELISA, which however are beyond the scope of this study, mostly focused on epitopes different from the well-known immunodominant sequence MOG(35–55) and possibly recognized by antibodies in the context of an intramolecular epitope spreading mechanism.

Taken together, these considerations enable us to assert the lack of a MOG intramolecular epitope spreading phenomenon in the case of the examined MS animal model, as we were able to detect IgG against the immunizing peptide and the recombinant protein, but not against the peptides mapping other portions of the examined sequence.

The presence of an immunological response against both MOG (35–55) and refolded MOG(1–117) allows us to hypothesize that the immunization procedure with MOG(35–55) peptide is able to elicit an antibody response against both linear and conformational epitopes, confirming the immunodominance of this epitope.

Acknowledgements

ANR Chaire d'Excellence PeptKit 2009–2014 (grant no. ANR-09-CEXC-013-01 to A. M. P.) and Ente Cassa di Risparmio di Firenze are gratefully acknowledged for their financial support.

References

1 Hohfeld R, Wekerle H. Autoimmune concepts of multiple sclerosis as a basis for selective immunotherapy: from pipe dreams to (therapeutic) pipelines. Proc. Natl. Acad. Sci. U. S. A. 2004; 101 (Suppl.2): 14599–14606.
2 Lassmann H, Brück W, Lucchinetti CF. The immunopathology of multiple sclerosis: an overview. Brain Pathol. 2007; 17: 210–218.
3 Compston A, Coles A. Multiple sclerosis. Lancet 2008; 372(9648): 1502–1517.
4 Lublin FD, Reingold SC. Defining the clinical course of multiple sclerosis: result of an international survey. National Multiple Sclerosis Society (USA) advisory committee on clinical trials of new agents in multiple sclerosis. Neurology 1996; 46(4): 907–911.
5 O'Connor P. Canadian Multiple Sclerosis Working Group. Key issues in the diagnosis and treatment of multiple sclerosis. An overview. Neurology 2002; 59(6 Suppl 3): S1–S33.
6 Mix E, Meyer-Rienecker H, Hartung HP, Zettl UK. Animal models of multiple sclerosis – potentials and limitations. Prog. Neurobiol. 2010; 92(3): 386–404.
7 Batoulis H, Recks MS, Addicks K, Kuerten S. Experimental encephalomyelitis – achievements and prospective advances. APMIS 2011; 119(12): 819–830.
8 Constantinescu CS, Farooqi N, O'Brien K, Gran B. Experimental autoimmune encephalomyelitis (EAE) as a model for multiple sclerosis. Br. J. Pharmacol. 2011; 164(4): 1079–1106.
9 Wekerle H, Kojima K, Lannes-Vieira J, Lassmann H, Linington C. Animal models. Ann. Neurol. 1994; 36(Suppl): S47–S53.
10 Robinson AP, Harp CT, Noronha A, Miller SD. The experimental autoimmune encephalomyelitis (EAE) model of MS: utility for understanding disease pathophysiology and treatment. Handb. Clin. Neurol. 2014; 122: 173–189.
11 Aharoni R, Vainshtein A, Stock A, Eilam R, From R, Shinder V, Arnon R. Distinct pathological patterns in relapsing-remitting and chronic models of experimental autoimmune encephalomyelitis and the neuroprotective effect of glatiramer acetate. J. Autoimmun. 2011; 37: 228–241.
12 Adelmann M, Wood J, Benzel I, Fiori P, Lassmann H, Matthieu JM, Gardinier MV, Dornmair K, Linington C. The N-terminal domain of the myelin oligodendrocyte glycoprotein (MOG) induces acute demyelinating experimental autoimmune encephalomyelitis in the Lewis rat. J. Neuroimmunol. 1995; 63(1): 17–27.
13 Mendel I, Kelero de Rosbo N, Ben-Nun A. A myelin oligodendrocyte glycoprotein peptide induces typical chronic experimental autoimmune encephalomyelitis in H-2b mice: fine specificity and T cell receptor V beta expression of encephalitogenic T cells. Eur. J. Immunol. 1995; 25(7): 1951–1959.
14 Slavin A, Ewing C, Liu J, Ichikawa M, Slavin J, Bernard CC. Induction of a multiple sclerosis-like disease in mice with an immunodominant epitope of myelin oligodendrocyte glycoprotein. Autoimmunity 1998; 28: 109–120.
15 Lee DH, Linker RA. The role of myelin oligodendrocyte glycoprotein in autoimmune demyelination: a target for multiple sclerosis therapy? Expert Opin. Ther. Targets 2012; 16(5): 451–462.
16 Aharoni R. New findings and old controversies in the research of multiple sclerosis and its model experimental autoimmune encephalomyelitis. Expert Opin. Ther. Targets 2013; 9(5): 423–440.
17 Lalive PH. Autoantibodies in inflammatory demyelinating diseases of the central nervous system. Swiss Med. Wkly. 2008; 138: 692–707.
18 von Büdingen HC, Bar-Or A, Zamvil SS. B cells in multiple sclerosis: connecting the dots. Curr. Opin. Immunol. 2011; 23: 713–720.
19 Ben-Nun A, Kaushansky N, Kawakami N, Krishnamoorthy G, Berer K, Liblau R, Hohlfeld R, Wekerle H. From classic to spontaneous and humanized models of multiple sclerosis: impact on understanding pathogenesis and drug development. J. Autoimmun. 2014; 54: 33–50.
20 Mayer MC, Meinl E. Glycoproteins as targets of autoantibodies in central nervous system inflammation: MOG and more. Ther. Adv. Neurol. Disord. 2012; 5: 147–159.
21 Reindl M, Di Pauli F, Rostásy K, Berger T. The spectrum of MOG autoantibody-associated demyelinating diseases. Nat. Rev. Neurol. 2013; 9: 455–461.
22 Eugster HP, Frei K, Kopf M, Lassman H, Fontana A. IL-6-deficient mice resist myelin oligodendrocyte glycoprotein-induced autoimmune encephalomyelitis. Eur. J. Immunol. 1998; 28(7): 2178–2187.
23 Calida DM, Constantinescu C, Purev E, Zhang GX, Ventura ES, Lavi E, Rostami A. Cutting edge: C3, a key component of complement activation, is not required for the development of myelin oligodendrocyte glycoprotein peptide-induced experimental autoimmune encephalomyelitis in mice. J. Immunol. 2001; 166(2): 723–726.
24 Zhang GX, Yu S, Gran B, Li J, Calida D, Ventura E, Chen X, Rostami A. T cell and antibody responses in remitting-relapsing experimental autoimmune encephalomyelitis in (C57BL/6 x SJL) F1 mice. J. Neuroimmunol. 2004; 148(1–2): 1–10.
25 Linington C, Lassmann H. Antibody responses in chronic relapsing experimental allergic encephalomyelitis: correlation of serum demyelinating activity with antibody titre to the myelin/oligodendrocyte glycoprotein (MOG). J. Neuroimmunol. 1987; 17(1): 61–69.
26 Schluesener HJ, Sobel RA, Linington C, Weiner HL. A monoclonal antibody against a myelin oligodendrocyte glycoprotein induces relapses and demyelination in central nervous system autoimmune disease. J. Immunol. 1987; 139(12): 4016–4021.
27 Linington C, Bradl M, Lassmann H, Brunner C, Vass K. Augmentation of demyelination in rat acute allergic encephalomyelitis by circulating mouse monoclonal antibodies directed against a myelin/oligodendrocyte glycoprotein. Am. J. Pathol. 1988; 130(3): 443–454.
28 Kerlero de Rosbo N, Honegger P, Lassmann H, Matthieu JM. Demyelination induced in aggregating brain cell cultures by a monoclonal antibody against myelin/oligodendrocyte glycoprotein. J. Neurochem. 1990; 55(2): 583–587.
29 Linington C, Engelhardt B, Kapocs G, Lassman H. Induction of persistently demyelinated lesions in the rat following the repeated adoptive transfer of encephalitogenic T cells and demyelinating antibody. J. Neuroimmunol. 1992; 40(2–3): 219–224.
30 Gori F, Mulinacci B, Massai L, Avolio C, Caragnano M, Peroni E, Lori S, Chelli M, Papini AM, Rovero P, Lolli F. IgG and IgM antibodies to the refolded MOG(1–125) extracellular domain in humans. J. Neuroimmunol. 2011; 233(1–2): 216–220.
31 Rentier C, Pacini G, Nuti F, Peroni E, Rovero P, Papini AM. Synthesis of diastereomerically pure Lys(N_ε-lipoyl) building blocks and their use in Fmoc/tBu solid phase synthesis of lipoyl-containing peptides for diagnosis of primary biliary cirrhosis. J. Pept. Sci. 2015; 21: 408–414.
32 Brunner C, Lassmann H, Waehneldt TV, Matthieu JM, Linington C. Differential ultrastructural localization of myelin basic protein, myelin/oligodendroglial glycoprotein, and 2′,3′-cyclic nucleotide 3′-phosphodiesterase in the CNS of adult rats. J. Neurochem. 1989; 52(1): 296–304.
33 Cornaby C, Gibbons L, Mayhew V, Sloan CS, Welling A, Poole BD. B cell epitope spreading: mechanisms and contribution to autoimmune diseases. Immunol. Lett. 2015; 163(1): 56–68.
34 McCluskey J, Farris AD, Keech CL, Purcell AW, Rischmueller M, Kinoshita G, Reynolds P, Gordon TP. Determinant spreading: lessons from animal models and human disease. Immunol. Rev. 1998; 164: 209–229.
35 Vanderlugt CL, Miller SD. Epitope spreading in immune-mediated diseases: implications for immunotherapy. Nat. Rev. Immunol. 2002; 2: 85–95.
36 Kidd BA, Ho PP, Sharpe O, Zhao X, Tomooka BH, Kanter JL, Steinman L, Robinson WH. Epitope spreading to citrullinated antigens in mouse

models of autoimmune arthritis and demyelination. Arthritis Res. Ther. 2008; 10: R119.
37 Pollinger B, Krishnamoorthy G, Berer K, Lassmann H, Bosl MR, Dunn R, Domingues HS, Holz A, Kurschus FC, Wekerle H. Spontaneous relapsing-remitting EAE in the SJL/J mouse: MOG-reactive transgenic T cells recruit endogenous MOG-specific B cells. J. Exp. Med. 2009; 206: 1303–1316.
38 Steinman L. Multiple sclerosis. Presenting an odd autoantigen. Nature 1995; 375: 739–740.
39 Bernard CC, Johns TG, Slavin A, Ichikawa M, Ewing C, Liu J, Bettadapura J. Myelin oligodendrocyte glycoprotein: a novel candidate autoantigen in multiple sclerosis. J. Mol. Med. 1997; 75: 77–88.
40 Rizzolo F, Testa C, Lambardi D, Chorev M, Chelli M, Rovero P, Papini AM.
Conventional and microwave-assisted SPPS approach: a comparative synthesis of PTHrP(1–34)NH(2). J. Pept. Sci. 2011; 17(10): 708–714.
41 Kaiser T, Nicholson G, Kohlbau H, Voelter W. Racemization studies of Fmoc-Cys(Trt)-OH during stepwise Fmoc-solid phase peptide synthesis.
Tetrahedron Lett. 1996; 37: 1187–1190.
42 Musiol H-J, Siedler F, Quarzago D, Moroder L. Redox-active bis-cysteinyl-peptides. I. Synthesis of cyclic cystinyl-peptides by conventional methods in solution and on solid supports. Biopolymers 1994; 34: 1553–1562.
43 Angell YM, Alsina J, Baranu G, Albericio F. Practical protocols for stepwise solid-phase synthesis of cysteine-containing peptides. J. Pept. Res. 2002;
60: 292–299.

Structure-Activity Relationship Studies, SPR Affinity Characterization and Conformational Analysis of Peptides Mimicking the HNK-1 Carbohydrate Epitope

(Draft)

INTRODUCTION

The design of glycomimetic novel molecules mimicking biologically relevant glycans, is a significant approach for understanding the molecular mechanisms of important biological processes, i.e., cell-cell recognition.[1,2] This strategy may lead to new potential therapeutic and diagnostic agents. While several carbohydrate-based glycomimetics have been reported,[3,4,5,6] only a few examples of peptides mimicking glycans are present in the literature.[7] The majority of peptides-mimicking carbohydrate epitopes have been selected using monoclonal antibodies to screen phage displayed random peptide libraries.[8,9,10] In the framework of our continuing interest toward the use of synthetic peptides as immunological probes to characterize antibodies,[11] we focused our attention on peptide-based mimetics of the trisaccharide human natural killer cell-1 epitope (HNK-1, Figure 1),[12] which is considered the antigenic determinant of myelin-associated glycoprotein (MAG), a quantitatively minor component of myelin sheaths.[13] Moreover, HNK-1 was also found on neural cell adhesion molecules (NCAM), myelin protein zero (P0), extracellular matrix proteins

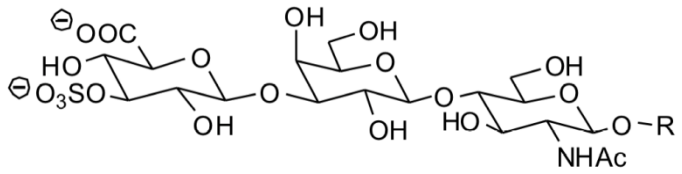

Figure 1. Structure of the trisaccharide HNK-1.

of the tenascin family, in glycolipids, i.e., the sulfate-3-glucuronyl paragloboside (SGPG),[2,14] acting as a ligand for adhesion molecules and appearing to be associated with developmental events such as outgrowth of astrocytes and neuronal processes.[15] Importantly, patients affected by autoimmune neurological disorders, such as IgM monoclonal gammopathy and demyelinating polyneuropathy often develop anti-MAG antibodies specifically targeting the HNK-1 epitope.[16,17] Therefore identification and characterisation of these antibodies is clinically relevant.[18] For this reason, since both the

chemical synthesis and the isolation from natural sources of HNK-1 appear extremely difficult and time consuming and very often can lead to inconsistent material, the development of glycomimetics of this carbohydrate is indeed a desirable goal. In fact, Simon-Haldi *et al.* selected HNK-1 peptide mimetics screening a phage-displayed peptide library with a rat monoclonal antibody,[19] while Bachle *et al.* further elaborated these linear sequences to obtain two cyclic hexapeptides, showing binding affinity to the monoclonal antibody in the high micromolar range.[20]

We report herein a structure-activity relationship (SAR) study of one of these previously reported HNK-1 mimetic peptide, based on the measurement of binding affinities by surface plasmon resonance (SPR) experiments. The final goal was the optimization in terms of binding affinity of a peptide mimicking the minimal epitope recognized by the commercially available monoclonal antibody. Subsequently this peptide could be used for the development of a novel and reliable diagnostic tool for anti-HNK-1 antibody identification in sera of patients affected by autoimmune neurological disorders.

SPR is an attractive technique for the evaluation and quantification of antigen-antibody interactions, enabling direct visualization of biomolecular interactions in real-time.[2122] The use of peptides for specific antibody recognition has been already widely employed in SPR, as exemplified by the glycopeptide-based SPR biosensor for the detection of specific antibodies in sera of patients affected by multiple sclerosis,[23] or the kinetic characterization through SPR of different antibody families in rheumatoid arthritis patients' sera, using a panel of citrullinated peptides, recently developed in our laboratory.[24]

RESULTS AND DISCUSSION

Peptide design and synthesis. The starting point of our effort to rationally design a high affinity peptide binder of the anti-HNK1 monoclonal antibody was the previously described cyclic hexapeptide c-(LSETTdL) (Entry **1** in Table 1, dL is used for D-Leu), reported to mimic the trisaccharide HNK-1 epitope.[20] Not surprisingly, the starting sequence, which mimics a carbohydrate epitope, contains amino acids with hydroxylated side chains (Ser, Thr), apolar amino acids to establish hydrophobic interactions with the target, and a Glu residue, bearing a negative charge, in the framework of the peptide backbone, with amide groups acting as hydrogen bond donors and acceptors.

Table 1. Sequences of the synthetic peptides and affinity binding constants[a] to the anti-HNK1 monoclonal antibody determined by SPR.

No	Sequence	k_a (1/Ms)	k_d(1/s)	K_D (M)
1	c-(LSETTdL)	$1.41 \cdot 10^{2}$	$1.55 \cdot 10^{-3}$	$1.09 \cdot 10^{-5}$
2	LSETTdL	$1.99 \cdot 10^{1}$	$43.6 \cdot 10^{-2}$	$2.18 \cdot 10^{-2}$
3	LSETETdL	$8.6 \cdot 10^{4}$	$0.9 \cdot 10^{-2}$	$1.04 \cdot 10^{-7}$
4	LSETETK(Ac)dL	$1.09 \cdot 10^{3}$	$50.2 \cdot 10^{-5}$	$4.62 \cdot 10^{-7}$
5	c-(LSETETK(Ac)dL)	$3.72 \cdot 10^{5}$	$40.7 \cdot 10^{-3}$	$1.09 \cdot 10^{-7}$
6	c-(LSETETKdL)	$1.05 \cdot 10^{2}$	$1.82 \cdot 10^{-3}$	$1.73 \cdot 10^{-5}$
7	c-(LSETKTdL)	$1.46 \cdot 10^{1}$	$6.30 \cdot 10^{-1}$	$4.33 \cdot 10^{-2}$
8	LSETY(OSO_3)TKdL		no interaction	
9	c-(LSETY(OSO_3)TKdL)		no interaction	
10	LSETYTKdL	$1.20 \cdot 10^{3}$	$23.0 \cdot 10^{-2}$	$1.92 \cdot 10^{-4}$
11	c-(LSETYTKdL)	$1.45 \cdot 10^{2}$	$1.0 \cdot 10^{-2}$	$6.90 \cdot 10^{-5}$
12	LSETETL	$5.16 \cdot 10^{2}$	$9.6 \cdot 10^{-4}$	$1.89 \cdot 10^{-6}$
13	Ttds-LSETETdL [b]	$8.5 \cdot 10^{2}$	$5.4 \cdot 10^{-4}$	$6.32 \cdot 10^{-7}$

[a] k_a: association rate constant, k_d: dissociation rate constant; K_D: equilibrium dissociation connt. [b] Ttds: 4,7,10-trioxa-1,13-tridecanediamino succinic acid.

Firstly, we synthesized the cyclic peptide c-(LSETTdL) (**1**) and its linear precursor LSETTdL (**2**), in order to investigate affinity differences between linear and cyclic structures. Afterward, taking into account that the HNK-1 trisaccharide bears two negatively charged functional groups, i.e. the carboxylic function and the sulfate group at positions C1 and C3, respectively, of the glucuronic acid (Figure 1), we focused our attention on the charged side chains exposed by the sugar-mimetic peptide. Accordingly, a second Glu residue was inserted into the sequence, with the aim of reproducing the trisaccharide double negative surface charge, obtaining the linear sequence LSETETdL (**3**), characterized by a net charge -2. Moreover, a Lys residue was also inserted in the sequence, with the aim of introducing a further functional group to be eventually used to covalently anchor this peptide to a solid support, such as the active surface of a sensor chip. Accordingly, to maintain a net charge of

-2 and mimic the involvement of the Lys side chain amino group in the anchoring linkage, this peptide was synthesized using acetylated Lys: LSETETK(Ac)dL (**4**). We also prepared the corresponding cyclopeptides, with either acetylated or free lysine (**5** and **6**, respectively), the latter showing net charge -1, as the parent peptide, as well as an analogue characterized by a total net charge zero, e.g., c-(LSETKTdL) (**7**). Moreover, we synthesized the linear peptide LSETY(OSO_3)TKdL (**8**) and the corresponding cyclic analog c-(LSETY(OSO_3)TKdL) (**9**), replacing the second Glu residue introduced in the sequence with Tyr(OSO_3), in an attempt to mimic more closely the sulfate group present on the glucuronic acid of the parent trisaccharide (Fig. 1). The two peptides with non-sulfated Tyr were also included (linear **10** and cyclic **11**). Finally, although it was previously described that the presence of Leu residue instead of D-Leu decreased antibody affinity,[20] we also prepared the peptide LSETETL (**12**), analogue of **3**, containing L-Leu in place of D-Leu.

All peptides were synthesized by microwave-assisted solid phase peptide synthesis, following the Fmoc/*t*Bu strategy. Cyclic peptides were synthesized following the general procedure for head-to-tail on-resin cyclization as described in the experimental section. Peptides were purified by semi-preparative RP-HPLC to obtain a final purity ≥95% and characterized by electrospray ionization mass spectrometry (ESI-MS). Analytical HPLC methods, retention times, and observed mass peaks for each peptide are summarized in Table 2.

Surface plasmon resonance experiments. Affinity measurements of binding of all the synthetic peptides to the mouse anti-HNK-1 monoclonal antibody were performed by SPR technique on a BiaCore T100 system (GE Healthcare,. Commercially available anti-HNK1 monoclonal antibodies produced in mouse (Sigma)were immobilized on the sensor chip surface following the amine coupling strategy according to the manufacturer recommendations. Synthetic peptides were flowed at different concentrations over immobilized antibodies in individual cycles of analysis based on the following steps: sample injection (association phase), washing with running buffer (dissociation step), and finally chip surface regeneration. Results reported in Table 1 were elaborated separately for each sample by fitting the experimental values to theoretical kinetic models, thus obtaining the kinetic constants and K_D values.

The results for the peptide c-(LSETTdL) (**1**) confirmed the performance of the SPR assay, since the observed K_D (1.09×10^{-5} M) is comparable to the previously published value (K_D = 6.7×10^{-5} M),[20] while the corresponding linear sequence LSETTdL (**2**) appears to be a much

weaker binder (K_D = 2.18 x 10^{-2} M), as also reported by Bachle *et al*. The linear peptide LSETETdL (**3**), bearing two negative net charges, was then tested in SPR, observing the highest affinity to the anti-HNK-1 monoclonal antibody, with K_D = 1.04 x 10^{-7} M. This result indicates that the increase in net negative charge due to the presence in the sequence of a second glutamic acid residue increases significantly the affinity for the antibody. This was confirmed by the analysis of the affinities registered for peptides c-(LSETKTdL) (**7**), K_D = 4.33 x 10^{-2} M, c-(LSETETKdL) (**6**), K_D = 1.73 x 10^{-5} M, and c-(LSETETK(Ac)dL) (**5**), K_D = 1.09 x 10^{-7} M, displaying net negative charges of 0, 1, and 2, respectively, corresponding to an affinity increase of almost 5 log units. The linear analogue of peptide **5**, LSETETK(Ac)dL (**4**), displays a slightly lower affinity, as compared to the corresponding cyclic one (**5**), but interestingly their K_D values are in the same range (K_D = 4.62 x 10^{-7} and 1.09 x 10^{-7} M, respectively), at variance with the marked difference observed in the case of the parent peptides **1** and **2**. Peptides LSETY(OSO_3)TKdL (**8**) and c-(LSETY(OSO_3)TKdL) (**9**), containing the sulfated tyrosine residue designed to mimic the sulfated glucuronic acid moiety characteristic of the HNK-1 carbohydrate, did not interact with the immobilized monoclonal anti-HNK-1 antibody, possibly because the bulky side-chain of the tyrosine residue does not fit into the antibody binding site, in spite of the presence of the sulfate moiety, as in the native sugar epitope. Surprisingly, the corresponding non sulfated peptides LSETYTKdL (**10**) and c-(LSETYTKdL) (**11**) show a weak, but significant binding interaction with the antibody (K_D = 1.92 x 10^{-4} and 6.90 x 10^{-5} M, respectively). Finally, the linear peptide bearing D-Leu instead of L-Leu, e.g., LSETETL (**11**), shows an affinity roughly one order of magnitude lower than that of the unmodified peptide **3** (K_D = 1.89 x 10^{-6} M), thus confirming the previously reported beneficial effect of a D-Leu residue in antibody interaction.[20]

Summarizing, the SPR affinity characterization of the interaction between a series of synthetic peptides and the anti-HNK1 monoclonal antibody allowed us to compare structural motifs involved in antibody recognition. The linear sequence LSETETdL (**3**), a 7-mer peptide bearing 2 net negative charges, was selected due to its K_D value as the best peptide mimetic of the HNK-1 epitope. This peptide could be considered an optimized HNK-1 epitope mimetic, showing higher affinity than the peptides reported in prior studies and derived by screening a phage-displayed random peptide library.[20] We also selected the cyclic peptide c-(LSETETK(Ac)dL) (**5**), showing similar K_D values as compared to **3** (1.04 x 10^{-7} M and 1.09 x 10^{-7} M, respectively), bearing an additional acetylated Lys residue, which may allow further modification with spacers enabling immobilization on a suitable sensor chip, in a future development of novel anti-HNK1 antibody detection tools. For this reason, we consider

peptide **5** as the cyclic counterpart of linear peptide 3, since the simple head-to-tail cyclization of **3** would yield a peptide without a functional group available for subsequent covalent immobilization. However, when peptide **6** was covalently linked to the BiaCore sensor chip through the Lys side chain, we were unable to observe a binding interaction with the anti-HNK-1 monoclonal antibody (data not shown), possibly because peptide immobilization hides the epitope fundamental for antibody recognition when the peptide is free in solution, a well-known phenomenon when dealing with solid-phase immunoenzymatic assays.[25]

Further modification of peptide 3 for solid-phase immunoassay. The two high affinity binders, mimetic of the trisaccharide HNK-1, could be proposed as antigenic probes to detect anti-HNK1 antibodies in a solid-phase immunoenzymatic assay (SP-ELISA), but they appear to be too short for an efficient adsorption on the SP-ELISA plastic plates.[25] Therefore, in order to obtain a molecule with the best physico-chemical properties, peptide **3** was modified by insertion in the N-terminal position of a flexible and hydrophilic moiety, such as the PEG chain 4,7,10-trioxa-1,13-tridecanediamino succinic acid linker 4,7,10-trioxa-1,13-tridecanediamino succinic acid (Ttds, Figure **2**).

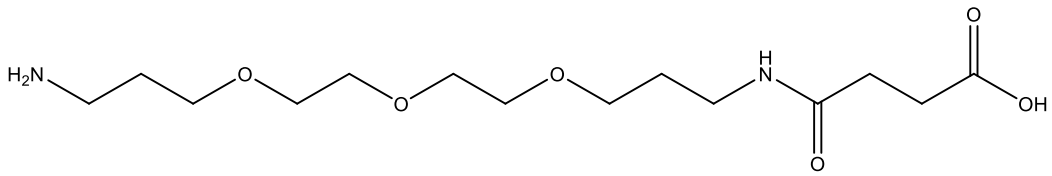

Figure 2. Structure of the spacer Ttds

The resulting peptide Ttds-LSETETdL (**13**) was preliminary tested in SPR experiments to verify if the introduced modification hampers the high affinity antibody binding observed with the unmodified peptide **3**. Indeed, despite the presence of the N-terminal PEG extension, when peptide **13** was tested in solution on the immobilized antibody, it showed a K_D value of 6.32 x 10^{-7} M, corresponding to a marginal loss of affinity (six-fold), as compared to the original sequence. We have previously observed a similar behavior, i.e. a modest decrease in affinity due to N-terminal modification of antigenic peptides, possibly due to the introduction of steric hindrance, which however did not hamper the use of these peptides in ELISA.[26] Accordingly, we tested in SP-ELISA the peptide Ttds-LSETETdL (**13**), which can be directly adsorbed on plastic plates.

SP-ELISA experiments. Initially, Ttds-LSETETdL (**13**) was tested for its ability to detect the anti-HNK-1 monoclonal antibody in SP-ELISA. The condition of the assay in terms of type of polymeric support of the ELISA plate, amount of peptide per well, coating buffer, blocking buffer, and concentration of the secondary antibody were evaluated (data not shown), in order to determine the optimal SP-ELISA conditions for the identification of anti-HNK1 antibodies, using the monoclonal antibody. Subsequently, the anti-HNK1 monoclonal antibody was titrated by SP-ELISA at the established optimal conditions. Titration results, shown in Figure **3**, suggest that the peptide-based ELISA is able to identify anti-HNK1 antibodies in a good range of concentrations. Moreover, the specificity of the signal obtained using peptide **13** as antigen was confirmed using in parallel a BSA-coated plate.

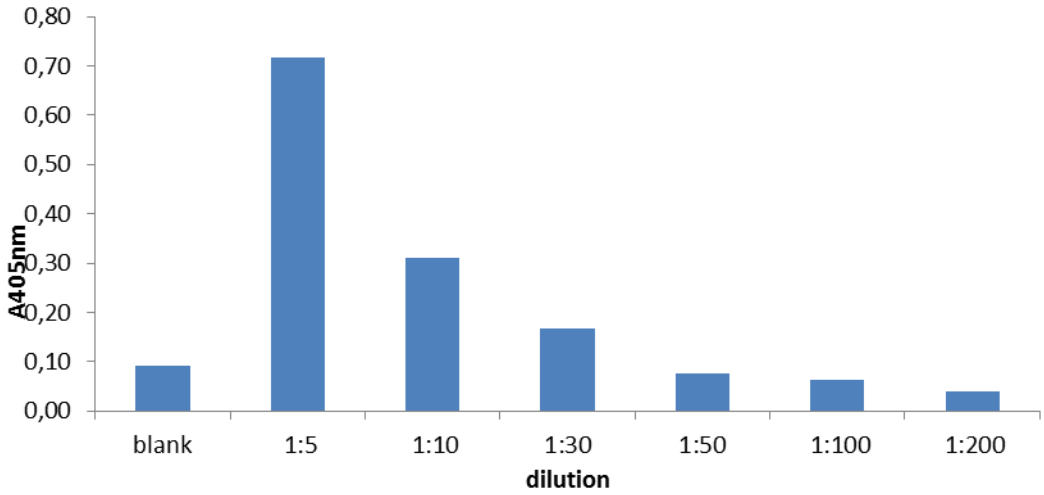

Figure 3. Anti-HNK1 monoclonal antibody titration in SP-ELISA with coated peptide **13**. Blank is obtained using BSA buffer instead of the monoclonal antibody.

To the best of our knowledge, this is the first example of a simple synthetic peptide probe that appears to be able to recognize specific anti-HNK-1 antibodies in SP-ELISA and therefore we propose it to be exploited for the development of a diagnostic tool for patients affected by autoimmune neurological disorders, such as IgM monoclonal gammopathy characterized by anti-HNK-1 antibodies circulating in blood. However, preliminary aspecific results obtained with human sera suggest that the monoclonal epitope of mouse is different from the human one.

Conformational studies. To explore the conformational preferences of the most interesting peptides **3** and **5**, we performed a CD analysis in water and HFA/water 30% solutions. CD spectra of peptide **5** in the two solutions were very similar showing a minimum at 204 nm and a shoulder at 222 nm characteristic of turn-helix structures (Figure 4a). Spectra similarity clearly indicates that the environment has little influence on the cyclic peptide structure. In contrast, CD spectra of peptide **3** (Figure 4b) change from water to HFA/water solution indicating an increase of the folded structure in the last medium. Spectra of peptides **3** and **5** in HFA/water solution were qualitatively similar (Figure 4c) indicating similar conformation of the two peptides but dichroic intensity was reduced for peptide **3** pointing to a lower conformational stability.

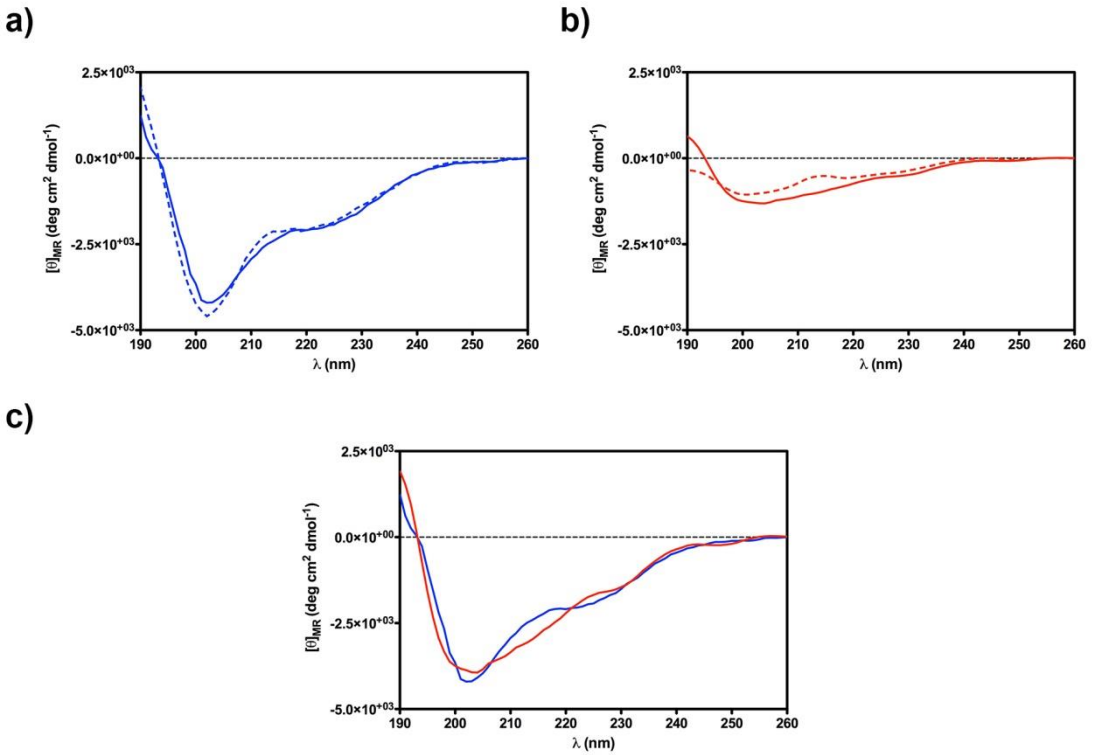

Figure 4. CD spectra of peptide **5** (a) and **3** (b) in water (dashed lines) and 30% HFA/water solution (solid lines) respectively. (c) Overlap of the CD spectra in HFA/water solution of **5** (blue) and **3** (red). For qualitative comparison, the last spectrum intensity was multiplied by three.

We then followed up with a detailed NMR conformational analysis of peptide **5** in HFA/water solution. Several NOE dipolar couplings observed in the NOESY spectrum of **5** pointed to the presence of turn-helical structures. In particular strong $d_{NN}(i,i+1)$ between Glu^3 and Thr^4 and between Thr^6 and $DLeu^8$, $d_{\alpha N}(i,i+2)$ between Ser^2 and Thr^4, and between

Thr[4] and Thr[6], $d_{\beta N}$(i,i+3) between Leu[1] and Glu[3], $d_{\beta N}$(i,i+4) between Leu[1] and Thr[4], $d\gamma_N$(i,i+3) between Thr[4] and Lys[7] were observed (Table S3). Also, side chain to side chain NOEs were observed between Ser[2] and Glu[5]. Using the NOE derived data as input, structure calculations by restrained simulated annealing gave the conformers of peptide **5** shown in Figure **5**. Structures are well defined (backbone rmsd is 0.20 Å), and analysis of the ensemble dihedral angles (Table S4) provides the presence of four β-turns along residues 1-4 (type III), 2-5 (distorted type VIII), 4-7 (type III), and 5-8 (distorted type VIII). Interestingly, side chains of residues Ser[2] and Glu[5] are spatially close and, in many cases, an H-bond is observed between Ser[2] hydroxyl and Glu[5] carboxyl groups. Previous conformational studies on parent peptide **1**, revealed the existence of a β-turn around Ser[2]-Glu[3]-Thr[4]-Thr[5] sequence.[27] In our peptide **5** (and **3**) a Glu residue replaces Thr[5] and the stable H-bond between the side chains of residues 2 and 5 (not reported for peptide **1**) can be one of the reasons for the increased affinity of peptide **5** (and **3**) for the antibody. Moreover, the other secondary structural elements of peptide **5**, not observed in peptide **1**, can be responsible of such binding improvement.

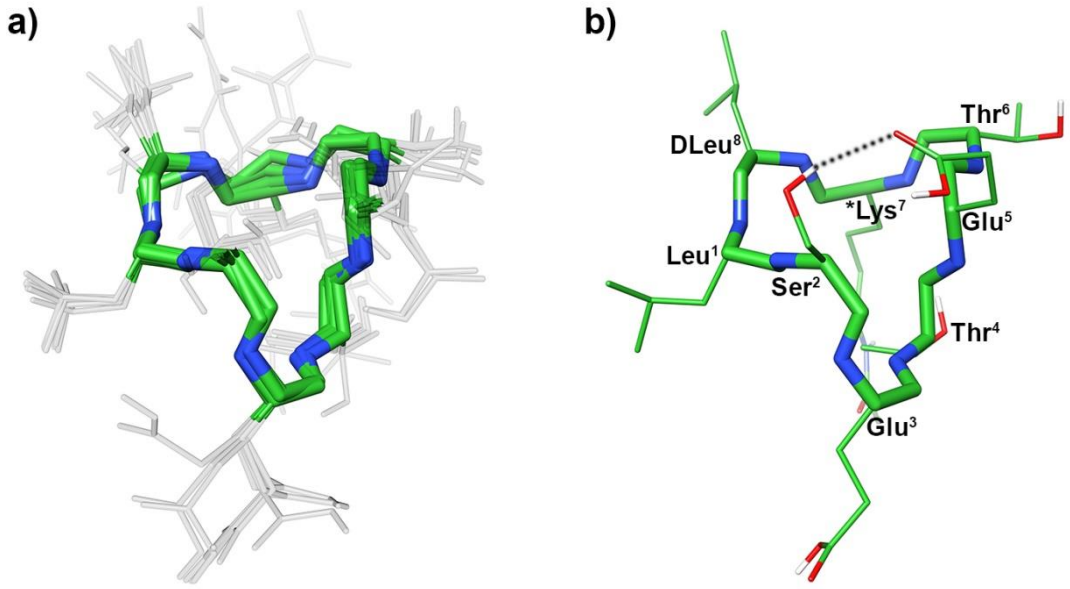

Figure 5. (a) Superposition of the ten lowest energy conformers of peptide **5**. Structures were superimposed using the backbone heavy atoms. Side chains are shown in light grey. (b) Lowest energy conformer of **5**: hydrogen bond between Ser[2] hydroxyl and Glu[5] carboxyl groups is shown as black dotted line. Heavy atoms have different colors (carbon, green; nitrogen, blue; oxygen, red; sulfur, yellow). Hydrogen atoms are hidden for a better view. *Lys: Acetyl-lysine.

Identification and reproduction of conformational epitopes involved in antibody recognition is a challenge, particularly if sugars are involved in antibody recognition. In this context peptide molecules can be instrumental to develop conformational epitope mimics to improveantibody affinity and specificity to carbohydrates. Nowadays, anti-MAG and anti-SGPG antibodies are used as biomarkers in clinical practice to support the diagnosis of patients affected by PNS disorders. The putative target of these antibodies circulating in patients' sera is considered the trisaccharide HNK-1 epitope, which synthesis is not straightforward (let Mallet).With the aim of producing a simple synthetic peptide mimicking the complex trisaccharide HNK-1 epitope and useit to develop a novel diagnostic tool for practical clinical use, we rationally designed a series of peptides mimicking the HNK-1 molecule that could be sufficient to ensure the specificity of antibody recognition. After a screening of a peptide library over the immobilized commercial monoclonal anti-HNK-1 antibody by SPR, a cyclic heptapeptide bearing 2 net negative charges was selected as the best mimetic of the HNK-1 epitope. Biological experiments helped to evaluate the effects of this analogue in the detection of autoantibodies in the sera of patients with polyneuropathies. Conformational analysis gave possible explanations of the increased antibody affinity displayed by some novel analogues. Overall the results can help in the development of novel …

EXPERIMENTAL SECTION

Materials and methods. All Fmoc-protected amino acids, Fmoc-Ile-Wang resin, Fmoc-dLeu-Wang resin, Fmoc-Glu(Wang resin)-OAll, DIC, Oxyma, HATU and N-methylmorpholine (NMM) were purchased from Iris Biotech GmbH (Marktredwitz, Germany). The following amino acid side-chain-protecting groups were used: OtBu (Glu), tBu (Ser,Thr) and Dde (Lys). Peptide-synthesis grade N,N-dimethylformamide (DMF) was purchased from Scharlau (Barcelona, Spain); acetonitrile (ACN) from Carlo Erba (Milan, Italy); dichloromethane (DCM), trifluoroacetic acid (TFA), piperidine were purchased from Sigma-Aldrich (Milan,Italy). The scavenger triisopropylsilane (TIS) for cleavage of peptides from resin was purchased from Acros Organics (Geel, Belgium). The $Pd(PPh_3)_4$ was purchased from Sigma-Aldrich (St. Quentin Fallavier, France) and every time was weighted under argon and dissolved in dry DCM immediately before use. Sensor chip CM5, chip SA, running buffer 10x (0.1M HEPES, 1.5M NaCl, 30mM EDTA, 0.5% v/v p20 yielding pH 7.4 when diluted), amine coupling reagents *N*-hydroxysuccinimide (NHS) and 1-ethyl-3-(3-dimethylaminopropyl) carbodiimide hydrochloride (EDC) were purchased from Biacore AB (GE Healthcare). The monoclonal anti-

HNK-1/N-CAM (CD57) antibody produced in mouse was commercially available from Sigma-Aldrich. Assays (SP-ELISA) were performed using 96 wells plates PVC (company). Washings steps were performed with Hydroflex Microplate Washer (Tecan, Männedorf, Switzerland). Bovine serum albumin was purchased by Euroclone (Milan, Italy). Anti-mouse IgM alkaline phosphatase conjugates were purchased by Sigma Aldrich (Milan, Italy). p-Nitrophenyl phosphate was purchased from Fluka (Milano, Italy). Absorbance values were measured on a Sunrise Tecan ELISA plate reader purchased by Tecan (Tecan Italia, Milano, Italy).

MW-assisted Solid Phase Peptide Synthesis. General Protocol. The linear peptides were synthesized on a 0.1 mmol scale (5 eq of activator and amino acid) by a high-efficiency Solid Phase Peptide Synthesis (HE-SPPS) strategy, using a Liberty Blue^{TM} automated microwave synthesizer (CEM) following the Fmoc/tBu methodology. The reactions were performed in a Teflon vessel and mixed by N_2 bubbling. Reaction temperatures were monitored by an internal fiber-optic sensor. The syntheses were performed on Fmoc-Ile-Wang resin (0.7 mmol/g) for the linear peptides 2, 3, 4, 8, 10, and 13, Fmoc-Glu(Wang resin)-OAll (0.21 mmol/g) for the cyclic peptides 1, 5, 6, 7, 9, and 11, and Fmoc-Leu-Wang resin (0.7 mmol/g) for peptide 12. The resins were swelled with DMF (1mL/100mg of resin) for 20 min.
A general coupling cycle was initiated with a double deprotection step with 20% piperidine in DMF, for 15 sec at 75 °C using 155W followed by 50 sec with a fresh deprotection solution at 90 °C reached with 30W. Three washes with DMF and N_2 bubbling were performed. Fresh stock solutions of the Fmoc-protected amino acids (0.2 M), Oxyma (1 M) and DIC (0.5 M) in DMF were prepared in separated bottles and used as reagents during the SPPS. The MW-SPPS protocol, consisted of two coupling steps (standard coupling), performed firstly at 75°C for 15 sec using 170W and then at 90°C for 110 sec using 30W. One wash was performed after the coupling step with DMF and N_2 bubbling.
General procedure for head to tail on-resin cyclization. *Removal of allyl protecting groups.* Peptide-resin protected by allyl group was swollen in anhydrous DCM under Ar atmosphere for 20 min. Then $Pd(PPh_3)_4$ (3 eq.) in a solution of dry DCM/AcOH/NMM (37:2:1) was added (15mg/gr of resin) and the resin was shaken for 2 h at room temperature. The reaction is air-sensitive and all manipulations were carried out under Ar. Finally, the resin was filtered and washed successively with 0.5% *N,N*-Diisopropylethylamine (DIPEA) in DMF and 0.5% sodium diethyldithiocarbamate in DMF to remove the catalyst. *Cyclization.* After performing the final Fmoc-deprotection, the resin was swollen in DMF and cyclized with NMM (5 eq.), Oxyma (5 eq.) and HATU (5 eq.). After shaken for 1.5 h at room temperature, the resin was

filtered and washed successively with DMF, DCM. The reaction was verified by Kaiser Test. *Acetylation.* Firstly the Dde protecting group was removed from the side chain of Lys with a solution of 2% hydrazine in DMF (25mL/g resin) at rt for 3min. The resin was filtered and the treatment with hydrazine was repeated two more times. At the end the partially protected resin was washed several times with DMF and DCM. For the peptides 4 and 5 which are modified with an acetyl group at the side chain of the residue of Lys, the acetylation was performed adding on the peptide-resin a solution of acetic anhydride (10 eq.) and NMM (10 eq.) in DMF. After shaken for 1 h, the resin was filtered and washed successively with DMF, DCM. The reaction was verified by Kaiser Test.

Deprotection, Cleavage, Purification and Characterization of Peptides. Cleavage from the resin and side-chain deprotection was achieved by treatment with a TFA/TIS/water solution (95:2.5:2.5 v/v/v, 1mL/100 mg of resin-bound peptide). The cleavage was carried out approximately for 3 h with vigorous shaking at room temperature. The resin was filtered and the combined filtrates were concentrated by flushing with N_2. The crude peptides were precipitated from the cleavage mixture by addition of ice-cold Et_2O, centrifuged, washed with ice-cold Et_2O (x3), dried and lyophilized. Lyophilized crude peptides were purified by semi-preparative Waters RP-HPLC on a Phenomenex Jupiter C18 (10 µm, 250 mm × 10 mm) column (Phenomenex, Castel Maggiore, Italy) at 4 mL/min. The solvent systems used were: 0.1% TFA in H_2O (A) and 0.1% TFA in CH_3CN (B) and the gradients used are presented in Table 2. All peptides were obtained with a purity >95%.

Characterization of the peptides was performed by analytical Waters Alliance RP-HPLC (model 2695) with UV detection at 215nm, coupled with an ESI-MS detector (Micromass ZQ, Waters, Milford Massachusetts, USA) using a BIOshell^{TM} A160 Peptide C18 (2.7µm, 10cm × 30mm) column and Phenomenex Kinetex C-18 column 2.6µm (100 × 3.0 mm) at 35 °C, with a flow rate of 0.6mL/min. The total run time of the analysis was 5 min and the solvent systems used were: 0.1% TFA in H_2O (A) and 0.1% TFA in ACN (B). The analytical data are reported in Table 2. Data were acquired and processed using MassLynx software (Waters, Milford, Massachusetts, USA).

Table 2. Analytical data of synthetic peptides.

No	Sequence	**HPLC** Rt (min)	**ESI-MS** $[M + H]^{2+}$ (m/z) found (calcd)
1	c-(LSETTdL)	4.71[a]	645.53 (645.75)
2	LSETTdl	3.37[b]	663.42 (663.75)
3	LSETETdL	3.37[c]	792.13 (792.36)
4	LSETETK(Ac)dL	3.63[c]	962.35 (961.5)
5	c-(LSETETK(Ac)dL)	3.15[d]	944.36 (944.5)
6	c-(LSETKTdL)	4.26[a]	773.67 (773.93)
7	c-(LSETETKdL)	4.15[a]	902.82 (903.04)
8	LSETY(OSO_3)TKdL	4.32[a]	1035.04 (1035.10)
9	c-(LSETY(OSO_3)TKdL)	4.43[a]	1017.04 (1017.10)
10	LSETYTKdL	4.14[a]	955.02 (955,10)
11	c-(LSETYTKdL)	4.77[a]	937.02 (937.10)
12	LSETETL	3.98[c]	744.26 (744.36)

Analytical HPLC conditions: column, BIOshell™ A160 Peptide C18 (2.7µm, 10cm × 30mm) and Phenomenex Kinetex C-18 column 2.6µm (100 × 3.0 mm); solvent systems, A: 0.1% TFA in H_2O, B: 0.1% TFA in CH_3CN; flow rate 0.6 mL min^{-1}. Gradient [a]10–60% B in 5 min, [b]20–60% B in 5 min, [c]15–50% B in 5 min , [d]25-50% B in 5 min, [e]isocratic 23%B in 5 min, [f]75–95% B in 5 min.

SPR studies. *Anti-HNK-1 antibody immobilization.* Antibody was covalently linked according to the *amine coupling* strategy. Immobilization buffer was selected to obtain the electrostatic pre-concentration of the antibody on CM5 chip surface, using the following buffers: D-PBS buffer pH 6 and 7.2, AcNa 5mM pH 6 and 5, AcNa 0.5mM pH 5.5 and 6.5, AcNa 0.1mM pH 6 and 7, NaCl 5 mM pH 6. Chip surface was activated with two injections of *N*-hydroxysuccinimide (NHS 0.1 M) and 1-ethyl-3-(3-dimethylaminopropyl)-carbodiimide (EDC 0.4 M) 50:50 for 420 and 60 seconds at a flow rate of 10 µl/min to give reactive

succinimide esters; antibody solubilized in the previously selected immobilization buffer [5 µg/mL], was injected for 420 seconds at a flow rate of 5 µl/min. Immobilization was continued in manual mode by changing ligand concentration and contact time in order to reach a satisfactory immobilization level around 730 RU. Non-reacted sites on sensor chip surface were blocked with ethanolamine-HCl 1 M pH 8.5 for 420 and 60 seconds at a flow rate of 30 µL/min. Reference channel was activated injecting NHS/EDC 50:50 and directly blocked with ethanolamine-HCl.

Kinetic and affinity experiments. Once the antibody was immobilized on the chip, kinetic studies were started. Peptides were tested at 3 different concentrations (2.0, 3.0 and 3.5 mM) in running buffer and injected in a different cycle of analysis. Each diluted peptide was injected over the immobilized antibody for 80 seconds at a flow rate of 30 µl/min, dissociation was followed for 120 seconds by injecting running buffer and finally the chip surface was regenerated with an injection of NaOH 0.1 M for 60 seconds. Experimental data were recorded and further elaborated with Bia Evaluation Software 2.0 and the kinetic parameters and the affinity constants were calculated according to a 1:1 binding model optimized for small analytes.

ELISA Assays. 1ug/well of antigen (peptide or protein) were dissolved in EtOH, then 100 µL of solution were dispensed in each well of 96-well PVC plates (company). Plates were incubated overnight at room temperature. Subsequently, plates were washed 3 times with 0.9% NaCl, and blocked 1 h at room temperature with 100µL/well of bovine serum albumin (BSA) Buffer [5% BSA in Washing Buffer (0.9% NaCl, 0,01% Tween 20)]. BSA Buffer was removed, and 100 µL/well of diluted monoclonal anti-HNK1 antibody in BSA Buffer were dispensed. Blank wells were included in all the plates, and were obtained using BSA Buffer instead of the monoclonal Ab. Plates were incubated at 4 °C overnight, then washed 3 times with Washing Buffer. 100 µL/well of secondary antibodies diluted in 2,5% BSA Buffer (goat anti-mouse IgM 1:7500) were dispensed, and plates were incubated 3 h at room temperature. Plates were washed 3 times with Washing Buffer, then 100 µL/well of Substrate Solution (1mg/mL p-NPP~~PNP~~ in Substrate Buffer: 10mM $MgCl_2$, 12 mM Na_2CO_3, 35 mM $NaHCO_3$, pH 9.6) were dispensed. Plates were incubated at room temperature, and then the absorbance (ABS) of each well was red with a multichannel ELISA reader (Tecan Sunrise, Männedorf, Switzerland) at 405 nm. ABS value for each serum was calculated as (mean ABS of triplicate) – (mean ABS of blank triplicate).

CD Studies. CD spectra (Figure 3) were recorded using a JASCO J710 spectropolarimeter at 20 °C between λ=260–190 nm (1 mm path, 1 nm bandwidth, 4 accumulations, and 100 nm min^{-1} scanning speed). Measurements were performed with peptides in H_2O (0.100 mM, pH 7.4) or in HFA/water 30% solution.

NMR Studies. [28] The samples for NMR spectroscopy were prepared by dissolving the appropriate amount of peptide **5** in 0.30 ml of ^1H_2O (pH 5.5), 0.05 ml of ^2H_2O and 0.15 ml of HFA to obtain a 2 mM concentration of peptide. NMR spectra were recorded on a Varian INOVA 700 MHz spectrometer equipped with a z-gradient 5 mm triple-resonance probe head. All the spectra were acquired at a temperature of 25 °C. The spectra were calibrated relative to TSP (0.00 ppm) as internal standard. One-dimensional (1D) NMR spectra were recorded in the Fourier mode with quadrature detection. The water signal was abolished by gradient echo.[a] 2D DQF-COSY,[b,c] TOCSY,[d] and NOESY[e] spectra were recorded in the phase-sensitive mode using the method from States.[f] Data block sizes were 2048 addresses in t_2 and 512 equidistant t_1 values. Before Fourier transformation, the time domain data matrices were multiplied by shifted sin^2 functions in both dimensions. A mixing time of 70 ms was used for the TOCSY experiments. NOESY experiments were run with mixing times in the range of 100-200 ms. The qualitative and quantitative analyses of DQF-COSY, TOCSY, and NOESY spectra, were obtained using the interactive program package XEASY.[g] $^3J_{HN\text{-}H\alpha}$ coupling constants were obtained from 1D ^1H NMR and 2D DQF-COSY spectra. ^1H NMR chemical shift assignments were effectively achieved according to the Wüthrich procedure[h] (Table S2, Supporting Information).

Structure Calculation. The NOE-based distance restraints were obtained from NOESY spectra acquired with a mixing time of 200 ms. The NOE cross peaks were integrated with the CARA program and were converted into upper distance bounds using the CALIBA program incorporated into the program package DYANA.[i] Only NOE derived constraints (Table S3, Supporting Information) were considered in the annealing procedures. NMR-derived upper bounds were imposed as semiparabolic penalty functions with force constants of 16 Kcal mol^{-1} $Å^{-2}$. A distance maximum force constant of 1000 Kcal mol^{-1} $Å^{-2}$ was used. Cyclic peptide **5** was built using the Insight Builder module (Accelrys Software Inc., San Diego). Atomic potentials and charges were assigned using the consistent valence force field (CVFF).[l] The conformational space of compound was sampled through 100 cycles of restrained simulated annealing (ε = 1r). In simulated annealing, the temperature is altered in time increments from an initial temperature to a final temperature by adjusting the kinetic energy of the structure (by rescaling the velocities of the atoms). The following protocol was

applied: the system was heated up to 1500 K over 2000 fs (time step = 1.0 fs); the temperature of 1500 K was applied to the system for 2000 fs (time step = 1.0 fs) with the aim of surmounting torsional barriers; successively, temperature was linearly reduced to 300 K in 1000 fs (time step = 1.0 fs). Resulting conformations were then subjected to restrained Molecular Mechanics (MM) energy minimization within Insight Discover module (ε = 1r) until the maximum RMS derivative was less than 0.001 kcal/Å, using Conjugate Gradient as minimization algorithm. Finally, conformations were subjected to 1000 steps of unrestrained MM Conjugate Gradient energy minimization. From the produced 100 conformations, 10 structures, whose interproton distances best fitted NOE derived distances, were chosen for statistical analysis (Table S4, Supporting Information). The final structures were analyzed using the InsightII program (Accelrys, San Diego, CA). Molecular graphics images of the complexes were realized using the UCSF Chimera package.[m]

ACKNOWLEDGMENTS

ANR Chaire d'Excellence PeptKit 2009–2014 (grant n° ANR-09- CEXC-013-01 to AMP) and Ente Cassa di Risparmio di Firenze are gratefully acknowledged for their financial support.

[1] Lis, H. and Sharon, N. Chem. Rev. **1998**, 98, 637−674.

[2] Kleene, R.; Schachner, M. *Nat.Rev. Neurosci.* **2004**, *5*, 195

[3] Rao N, Anderson MB, Musser JH, Gilbert J, Schaefer M, Foxall C, Brandley B Sialyl LewisX mimics derived from a pharmacophore search are selectin inhibitors with anti-inflammatory activity. *J Biol Chem* **1994**, *269*, 19663–19666.

[4] Mikkelsen LM, Hernáiz MJ, Martín-Pastor M, Skrydstrup T, Jiménez-Barbero J. Conformation of glycomimetics in the free and protein-bound state: structural and binding features of the C-glycosyl analogue of the core trisaccharide alpha-D-Man-(1-3)-[alpha-D-Man-(1-6)]-D-Man. *J Am Chem Soc* **2002**, 124, 14940-51.

[5] Magniani, J.L., Ernst, B., *Nat. Rev. Drug Discov.* **2009**, *8*, 247-252.

[6] Fernández-Tejada A, Cañada FJ, Jiménez-Barbero J. Recent Developments in Synthetic Carbohydrate-Based Diagnostics, Vaccines, and Therapeutics. *Chemistry* **2015**, *21*, 10616-10628.

[7] Johnson MA, Pinto BM. Molecular mimicry of carbohydrate by peptides. *Aust. J. Chem.* **2002**, *35*, 13-25.

[8] Torregrossa, P., Buhl, L., Bancila, M., Durbec, P., Schafer, C., Schachner, M., Rougon, G., *J. Biol. Chem.* **2004**, 29, 30707-30714

[9] Mehanna, A., Mishra, B., Kurschat, N., Schulze C., Bian, S., Loers, G., Irintchev, A., Schachner, M., *Brain* **2004**, 132, 1449-1462.

[10] Katagihallimath, N., Mehanna, A., Guseva, D., Kleene, R., Schachner, M., *J. Cell Biol.* **2010**, 89, 77-86.

[11] M.C. Alcaro, F. Lolli, P. Migliorini, M. Chelli, P. Rovero, A.M. Papini. Peptides as autoimmune diseases antigenic probes: a peptide-based reverse approch to detect biomarkers of autoimmune diseases.*Chem. Today*, **2007**, *25*, 14-16.

[12] Voshol, H.; Carol, W. E. M.; Georg, O.; Johannes, F. G. V.; Melitta, S. *J. Biol. Chem.***1996**, 271, *38*, 22957

[13] Quarles, H., Everly, L., Brandy, O., *J.Neurochem.* **1973**, *21*, 1171-1191

[14] Morita, I., Kizuka, Y., Kakuda, S., Oka, S. *J.Biochem.* **2008**, 143, 719-724

[15] Künemund, V., Jungalwala, F., Fischer, G., Chou, D., Keilhauer, G., Schachner, M., *J. Cell Biol.* **1988**, 106, 213-223

[16] Ilyas, A.A., Quarles, R.H., MacIntosh, T.D., Dobersen, M.J., Trapp, B.D., Dalakas, M.C., Brady, R.O. IgM in a human neuropathy related to paraproteinemia binds to a carbohydrate determinant in the myelin-associated glycoprotein and to a ganglioside. *Proc. Natl. Acad. Sci. USA* **1984**, *81*, 1225–1229.

[17] Burger, D., Perruisseau, G., Simon, M., Steck, A.K. Comparison of the N-linked oligosaccharide structures of the two major human myelin glycoproteins MAG and P0: assessment of the structures bearing the epitope for HNK-1 and human monoclonal immunoglobulin M found in demyelinating neuropathy. *J. Neurochem.* **1992**, *58*, 854–861.

[18] Matà, S., Ambrosini, S., Mello, T., Lelli, F., Minciacchi, D. Anti-myelin associated glycoprotein antibodies recognize HNK-1 epitope on CNS. *J. Neuroimmunol.* **2011**, *236*, 99-105.

[19] Simon-Haldi, M., Mantei, N., Franke, J., Voshol, H., Schachner, M., *J. Neurochem.* **2002**, 83, 1380-1388

[20] Bächle, D., Loers, G., Guthöhrlein, E.W., Schachner, M., Sewald, N. *Angew. Chem. Int. Ed.* **2006**, *45*, 6582 –6585

[21] Gomara, M. J.; Ercilla, G.; Alsina, M. A.; Haro, I. *J. Immunol. Methods* **2000**, *246*, 13-24

[22] Gomes, P., Giralt, E., Andreu D. *J. Immunol. Methods* **2000**, *235*, 101–111

[23] Real-Fernández, F., Passalacqua, I., Peroni, E., Chelli, M., Lolli, F., Papini, A-M., Rovero, P. *Sensor* **2012**, *12*, 5596-5607

[24] Rossi, G.; Real Fernandez, F.; Panza, F., Barbetti, F., Pratesi, F., Rovero P., Migliorini, P., *Analytical Biochemistry* **2014**, 465C, 96-101.

[25] Van Regenmortel MHV, Muller S. Synthetic Peptides as Antigens. Amsterdam, Elsevier, 1999: pp. 1–381.

[26] Real Fernández F, Di Pisa M, Rossi G, Auberger N, Lequin O, Larregola M, Benchohra A, Mansuy C, Chassaing G, Lolli F, Hayek J, Lavielle S, Rovero P, Mallet JM, Papini AM. Antibody Recognition in Multiple Sclerosis and Rett Syndrome Using a Collection of Linear and Cyclic N-Glucosylated Antigenic Probes. *Biopolymers*. **2015**, *104*, 560-576.

[27] Bhunia, A.; Vivekanandan, S.; Eckert, T.; Burg-Roderfeld, M.; Wechselberger, R.; Romanuka, J.; Bächle, D.; Kornilov, A.V.; von der Lieth, C-W.; Jimenez-Barbero, J.; Nifantiev, N.E.; Schachner, M.; Sewald, N.; Lütteke, T.; Siebert, H-C. Why structurally different cyclic peptides can be glycomimetics of the HNK-1 carbohydrate antigen. *J. Am. Chem. Soc.* **2010**, *132*, 96–105

[28] a) Hwang, T. L.; Shaka, A. J. Water suppression that works. Excitation sculpting using arbitrary wave-forms and pulsed-field gradients. J. Magn. Res. 1995, 112, 275-279.

b) Piantini, U.; Sorensen, O.W.; Ernst, R.R. Multiple quantum filters for elucidating NMR coupling network. J. Am. Chem. Soc. 1982, 104, 6800-6801.

c) Marion. D.; Wüthrich, K. Application of phase sensitive two-dimensional correlated spectroscopy (COSY) for measurements of 1H-1H spin-spin coupling constants in proteins. Biochem. Biophys. Res. Commun. 1983, 113, 967-974.

d) Braunschweiler, L.; Ernst, R. R. Coherence transfer by isotropic mixing: application to proton correlation spectroscopy. J. Magn. Reson. 1983, 53, 521–528.

e) Jenner, J.; Meyer, B.H.; Bachman, P.; Ernst, R.R. Investigation of exchange processes by two-dimensional NMR spectroscopy. J. Chem. Phys. 1979, 71, 4546-4553.

f) States, D.J.; Haberkorn, R.A.; Ruben, D.J. A two-dimensional nuclear overhauser experiment with pure absorption phase in four quadrants. J. Magn. Reson. 1982, 48, 286-292.

g) Bartels, C.; Xia, T.; Billeter, M.; Guentert, P.; Wüthrich, K. The program XEASY for computer-supported NMR spectral analysis of biological macromolecules. J. Biomol. NMR 1995, 6, 1-10.

h) Wüthrich, K. In NMR of Proteins and Nucleic Acids; John Wiley & Sons: New York, 1986.

i) Güntert, P.; Mumenthaler C.; Wüthrich, K.; Torsion angle dynamics for NMR structure calculation with the new program DYANA. J. Mol. Biol. 1997, 273, 283-298.

l) Maple, J.; Dinur, U.; Hagler, A.T. Derivation of force fields for molecular mechanics and dynamics from Ab Initio energy surface. Proc. Natl. Acad. Sci. U.S.A. 1988, 85, 5350-5354.

m) Pettersen, E. F.; Goddard, T. D.; Huang, C. C.; Couch, G. S.; Greenblatt, D. M.; Meng, E. C.; Ferrin, T. E. UCSF Chimera – a visualization system for exploratory research and analysis. J. Comput. Chem. 2004, 25, 1605-1612.